

February 2020

Evaluation of Optimal Technique for Left Breast Irradiation

Amitpal Singh Saini
University of South Florida

Follow this and additional works at: <https://digitalcommons.usf.edu/etd>



Part of the [Biophysics Commons](#)

Scholar Commons Citation

Saini, Amitpal Singh, "Evaluation of Optimal Technique for Left Breast Irradiation" (2020). *USF Tampa Graduate Theses and Dissertations*.
<https://digitalcommons.usf.edu/etd/8682>

This Dissertation is brought to you for free and open access by the USF Graduate Theses and Dissertations at Digital Commons @ University of South Florida. It has been accepted for inclusion in USF Tampa Graduate Theses and Dissertations by an authorized administrator of Digital Commons @ University of South Florida. For more information, please contact digitalcommons@usf.edu.

Evaluation of Optimal Technique for Left Breast Irradiation

by

Amitpal Singh Saini

A dissertation submitted in partial fulfillment
of the requirements for the degree of
Doctor of Philosophy
Department of Medical Engineering
College of Engineering
University of South Florida

Major Professor: William E. Lee III, Ph.D.
Indra Das, Ph.D.
Robert Frisina, Ph.D.
Matthew Biagioli, M.D.
Piyush Koria, Ph.D.
Geoffrey Zhang, Ph.D.

Date of Approval:
January 31, 2020

Keywords: Lt breast radiation, prone, DIBH, Heart dose, Lung dose, Biological dosimetry

Copyright © 2020, Amitpal Singh Saini

Dedication

To my father (Late) Sardar Surinder Singh Saini, who has been my role model and inspiration.

Acknowledgments

I am thankful to Dr. William Lee III, Ph.D., for serving as a major professor and guiding me throughout my graduate career. Without Dr. Lee's help, I would not have been able to continue my Ph.D. I would like to thank my advisor Indra J. Das, Ph.D., for providing me the opportunity to work on this project and for providing time and resources for this project. His guidance has been invaluable, and he has provided productive advice on this project. Then, I would like to thank Dr. Matthew Biagioli, M.D., for his tremendous support and motivation. I would also like to express my gratitude towards Robert Frisina, Ph.D. for not only guiding me as a department chair but also agreeing to serve on the committee. Next, I would like to thank Geoffrey Zhang, Ph.D., and Piyush Koria, Ph.D., for serving in my supervisory committee and their encouraging support, as well as my colleague Catherine Hwang, M.D., who has helped me immensely with this project. She worked very hard to set up all the patients for treatment planning. This project would not have been possible without her help. Then, I would like to thank my brother-in-law, Amarjit Saini, very much; he has provided guidance, support, and encouragement not only in my academic career since high school but also in my personal life. I also immensely thank my uncle, Daljit Saini, for his guidance and interest in my career. Finally, I could not have achieved much without the unconditional support of my mother, Kailash Kaur, and my wife, Amarjit Kaur, who have both been a great source of inspiration that kept me going despite a few difficult stints in the last few years. My wife has taken the entire responsibility of caring for our children and household in the last few years. My children Suhavi and Sohum have also contributed by being so understanding when I could not give them enough time in the last few years. Thanks to all my special friends and family, who have stood with me through my tough times.

Table of Contents

List of Tables	iii
List of Figures	iv
Abstract.....	v
Chapter 1: Background	1
1.1 What is Cancer?	1
1.2 What is Breast Cancer?	1
1.3 Treatment for Breast Cancer	1
1.3.1 Surgery	2
1.3.1.1 Breast-Conserving Surgery (Lumpectomy)	2
1.3.1.2 Mastectomy	2
1.3.2 Systematic Medical Therapy	3
1.3.2.1 Neoadjuvant Therapy.....	3
1.3.2.2 Adjuvant Therapy.....	3
1.3.3 Radiation Therapy.....	3
1.3.3.1 Computed Tomography Scan	4
1.3.3.2 Treatment Planning System.....	5
1.3.3.3 Linear Accelerator	6
1.4 Radiation Therapy Treatment Techniques	8
1.4.1 Prone Technique.....	10
1.4.2 Deep Inspiration Breath Hold (DIBH) Technique	12
1.5 Design of Dissertation.....	14
Chapter 2: Introduction.....	15
2.1 Treatment Planning and Dosimetry.....	19
2.2 Laser-Based DIBH.....	22
2.3 Radiobiological Modelling Biological Evaluation.....	23
2.4 Statistical Analysis.....	24
Chapter 3: Objective of the Dissertation	26
Chapter 4: Discussion	28
4.1 First Study	28
4.2 Second Study	30
4.3 Third Study.....	32
Chapter 5: Conclusion.....	37
5.1 Future Work.....	39
References	40

Abbreviations	47
Appendix A: Lasers Based DIBH Procedure	49
A.1 Procedure 1: Computed Tomography (CT) Scan with Lasers Based DIBH	49
A.1.1 Prepare Patient.....	49
A.2 Procedure 2: Treatment Procedure with Lasers Based DIBH.....	51
A.2.1 Prior to Bringing the Patient into the Treatment Room	51
A.2.2 Prepare Patient.....	51
A.2.3 Patient Coaching from Treatment Console	52
A.2.4 Perform Pretreatment Verification/Filming (KV)	52
A.2.5 Perform Pretreatment Verification/Filming (MV).....	53
A.2.6 Begin Treatment.....	54
Appendix B: Biological Evaluation Models and Parameters	55
Appendix C: Published Study 1—Evaluation of Sparing Organs at Risk in Left-Sided Breast Irradiation in the Supine and Prone Positions with Deep Inspiration Breath Hold	59
Appendix D: Published Study 2—Biological Indices Evaluation of Various Treatment Techniques for Left-Sided Breast Treatment	70
Appendix E: Submitted Study 3—Skin Dose in Radiation Treatment of Left Breast: Analysis in the Context of Prone Versus Supine Treatment Techniques	82
Appendix F: Permission to Publish Study 1	99
Appendix G: Permission to Publish Study 2	100

List of Tables

Table 2.1 Table for recording SDIBH measurements	22
Table 2.2 NTCP parameters for models used to evaluate OAR with specific end stage	25
Table 4.1 Dosimetry parameters (median values and quartiles) in supine free-breathing (SFB), supine deep inspiration breath-hold (SDIBH), prone free-breathing (PFB), and prone deep inspiration breath-hold (PDIBH) techniques for heart, left ventricle (LV), left anterior descending artery (LAD), and left lung	28
Table 4.2 Mean dosimetric parameters (median values and quartiles) of OAR in SFB, SDIBH, and PFB based on breast PTV volume < 750 cm ³ and ≥ 750 cm ³	30
Table 4.3 Dosimetry parameters (median values and quartiles) in supine free-breathing (SFB), supine deep inspiration breath-hold (SDIBH), prone free-breathing (PFB), and prone deep inspiration breath-hold (PDIBH) techniques for heart, left ventricle (LV), left anterior descending artery (LAD), and left lung.	31
Table 4.4 Calculated NTCP values (median values and quartiles) in supine free-breathing (SFB), supine deep inspiration breath-hold (SDIBH), prone free-breathing (PFB), and prone deep inspiration breath-hold (PDIBH) techniques with end-stage for heart, left ventricle (LV), left anterior descending artery (LAD), and the lung	33
Table 4.5 Dose (median value and quartile range) in percentage from a depth of 0–5 mm for prone and supine techniques with grid sizes of 1.5 mm and 2.5 mm respectively	34
Table 4.6 Dose (median value and quartile range) in Gy for OAR in prone and supine position	37

List of Figures

Figure 1.1 Anatomy of normal breast tissue	2
Figure 1.2 Computed tomography scanner	4
Figure 1.3 Eclipse Treatment planning system unit used for treatment planning	5
Figure 1.4 a) Schematic b) Actual image of medical linear accelerator	7
Figure 1.5 Prone and supine CT images showing the heart, lungs, and left breast contours.....	11
Figure 1.6 Fused SFB and SDIBH CT scan images of the same patient. Please note the position of the heart in SFB and SDIBH scans with respect to the radiation field edge.....	13
Figure 1.7 Fused CT scan images of the PFB and PDIBH techniques of the same patient	13
Figure 2.1 Typical beam placement for (a) Prone and (b) Supine set up for left Breast.....	20
Figure 4.1 (a) Prone and (b) Supine treatment techniques with 100% isodose line	36
Figure B.1 Organ: heart; end point/stage: cardiac mortality; model: NTCP poisson-LQ.....	53
Figure B.2 Organ: lung; end point/stage: pneumonitis (1) grade ≥ 2 ; model: NTCP lyman.....	54
Figure B.3 Organ: lung; end point/stage: pneumonitis (2) grade ≥ 2 ; model: NTCP lyman.....	54
Figure B.4 Organ: lung; end point/stage: symptomatic or radiographic pneumonitis (≤ 6 months); model: NTCP lyman.....	55
Figure B.5 Organ: lung; end point/stage: symptomatic pneumonitis (≤ 6 months); model: NTCP lyman.....	55
Figure B.6 Organ: lung; end point/stage: symptomatic or radiographic fibrosis (> 6 months); model: NTCP lyman.....	56
Figure B.7 Organ: lung; end point/stage: symptomatic fibrosis (> 6 months); model: NTCP lyman	56

Abstract

Numerous studies have indicated that radiation therapy reduces the risk of the local recurrence of breast cancer in several cases and that it has increased the overall survival rate. Although radiation therapy is beneficial for the treatment of breast cancer, it is known to increase the risk of both radiation toxicity and secondary breast cancer. In left-sided breast cancer, radiation therapy treatment often leads to the heart and its components—such as the left ventricle and left anterior descending artery—being exposed to high doses of radiation because of the proximity of the heart to the left breast, resulting in cardiac complications several years after the treatment. Further, it is important to deliver low doses to the left lung to reduce the risk of pneumatic and lung fibrosis, particularly for patients with long survival rates. Modern 3D techniques can deliver a reduced dose to the cardiac components and lungs. However, the risk of radiation to cardiac components remains unclear, because complications are directly related to radiation dose. Treatment techniques play an important role in sparing organs at risk (OAR) without compromising the target. Specific techniques for left-sided breast cancer treatment result in higher cardiac and pulmonary toxicity, which has been shown to be related to increased risk of heart and lung diseases.

In the first two studies in this dissertation, the dose-volume metrics of the OAR were calculated for different techniques for treating patients with left-sided breast cancer. In the first study, the supine free-breathing (SFB), deep inspiration breath-hold in supine (SDIBH), and prone free-breathing (PFB) techniques were evaluated to reduce the cardiac and left lung doses. Most left-sided breast cancer patients undergoing radiation treatment are treated using the SFB technique. The deep inspiration breath hold (DIBH) technique has been proven to reduce the

cardiopulmonary doses for breast radiation therapy. In DIBH, a patient takes a deep breath and holds the breath during irradiation. The prone position is another technique used to reduce doses to OAR. Our first study is the only one that compares the dose-volume metrics of OAR for the same patient scanned in three different positions with respect to breast size. This study demonstrates a novel, yet simple and cost-effective, technique to implement the DIBH technique by utilizing lasers and high definition cameras. This method can be used in clinics without the need to purchase expensive breath-hold equipment to implement the DIBH technique clinically. In our second study, we included the prone deep inspiration breath-hold (PDIBH) method in addition to SFB, SDIBH, and PFB techniques to evaluate the OAR. In this study, the normal tissue complication probability (NTCP) is calculated to determine the probability of damage induced on normal tissues for given radiation doses to OAR. This study is the first to perform a biological evaluation based on radiobiological models for each OAR with specific endpoints in left-sided breast cancer treatment. The NTCP values for each OAR are compared and evaluated in addition to dose-volume histogram-based evaluations for four different techniques. In the third study, the surface dose of the prone and supine treatments was evaluated. Skin dose can be an important factor regarding the outcome and cosmesis for patients. Further, a superficial dose has a large variance that depends on the incident angle relative to the surface. Understanding surface dose dosimetry in the tangential or oblique beam is important to evaluate the skin dose, because a higher dose leads to toxicity and a lower dose can lead to recurrences. This study also evaluates superficial doses in the prone and supine positions with respect to two different grid sizes.

This dissertation establishes a basis for a comprehensive evaluation to help clinicians decide on the best possible treatment techniques for left-sided breast cancer patients. Patients with healthy lungs can be recommended the DIBH technique for a reduced dose to cardiac components, whereas patients with compromised lung function can be recommended the prone technique to spare the OAR. The clinician must be careful of lower skin dose when treating patients using the prone technique, particularly for tumor bed close to the skin surface.

Chapter 1: Background

1.1 What is Cancer?

Cancer is caused when the growth of cells becomes uncontrollable, consequently forming a mass or tumor. Normal and healthy cells divide systematically, stopping reproduction and growth when they touch other cells. On the contrary, cancer cells continue to divide disorderly and constantly grow. Cancer cells, which make up tumors, grow and reproduce rapidly.

1.2 What is Breast Cancer?

Cancer that develops in breast is known as breast cancer. Thus, breast cancer is a malignant tumor arising from the cells in the breast. Breast cancer can originate in different parts of the breast. A breast comprises three main parts, namely, glands, ducts, and connective tissue. The glands produce milk, and ducts are passages that carry milk to the nipple. The connective tissue connects and holds all the parts together. The most common breast cancers are ductal carcinoma, invasive ductal carcinoma, lobular carcinoma, and invasive lobular carcinoma. Breast cancer occurs predominantly in women but could affect men as well.

1.3 Treatment for Breast Cancer

Primary methods to treat breast cancer consist of surgery, adjuvant radiation therapy (RT), and systematic medical therapy, e.g., chemotherapy and endocrine treatment.¹ The most commonly used breast treatment methods are briefly explained below; because the primary research topic is RT, it is explained in more detail.

1.3.1 Surgery

According to the American cancer society, most breast cancer patients undergo some form of surgery as part of their treatment.¹ Two main types of surgery are available to remove breast cancer.

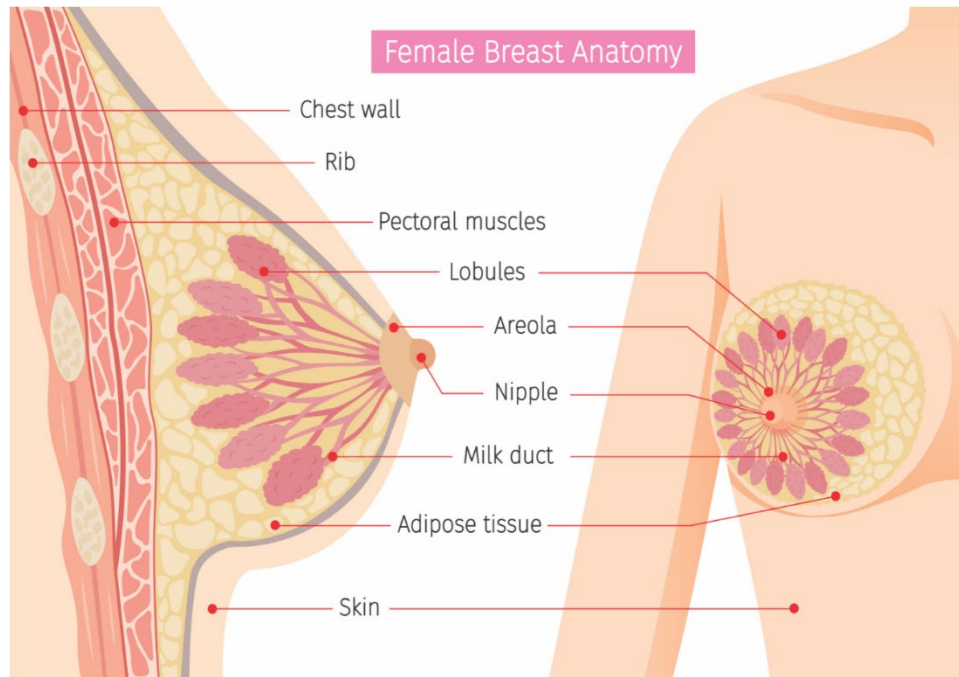


Figure 1.1 Anatomy of normal breast tissue.

1.3.1.1 Breast-Conserving Surgery (Lumpectomy)

This surgery involves the removal of only part of the breast containing the cancer. In this surgery, only tumor and some surrounding breast tissue around the tumor is removed. This method conserves the breast and is thus called breast-conserving surgery (BCS).

1.3.1.2 Mastectomy

This surgery involves the surgical removal of the entire breast and some surrounding tissue. A few women undergo double mastectomy or bilateral mastectomy in which both breasts are removed.

1.3.2 Systematic Medical Therapy

Systemic therapy refers to the treatment of the circulation of pharmaceuticals in the bloodstream after injection or ingestion. This treatment affects all parts of the body because blood circulates across the whole body. Although chemotherapy, hormone therapy, and targeted therapy are systemic medical treatments, each has a distinct underlying mechanism. They can be further categorized into neoadjuvant therapy and adjuvant therapy.

1.3.2.1 Neoadjuvant Therapy

Administering systematic therapies on patients before surgery is known as neoadjuvant therapy, whose objective is to shrink the tumor, thereby making the surgical procedure less extensive. Moreover, neoadjuvant therapy has been found to be as effective as **adjuvant** therapy—which is performed after surgery—in terms of survival, disease progression, and distant recurrence.¹

1.3.2.2 Adjuvant Therapy

Administering systematic therapies after the surgery is known as adjuvant therapy. Systemic therapy is given after surgery to kill undetected tumor cells remaining after the surgery. Cancer that has spread from the breast to the other parts of the body is called metastatic breast cancer. Metastatic breast cancer patients are considered good candidates for adjuvant therapy because of the spread of the disease.¹

1.3.3 Radiation Therapy

RT is one of the most widely used therapies to treat cancer. It uses ionizing radiation to destroy malignant tumors, thus minimizing damage to normal tissues. RT damages the DNA within the cancer cells, thereby destroying the ability of the cells to reproduce. The damaged cancer cells are eliminated naturally by the body. Although normal cells surrounding the tumor are affected by the radiation, they can repair themselves. The objective of RT is to destroy cancerous cells by irradiating the target with radiation beams and simultaneously preserving the surrounding healthy tissue.

About half of all cancer patients undergo radiotherapy as an independent treatment or in combination with other treatment modalities, i.e., surgery and chemotherapy.¹ The concept of treating cancer with ionizing radiation was first used at the end of the 19th century. Since then, technology has undergone major advancements and the current technology can offer increasingly sophisticated treatment methods. To avoid undesirable side effects or radiation-induced cancer, sparing as much normal tissue as possible is important when targeting the PTV. Accordingly, various treatment techniques are being continuously developed to realize the objective of maximizing the dose and radiation damage to the target volume and sparing the healthy tissues surrounding it.

The treatment process using radiation involves three major processes, namely, computed tomography (CT) scan, treatment planning, and RT treatment.

1.3.3.1 Computed Tomography Scan

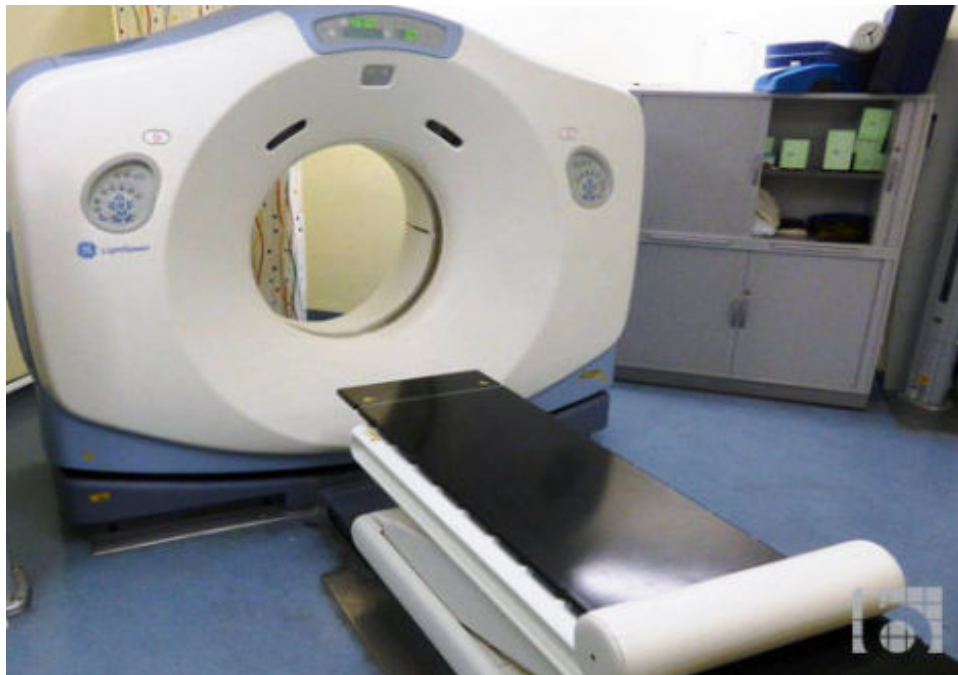


Figure 1.2 Computed tomography scanner.

CT scan is an imaging procedure that uses special x-ray equipment to create images or scan of areas inside the body. A typical CT machine used in RT is shown in Figure 1.2. The X-rays from the CT scanner pass through the body and are detected by detectors after exiting the

body. The CT scan images are used for contouring various normal surrounding tissues, organs at risk (OAR), and target volumes. A CT scan of the treatment region is performed to obtain accurate information on locating the tumor, OAR, and treatment planning. These 3D images are sent to the treatment planning system for performing treatment planning.

1.3.3.2 Treatment Planning System

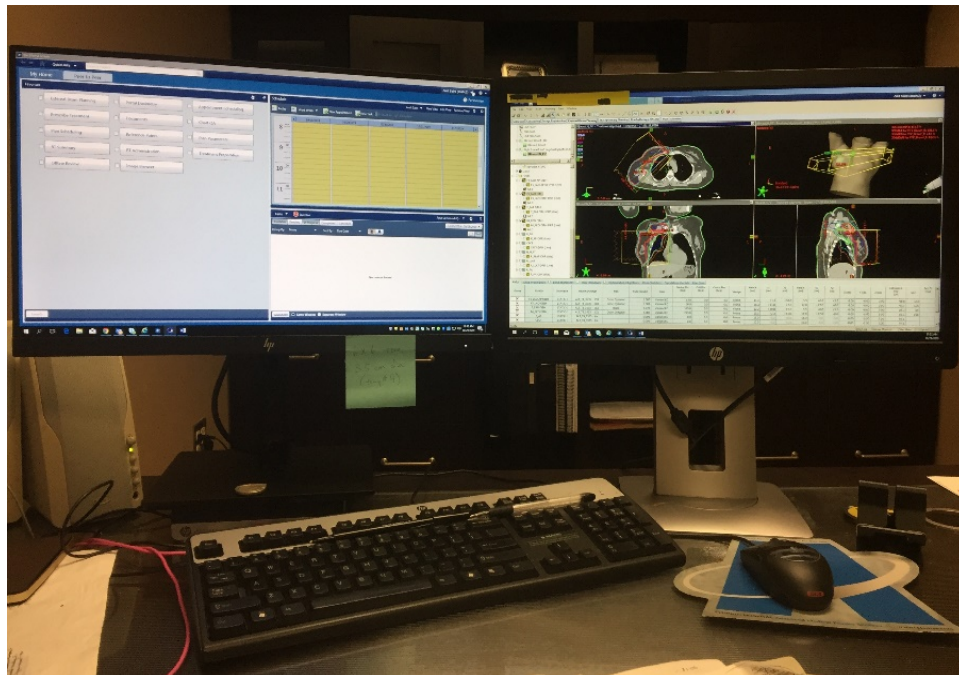


Figure 1.3 Eclipse Treatment planning system unit used for treatment planning.

Treatment planning systems (TPS) are of prime importance in the RT treatment procedure. It is a sophisticated software where all the data of linear accelerators and their characteristics are used to simulate the linear accelerator. The TPS is key to improved dose calculation, distribution, and patient outcomes. The CT scan images are imported into the TPS as the input data in the treatment planning process. Once the image datasets are loaded and the tumors are identified, the CT scan images are used to contour the normal surrounding tissues or OAR. CT images contain quantitative data that are expressed in Hounsfield units (HUs). Electron densities are directly related to the linear attenuation coefficients of tissues in the photon beam

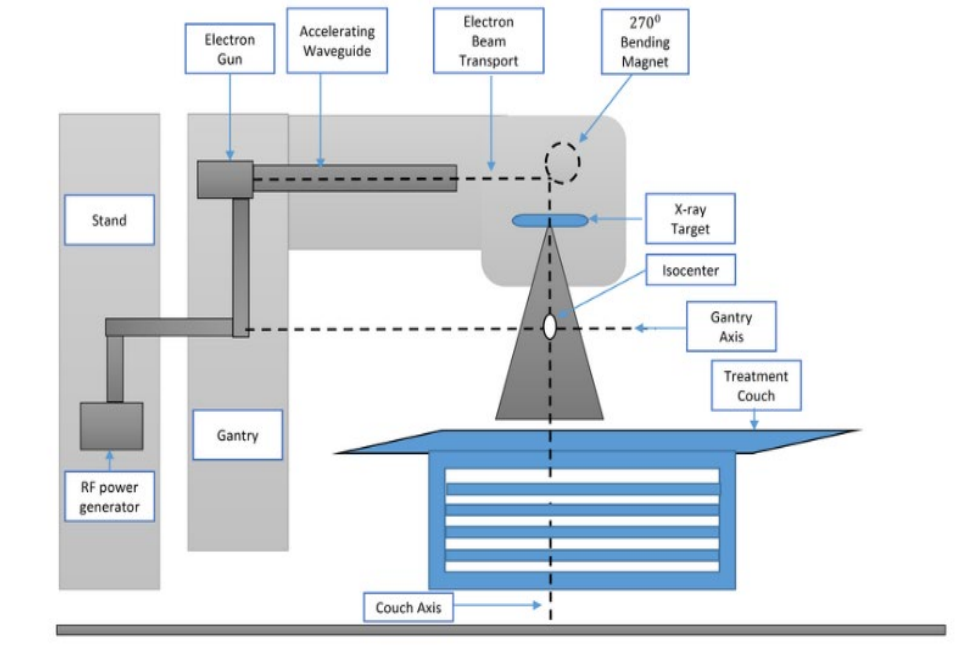
path length.² Thus, it is important to provide the correct relationship between HUs and electron density in the TPS for accurate dose calculation by the algorithm.

The TPS then develops a complex plan for each beamlet to deliver radiation. The software computes the expected dose distribution in the patient's tissue, including variables such as tissue type, energy, and tumor depth. Treatment beam shapes and dose distribution are chosen with the intent to minimize the dose to critical structures and maximize the dose to the target based on published guidelines.³

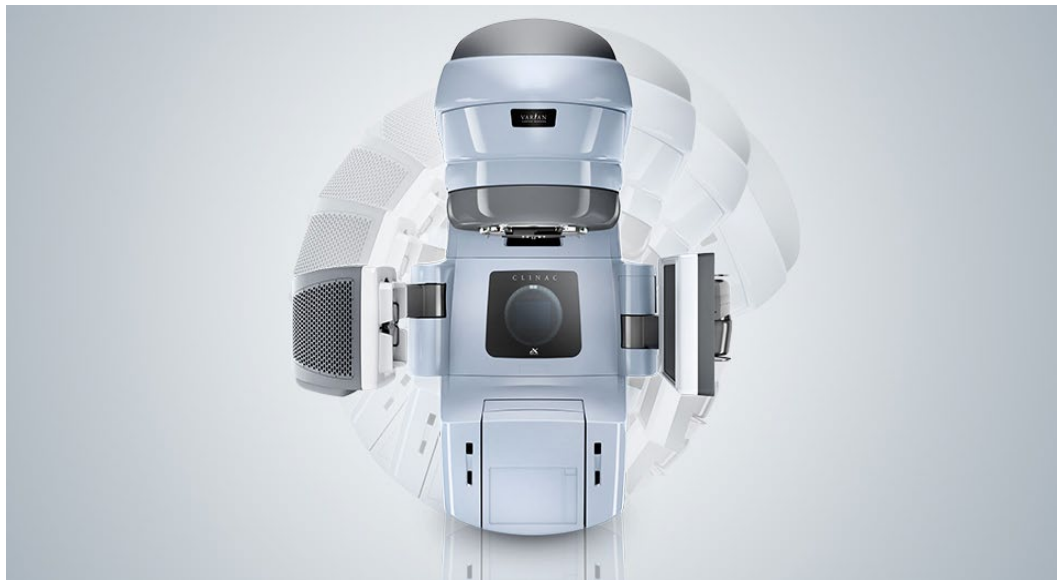
1.3.3.3 Linear Accelerator

The medical linear accelerator (LINAC) is the most used device for external beam RT treatments for cancer patients. It delivers high-energy photons or electrons to the tumor volume of the patient undergoing RT. These treatments are designed to damage the cancer cells while sparing the healthy tissue around them. An electron gun produces electrons that are injected into the waveguide. The LINAC employs microwave technology to accelerate electrons in a part of the accelerator called the waveguide; subsequently, these electrons are collided with a heavy metal target to produce high-energy x-rays, as shown in Figure 1.4a (schematic) and 1.4b (actual image).

The patient lies on a moveable treatment couch that can be moved in multiple directions; i.e., right, left, in, out, up, down; some couches can perform pitch and roll as well. The beam exits the accelerator from the gantry. The gantry of the accelerator can be rotated a full 360 degrees around the patient. The beam is usually shaped by a multi-leaf collimator (MLC) that is incorporated into the head of the gantry. A modern-day LINAC usually consists of 120 MLCs, with the MLC width varying from 0.25 cm to 1 cm. These high-energy photons are customized using MLCs to conform to the shape of the patient's tumor. Specifically, the MLCs aid the irradiation of the patient by shaping the tumor, with many different gantry angles being used by rotating the gantry and the couch to maximize the dose to the target while sparing the surrounding OAR. The major difference between 3D conformal therapy and intensity-modulated radiation therapy (IMRT)



(a)



(b)

Figure 1.4 a) Schematic and b) Actual image of medical linear accelerator.

or volumetric arc therapy (VMAT) is that in 3D conformal therapy, the MLC and collimator helps to form the shape of the target, whereas in IMRT and VMAT the software moves the MLCs to modulate the beam to conform to the shape of the target.

1.4 Radiation Therapy Treatment Techniques

As patients now have a prolonged life expectancy, they could be at higher risk of developing long-term complications because of radiation of OARs. Thus, different techniques are being used to study the possibility of reducing dose to OARs without compromising the coverage of target volume. As mentioned earlier, the current most common treatment techniques for breast cancer include (but not limited to) the use of supine 3D Tangent technique, IMRT, and VMAT. The 3D technique uses the MLC and the collimators to shape the beam to conform to the target and spare the OAR in three dimensions. It helps maximize the dose to the target and spare the healthy tissues. In addition, beam modifying devices such as wedges are included to shape the dose around the target volume. The supine free-breathing (SFB) 3D tangent technique is predominantly used over the others and has become a standard practice because of its easy, reproducible, and practical set up. Thus, free-breathing in supine position is the most used treatment technique for breast radiation treatment. A typical supine set up with the heart and left lung, and left breast in a CT slice is shown in Figure 1.5(a). The arrows in Figure 1.5(a) represent the volume of heart and left lung inside the treatment field edges, which is radiated. Although technology has advanced in the last decade, the dose delivered in this position to the heart and the left lung remains significant.

IMRT is a sophisticated method of three-dimensional (3D) conformal radiation therapy (CRT). IMRT uses the MLC to modulate the fluences and thus optimizes the delivery of irradiation to irregularly shaped tumor volumes. The IMRT technique thus has the capability to deliver radiation treatment to concave volumes. This helps administer the maximum dose to target volumes while sparing critical organs more than 3D CRT. VMAT is the latest technique to produce IMRT-like dose distributions. IMRT uses static gantry angles while the MLCs move continuously

to modulate the intensity of the beam. By contrast, in VMAT, the gantry also rotates at varying speeds and dose rates to deliver doses in single or multiple rotations of the gantry. Planning studies comparing both techniques indicate that a better conformity and dose homogeneity, shorter treatment time, fewer monitor units for treatment delivery, and better normal tissue sparing are achieved with VMAT.

Many other 3D treatment techniques have been evaluated to reduce the dose to cardiac components, such as the supine deep inspiration breath-hold (SDIBH) technique,^{4,5} prone free-breathing (PFB) technique,⁶⁻¹⁰ and the prone deep inspiration breast hold (PDIBH) technique^{11,12}; however, a consensus has not been reached over the superiority of a particular treatment technique.^{4,13-18} Few studies have compared the SFB, SDIBH, and PFB techniques to evaluate doses to OAR.^{10,19} In addition, newer techniques such as IMRT and VMAT have been used to reduce dose to the OAR. Although modern techniques such as IMRT decrease the volume of the heart and lung that receives high doses, a larger volume may receive lower doses owing to the low dose spread associated with these techniques.^{20,21}

Irradiation in the prone position (Figure 5(b)) is another method to minimize the doses to heart and lungs.^{6,8,10,12,13,19,22,23} Studies have shown a reduction of irradiated lung volume in all patients, and a few studies have shown a higher reduction of dose to the heart volume in the prone position compared with the supine position.^{8,10,13,22} Further, the deep inspiration breath-hold (DIBH) technique is used in combination with any of the above techniques to reduce the dose to the heart.^{10,11,22,24-27} In DIBH, the patient takes a deep breath and holds the breath during radiation. The DIBH has been proven to reduce cardiopulmonary doses in breast RT.^{5,10,19,22,28}

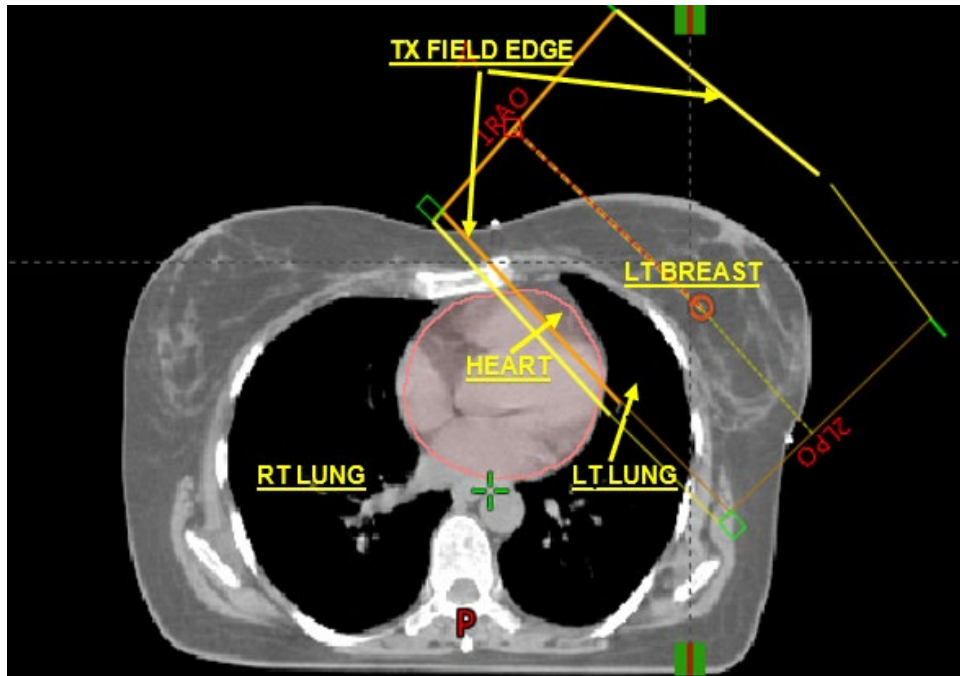
In our study, we compare only the 3D techniques because they are predominantly used for breast cancer treatment; we did not compare the treatments based on IMRT or VMAT technique. Furthermore, 3D CRT, in conjunction with DIBH and prone techniques, is an alternative

to free breathing-based 3D CRT. In this section, two techniques are demonstrated in addition to the supine technique, i.e., the prone and DIBH techniques used in this dissertation are explained briefly.

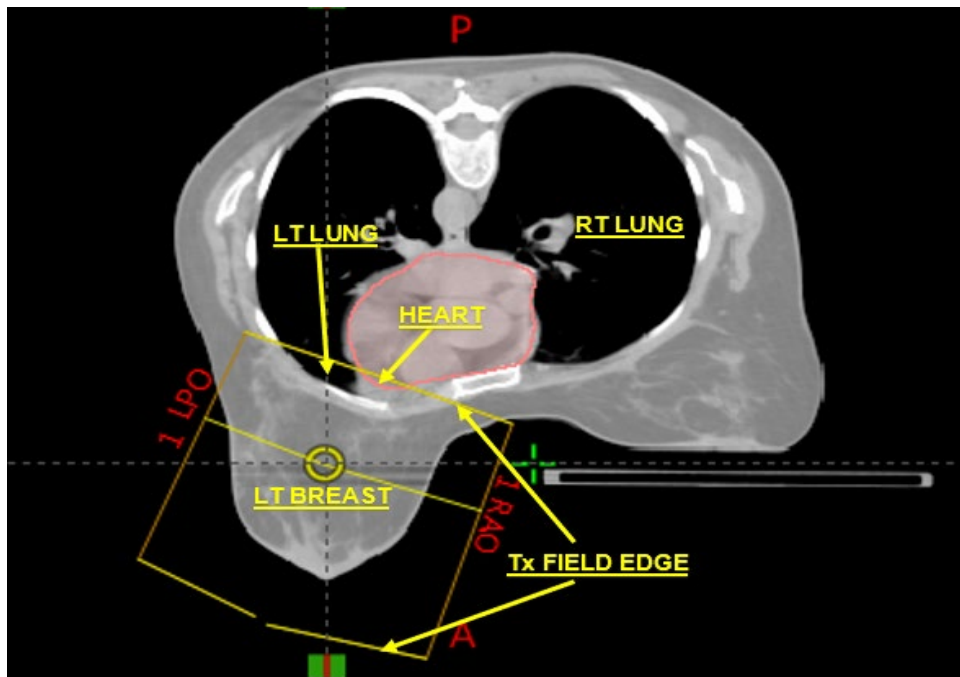
1.4.1 Prone Technique

In the prone technique, the patient is simulated and treated, lying on the abdomen to pull the breast away from the heart.^{10,18,22} This changed shape, motion, and position of the breast and OAR present in the treatment field raises unique concerns specific to prone breast irradiation. The hanging down of the breast from the aperture of the positioning device results in a different dose distribution relative to that in the supine position. The prone technique has become feasible and reproducible with the beginning of CT scan-based treatment planning. This prone technique has been developed to improve the dose distribution and homogeneity within the breast. It also helps to reduce the volume of normal tissues irradiated during whole breast treatment. The dosimetry of breast irradiation is improved by optimizing the shape of the breast, resulting in a reduction in the magnitude of high-dose regions and isodose gradients in the breast PTV. Reduction in the scale of high dose regions in the breast tissues can be achieved by optimization of the MLCs to conform to the shape of the breast. Improved dose homogeneity and reduction of overdosage within the PTV in the prone technique have been associated with better cosmetic outcomes.

Prone breast irradiation has generally been recommended for women with large pendulous breasts to decrease acute and late toxicities. In addition, this technique has been proven to be advantageous for most patients because it consistently reduces—if not eliminates—the inclusion of the heart and lungs within the field. The latest technological developments in linear accelerators and the increased accuracy of treatment planning algorithms, coupled with better imaging and verification reproducibility, have made an accelerated fraction scheme in which 42.66 Gy are delivered in 16 fractions is possible.^{6,29,30}



(a)



(b)

Figure 1.5 Prone and supine CT images showing the heart, lungs, and left breast contours. Yellow arrows represent the volume of organs in the radiation treatment field in a) Supine technique and b) Prone technique. Please note that the prone technique has lower heart and lung volumes in the treatment field compared with those of the supine technique.

1.4.2 Deep Inspiration Breath Hold (DIBH) Technique

The DIBH technique can be used to decrease heart, LV, and LAD doses during left-sided breast cancer radiation treatment. During both CT simulation and RT treatment, the patient takes a deep breath and holds it for a period, during which radiation can be administered. The technique is based upon the theory that during inspiration the expansion of the lungs and the flattening of the diaphragm pull the heart away from the chest wall. Thus, during inspiration, the heart and the target volume are separated, and a reduction in lung density is seen. This allows for a decrease in the volume of heart in the radiation beam, which reduces dose to the heart, as shown in Figure 1.6.³¹ In addition, a fused CT image of SFB with the SDIBH technique for the same patient, along with the heart position in both scans and radiation field edge, is shown in Figure 1.6. Please note how heart volume is pushed away from the chest wall in the SDIBH technique, thus sparing heart (Figure 1.6). The DIBH can be alternatively used for prone breast irradiation; the two techniques can be (and have been) used in conjunction with the PDIBH technique as well.²² The fused CT image of PFB with the PDIBH technique for the same patient, along with the heart position in both scans and radiation field edge, is shown in Figure 1.7; similar observation is made for PFB and PDIBH scans, which indicate that the heart is pushed away from the chest wall.

Both the initial imaging and the treatment delivery are performed during inhale breath-hold, which may be voluntary or involuntary. The DIBH methods, which are based on voluntary breath-hold and rely on external surrogates for monitoring, could have the disadvantage of variability in patient immobilization, which may not be quantified well during the imaging procedure.³²⁻³⁴ Involuntary breath-hold, on the other hand, uses an active breathing control (ABC) device, which holds the patient's lung at a specified and reproducible volume.^{35,36} A drawback of all the DIBH methods is that the patients cannot always tolerate breath-hold.

In this study, we propose an in-house technique to verify voluntary breath-hold without using expensive technology for monitoring breath-hold using RPM system or involuntary breath-hold based device to consistently achieve breath-hold. In our clinic, we used room lasers, which

are used for patient set up, along with high-definition cameras to implement the DIBH technique for the treatment.

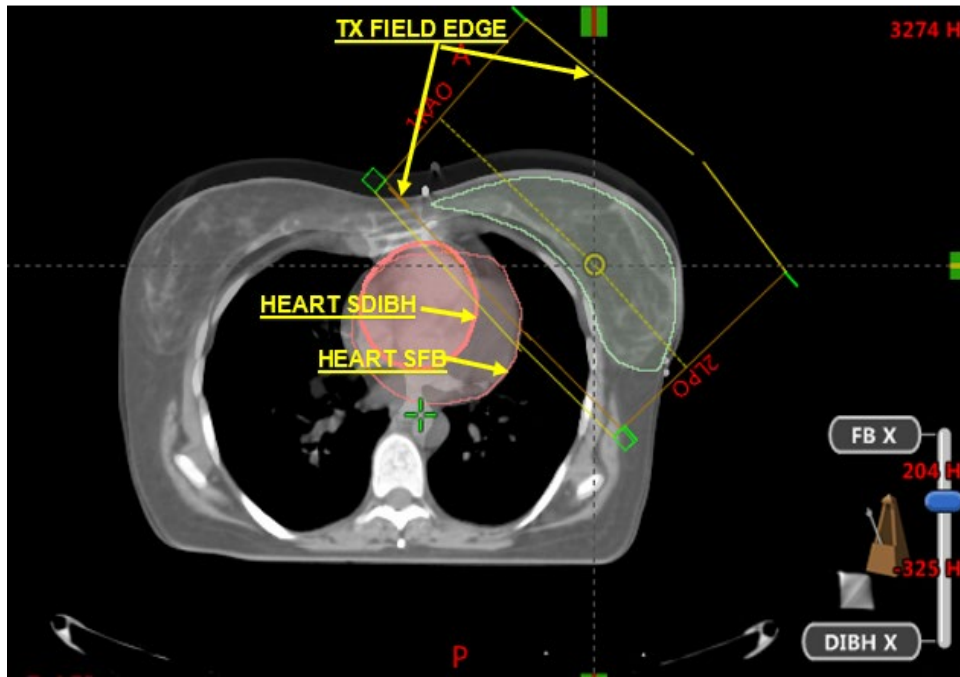


Figure 1.6 Fused SFB and SDIBH CT scan images of the same patient. Please note the position of the heart in SFB and SDIBH scans with respect to the radiation field edge.

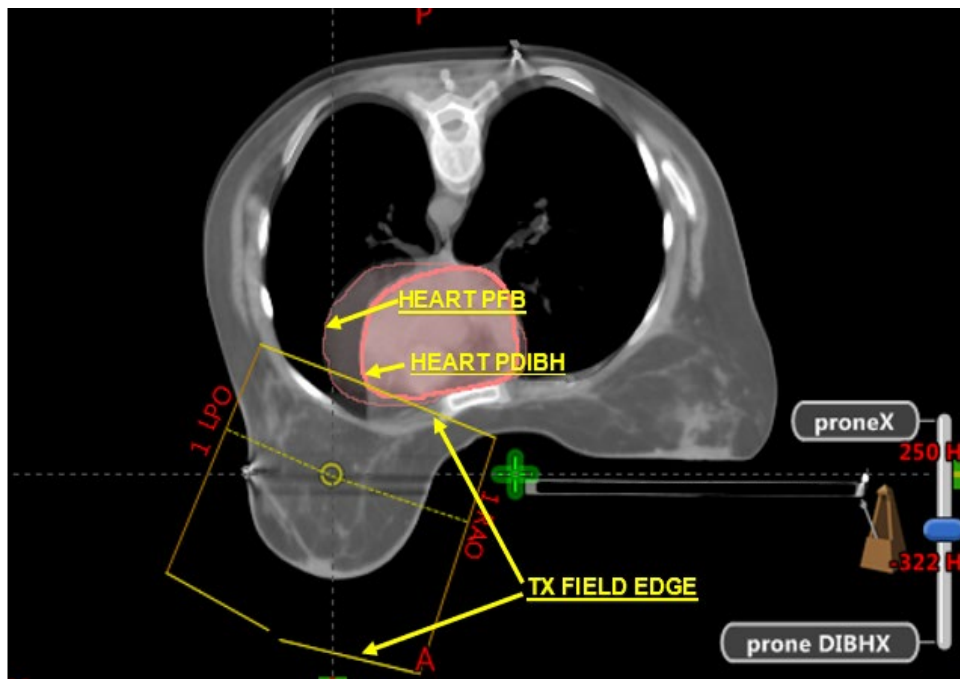


Figure 1.7 Fused CT scan images of the PFB and PDIBH techniques of the same patient. Please note the position of the heart in PFB and PDIBH scans with respect to the radiation field edge.

1.5 Design of Dissertation

We used the European format of introduction, discussion, and conclusion based on the three studies attached in the appendix section for this dissertation. Owing to the similarity of the topics between studies, they could overlap.

Chapter 2: Introduction¹

Breast cancer (BC) is a major global health problem among women, with about 1.7 million new cases diagnosed annually.³⁷ Breast cancer mortality rate is the second highest after lung cancer for women in the United States.³⁸ Approximately 1 in 8 women is diagnosed with invasive breast cancer in their lifetime and 1 in 39 women die of breast cancer.³⁹ Adjuvant radiotherapy has been used for the treatment of breast cancer since the 1930s. The first randomized trials for adjuvant RT were reported by the end of 1940s. Several randomized trials conducted since then have indicated clinically significant reduction of local recurrence and no adverse effect on the overall survival. Combined modality, breast conserving surgery, and chemotherapy, followed by whole breast RT, is currently becoming a standard in the treatment of early-stage breast cancer.⁴⁰

Many women with early stage breast cancer undergo radiation treatment as part of their cancer management.¹⁰ More than 20 years of follow-up data confirm that, after breast conservative surgery, higher risk of local recurrence is present. However, women undergoing breast conservative surgery followed by radiation treatment have the same long-term survival similar to that in mastectomy.⁴¹ It has been shown that RT reduces the risk of breast cancer local recurrence in a large number of cases, which has led to an increased overall survival rate.⁴² A large meta-analysis by early breast cancer trials found that patients treated without RT after breast-conserving surgery have 26% chance of local recurrence at five years follow up, compared with 7% in patients, who were administered RT.⁴² The analysis further indicated that, at 15 years

¹ This chapter is partially reproduced from work published in a peer reviewed journal. The author of this dissertation is the first author of the published work. See Appendix C,D,F,G for the published studies and permissions.

after diagnosis, an absolute risk reduction of 5.4% exists in breast cancer mortality with RT after breast-conserving therapy, compared with no RT after breast conserving therapy⁴².

Although RT to breast is beneficial, it is known to increase both the radiation toxicity and secondary breast cancer.⁴³ Specific techniques and treatment for left-sided breast cancer lead to higher cardiac and pulmonary toxicity, which have been shown to be related to increased risk of heart and lung diseases.^{40,42-45} It has been considered that the primary reason for higher complication and mortality in left-sided breast cancer is the proximity of the heart to the radiation beams, which can result in the delivery of high doses to the heart. This can lead to higher risk of cardiac complications to the patient undergoing RT. During regular breathing, the heart moves in and out of the radiation beams, often in an irregular and unpredictable pattern. It is difficult to predict the correct dose to the heart owing to uncertainties in breathing motion and its correlation to the position of the heart in the treatment field. Thus, it can be challenging to predict the accurate dose-volume received by the cardiac component in the free breathing technique.

Darby et al.⁴⁶ have shown that an increase of 1 Gy in mean dose to the heart results in a 7.4% relative increase of major coronary events; however Taylor et al.⁴⁵ have indicated a lower risk based on a recent dosimetry study. This study further demonstrated that exposure of heart to the ionizing radiation during RT for breast cancer significantly increases the rate of ischemic heart disease. Another research compared a group of irradiated patients and non-irradiated patients, and showed a significantly higher non-breast cancer-related mortality, primarily for heart disease (R.R, 1.27) and lung cancer (R.R, 1.78).⁴² A retrospective study compared the ratio of patients receiving radiation to left-sided and right-sided breast cancers and died of heart disease. The cardiac mortality ratio was 1.21, 1.08, and 0.99 for patients diagnosed between 1973–1982, 1983–1992, and 1993–2001, respectively.⁴³ Thus, the advantage of RT on survival rate was overshadowed by an increased risk of non-breast cancer-related deaths. Several investigations showed that the leading cause for these deaths was heart disease.^{43,46-48} However, these results are based on data using older treatment modalities and radiation techniques. RT techniques and

equipment have significantly improved since these reports were published. With the advent of modern technology, radiation exposure to the heart and lung is currently lower than that in the past. In spite of this improvement, a few studies have shown that patients receiving RT treatment for left-sided breast cancer are at a higher risk of long-term cardiac morbidity after the treatment.⁴⁹⁻⁵² These results were further correlated to the heart volume exposed to radiation during treatment.^{53,54}

A few studies suggest that arteries are particularly sensitive to radiation, and the left anterior descending artery (LAD) is one of the typical sites of origin of ischemic heart disease.^{51,52} It is further recommended that minimizing the absorbed dose to heart and LAD must be a priority, until evidence is found for a threshold absorbed dose below which no additional risk of cardiac morbidity and cardiac mortality is present.⁵⁵ In addition to cardiac complication, an increase in lung complications with increased absorbed lung dose is present.^{43,56} The lung cancer mortality for ipsilateral lung cancer was higher than that for contralateral lung cancer for the women who developed lung cancer after undergoing breast RT.⁴³ The increased absorbed lung dose further increases the incidences of radiation pneumonitis.⁵⁶

In left-sided breast cancer patients, parts of the heart, left ventricle (LV), LAD, and the left lung are usually inside the treatment field, and are considered as OAR. Various techniques such as DIBH and prone position have been used since then to spare the OAR without compromising the breast planning target volume (PTV) coverage. A few studies have compared the SFB and SDIBH or SFB and PFB techniques; however, no study has compared the dose for heart, LV, LAD, and left lung with respect to breast PTV in three different positions on the same patient. In our study, instead of commercially available gating systems, we developed an inhouse technique to use a high-definition camera to check the position of the patient during treatment with respect to lasers, as explained in section 2A. It is a simple, quick, and cost-effective technique that passes on the benefits of the DIBH techniques to the patients and eliminated the need for expensive devices to implement DIBH in clinics.

Recently, radiobiological evaluation tools have become available in many treatment planning systems. Normal tissue complication probability (NTCP) tool could be used to biologically evaluate the plan along with dose-volume histogram (DVH)-based evaluation for OAR.^{5,56,57} Biological parameters, when applied to these biological models, help predict the biological effects on OAR, and are believed to be more directly correlated with treatment outcome than the DVH based parameters.^{58,59} Our second study additionally involved biological evaluation of the OAR in four treatment positions in addition to commonly used dosimetric evaluation. Our study is the first to perform a biologic evaluation on OAR of left-sided breast cancer patients and calculate the NTCP for each treatment position of every patient. The radiobiological model and radiobiologic evaluation are further explained in section 2.3.

Skin dose in breast cancer radiation treatment is another important factor regarding not only the outcomes but also the cosmesis. The skin toxicity is often considered a dose-limiting factor.^{60,61} Radiation dermatitis has consistently been a concern for high dose treatments for radiation oncologists.^{62,63} Skin dose toxicity influences the tolerance of treatment by patients and the cosmetic outcomes of breast cancer patients.⁶⁴⁻⁶⁸ However, a recent study by Katz et al.⁶⁹ provided a case report of inadequate skin dose that leads to skin recurrence in the prone treatment technique. Therefore, evaluating the dose delivered to the skin to avoid recurrences, and (particularly) underdosing tumors near the surface in breast RT, are of significant interest.

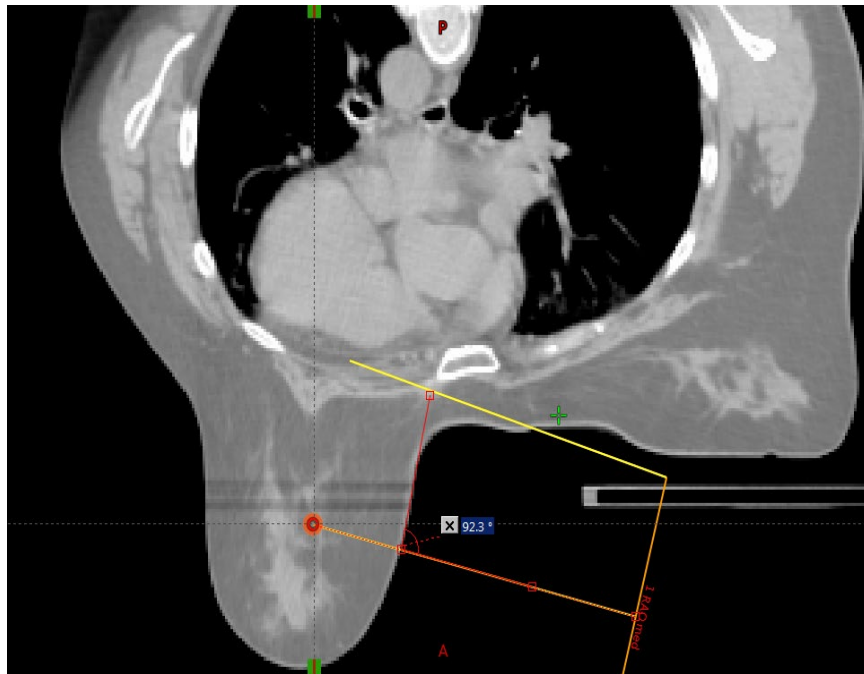
Generally, the surface/skin dose depends on the incident beam angle, field size, source to skin distance, beam energy, and beam modifying devices. Typical prone and supine set ups with gantry angle relative to the skin surface are shown in Figure 2.1. In our third study, we hypothesized that a beam incidence angle close to perpendicular in the one breast technique could result in lower superficial dose compared with the supine position, where the breast is treated at a tangential angle of 45–55°. Such a steep angle produces an increased surface dose based on the obliquity factor defined by Gerbi et al.⁷⁰ Das et al.⁷¹ showed that a smaller grid size can produce a more accurate dose calculation in the buildup region. The smallest grid size

available in the Eclipse version 13.7 is 1 mm; thus, we chose a grid size of 1 mm and clinically used 2.5 mm to evaluate the dose in the superficial region. Thus, understanding the skin dose for each treatment technique helps radiation oncologists in choosing the appropriate treatment plan to elicit positive outcomes.

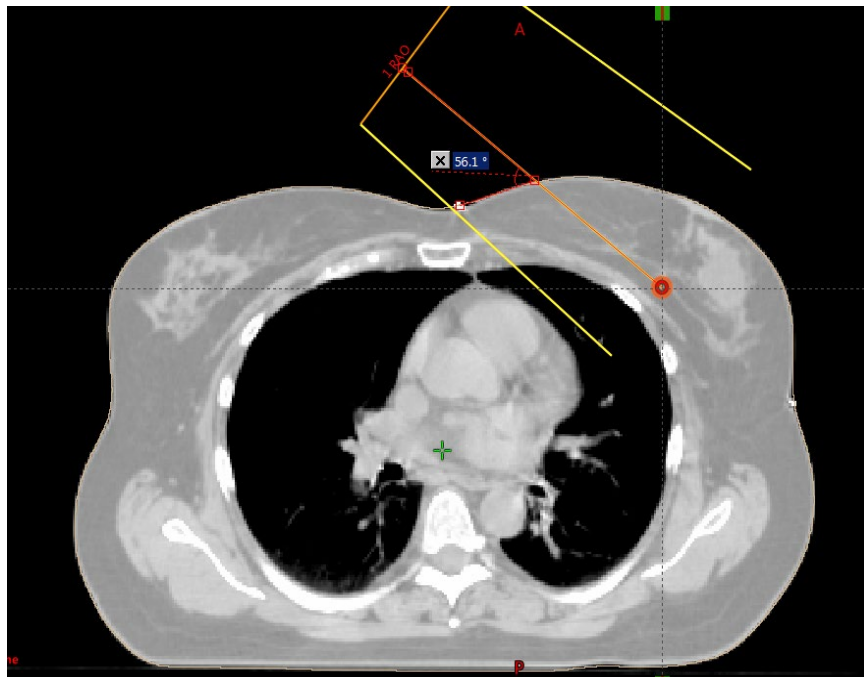
In this study, organ contouring, treatment planning, and dosimetric evaluation were performed on more than 100 patients, and more than 300 treatment plans were created and evaluated. Biological evaluation was performed on 100 treatment plans. For consistency, contouring on all CT scans was performed by a radiation oncologist in accordance with the national guidelines, and all the treatment plans were created by a physicist. Treatment planning, dosimetry, laser-based DIBH, and biological evaluation procedures are explained briefly in the next section.

2.1 Treatment Planning and Dosimetry

After the CT scans were obtained, the images were transferred to the treatment planning system. At our institute, for the first study, we used the Eclipse planning system V11 (Varian Medical System version 11). Furthermore, the Anisotropic Analytical Algorithm (AAA Version 11.0.31) was used for calculations, and the grid size was set to 2.5 mm for the first and second studies. For the second and third studies the calculations were performed in the Eclipse (Varian Medical Systems Inc., Version 13.7) TPS using the Anisotropic Analytical Algorithm (AAA; Version 13.7) for both 1 mm and 2.5 mm calculation grid sizes. Our breast radiation oncologist contoured the breast PTV, heart, LV, LAD, and contralateral breast of each patient based on the RTOG-1304²⁴ guidelines and RTOG Breast Cancer Atlas for planning (<https://www.rtog.org/CoreLab/ContouringAtlases/BreastCancerAtlas.aspx>). According to the atlas, the breast was defined as an all apparent CT glandular breast tissue, considering the RTOG consensus definition of anatomical borders. The cranial border was defined as the second rib insertion, the caudal border was defined as the loss of CT apparent breast tissue, and the anterior



(a)



(b)

Figure 2.1 Typical beam placement for (a) Prone and (b) Supine set up for *left breast*. Please note the gantry angle with respect to the skin surface.

boundary was defined as the skin. The posterior boundary was the anterior aspect of the pectoralis muscles. The medial border was the sternal-rib junction and the lateral border was at the mid-axillary line.

The LAD was defined as the vessel that descends anteriolaterally from the anterior interventricular groove to the apex of the heart.⁷² Cardiac contouring started superior at the level of great vessel insertion into the heart and extended inferior to the apex of the heart. The contours were drawn by a single physician. The lungs were contoured using an automatic segmentation tool available in Eclipse TPS, and the lung contours were manually edited by the physician as needed. The breast PTVs were cropped by 5 mm from the skin surface for planning because the dosimetry in the buildup region is not well defined.⁷¹ The contralateral breast was not cropped from the skin surface.

For treatment planning, heterogeneity correction was turned on for all the calculations. Opposing tangential beams with Field in field techniques (FIF) were used for planning. All the treatment plans were calculated only using a 6 MV beam, and wedges were not used in any plan. Treatments for all patients were planned using the hypo-fractionated fractionation scheme defined by Whelan et al.⁷³ The doses were prescribed as a total dose of 42.56 Gy in 16 fractions. The plan was normalized to the isocenter placed in the PTV. As per the RTOG protocol, a margin of 7 mm was given to PTV to form the field shapes using MLC.⁷⁴ The most optimal plan was made for each patient on each scan to compare the plans. The guideline was to have a minimum of 95% of PTV receiving 100% of the prescribed dose, with no more than 5% of the PTV volume receiving more than 110% of the dose, and simultaneously achieve maximum sparing of the OAR. Further, DVHs were used to analyze the PTV, dose homogeneity, and doses to OAR. For OAR, the dose parameters were used based on the evaluated organ. For heart and left ventricle mean dose, V2.5, V5, V10, V20, and V30 were recorded; for LAD mean dose, V2.5, V5, V10, and V20 were recorded; for lung mean dose, V10, V20, and V30 were recorded.

2.2 Laser-Based DIBH

For DIBH, our institution developed a technique using lasers to mark the position of patients in the FB and DIBH positions. Before scanning the patient, the breast tissue was marked with radio-opaque wire by a radiation oncologist. The patients were first scanned in the FB position. Patients were first marked in the medial and lateral direction with respect to lasers in the CT room while breathing freely; they were then coached to take a deep breath and hold it i.e., DIBH. New positions on the patient's skin in the medial and lateral positions were marked again. Now the patient has two marks, one representing the FB position and the second the DIBH position with respect to lasers. The patients were asked to repeat DIBH, and a CT sim therapist verified that they are consistently able to achieve the same position marked on their skin with respect to lasers. Only the patients who followed the instructions, and those who held the breath for 20 s were considered. Further, audio coaching was utilized to guide the patients for the second scan to realize DIBH and release the breath-hold after scanning. High-definition cameras were installed in the treatment room to clearly see the DIBH marks from outside the room. The high-definition cameras were used to check the position of the patients during treatment with respect to lasers to ensure the patient remains in the DIBH position. Table 2.1 represents the DIBH simulation sheet created during CT simulation to record the shifts with respect to FB laser marks. Please see the step by step procedure in the appendix A.

Table 2.1 Table for recording DIBH measurements.

Max breath-hold achieved (s)	
Anterior FB marks and DIBH marks distance (mm)	
Lateral FB marks and DIBH marks distance (mm)	

2.3 Radiobiological Modelling Biological Evaluation

Clinical radiobiology denotes the relationship between a delivered radiation dose and the resulting biological effect on the tumor, normal tissues, and OAR. The goal of RT is to attain a high local tumor control probability (TCP) at a low risk of normal tissue complication probability (NTCP). NTCP models that are currently used in the TPS provide a simpler interpretation of clinical radiobiology. Radiobiological evaluation is a complement to evaluation treatment plans using dose distribution and the DVHs.^{56,57} The estimated probabilities of the clinical outcome are evaluated in terms of NTCP for the OAR. These biological indices are used to compare rival dose distributions, as well as fractionation schedules.

The main objective of RT is to deliver a sufficiently high dose to the tumor, so that all the tumor cells are killed, along with minimal radiation-induced damage to the surrounding normal tissue. In physical dose-based evaluations, the dose distribution and the dosimetric endpoints are based on a clinician's individual clinical experience and published literature to define the dose-volume (DV) constraints. The physical quantities, such as DV, are conventionally used for plan comparison and plan evaluation to find the coverage of target and radiation-induced complications on the patient; it is generally evaluated using DVHs. In biological planning, the biological endpoints are directly inputted and evaluate the actual effect of physical dose distribution on the tissues using biological modeling. Furthermore, it is known that biologically related parameters such as NTCP have a more direct correlation with radiation-induced complications than the DV based parameters.^{58,59} Thus, they help avoid variability and a dependence on the clinician's knowledge of dose-tissue response on radiation-related OAR complications.

This study calculates the NTCP of radiotherapy plans for 3D conformal RT of left-sided breast cancer patients undergoing treatment. Biological modeling basically utilizes the DVH of a given plan, biological parameters of the tumor type, and normal critical tissues to calculate the normal tissue complication probability. In this study, two NTCP models—namely, NTCP-Poisson LQ and NTCP-LKB, which are available in Eclipse TPS—were used with the default parameters

listed in Table 3. The user can select a specific endpoint for the NTCP calculations.⁷⁵⁻⁷⁷ The treatment plans were exported to the Eclipse biological evaluation module and the NTCP was calculated from DVH. The NTCP Poisson LQ function was used to calculate the NTCP of heart, LV, and LAD with cardiac mortality as the endpoint.⁵⁷ Further, the NTCP-LKB model of the lung with all the available endpoints in Eclipse TPS was used to calculate the lung NTCP.⁷⁸⁻⁸⁰ The NTCP input factor and the associated endpoints for each OAR for the NTCP calculations are listed in Table 2. Detailed mathematical equations of both the models are presented in appendix E of this dissertation. The NTCP-LKB is based on the probit function,⁷⁶ whereas the NTCP-Poisson LQ model is based on cell survival models, Poisson statistics, and the relative seriality model⁷⁵.

A cell survival curve describes the relationship between the absorbed dose and the fraction of cells that survive. The shape of the dose response curve indicates the tissue-specific α/β -ratio. Normal tissue cells have α/β -ratios of approximately three, while the cells of late-responding tissues have lower α/β -ratios. The alpha, beta, D50, m, and n values used for each evaluation are shown in appendix B.

2.4 Statistical Analysis

The mean dose, V2.5, V5, V10, V20, and V30 of different scans were compared for statistical analysis. In addition, the skin surface dose of the prone and supine techniques—from the surface to a depth of 5 mm—for both grid sizes was evaluated for statistical analysis. The dosimetry parameters of the heart, LV, LAD, left lung, and skin dose of each scan were compared using a Wilcoxon signed-rank test for the related sample using the SPSS statistical software (version 23.0 and 25.0), because the data had a non-normal distribution. The data were considered to be statistically significant at P-value ≤ 0.05 .

Table 2.2 NTCP parameters for models used to evaluate OAR with specific end stage.

Structure	Organ Model	Model	End point/Stage	D50 (Gy)	Y	Alpha/Beta	Seriality	Parameter N	Parameter M	Reference
Heart	Heart	NTCP Poisson-LQ	Mortality	52.4	1.3	3.0	1	NA	NA	Gagliardi et al., Br J Radiol. 1996; 69:839-846 ⁵⁷
LV	Heart	NTCP Poisson-LQ	Mortality	52.4	1.3	3.0	1	NA	NA	Gagliardi et al., Br J Radiol. 1996; 69:839-846 ⁵⁷
LAD	Heart	NTCP Poisson-LQ	Mortality	52.4	1.3	3.0	1	NA	NA	Gagliardi et al., Br J Radiol. 1996; 69:839-846 ⁵⁷
Lung	Lung	NTCP Lyman	Pneumonitis (1), Grade >= 2	30.5	NA	3.0	NA	1	0.3	Kwa et al., <i>Radiother Oncol</i> 1998;48:61-69 ⁷⁹
Lung	Lung	NTCP Lyman	Pneumonitis (2), Grade >= 2	30.8	NA	3.0	NA	0.99	0.37	Seppenwoolde et al., Int J rad Onc bio, Phys, 2003;55:724-735 ⁷⁸
Lung	Lung	NTCP Lyman	Symptomatic or Radiographic pneumonitis (<= 6 months)	21.9	NA	3.0	NA	0.37	0.8	Moiseenko et al., <i>Radiother Oncol</i> 2003;67:265-274 ⁸⁰
Lung	Lung	NTCP Lyman	Symptomatic Pneumonitis (<= 6 months)	21.0	NA	3.0	NA	1.02	0.26	Moiseenko et al., <i>Radiother Oncol</i> 2003;67:265-274 ⁸⁰
Lung	Lung	NTCP Lyman	Symptomatic or Radiographic Fibrosis (> 6 months)	28.8	NA	3.0	NA	0.34	0.5	Moiseenko et al., <i>Radiother Oncol</i> 2003;67:265-274 ⁸⁰
Lung	Lung	NTCP Lyman	Symptomatic Fibrosis (> 6 months)	25.0	NA	3.0	NA	0.15	0.85	Moiseenko et al., <i>Radiother Oncol</i> 2003;67:265-274 ⁸⁰

Chapter 3: Objective of the Dissertation

The purpose of this research is to compare the dose to OARs and the skin dose for left-sided breast RT with comparable planning target volume coverage. This study primarily uses four techniques to compare the dose to OAR: SFB, SDIBH, PFB, and PDIBH techniques. In addition, it compares the skin dose of the SFB and PFB techniques, from the surface to a 5 mm depth. The objective of this study is to determine the best treatment technique to spare the heart without compromising the PTV coverage and underdosing skin. This study additionally provides guidelines to implement DIBH in clinics that do not have the software, state-of-the-art technology (such as real-time position management system), surface mapping, and devices for involuntary breath holds.

This dissertation comprises three studies: first, the three treatment positions SFB, SDIBH, and PFB were compared for the same patient. In this study the dosimetric evaluation of OAR is recorded and a statistical comparison was performed. In addition, an evaluation was performed based on the small or large breast volume of the patient, i.e., left breast volume $< 750 \text{ cm}^3$ and $\geq 750 \text{ cm}^3$. Second, the four treatment positions SFB, SDIBH, PFB, and PDIBH were dosimetrically compared and evaluated for statistical significance. In addition, a biological evaluation of the OAR was performed for all the four techniques. These studies provide clinicians with both DVH based dosimetric comparison and various biological model based biological evaluations of OAR in all four techniques. The radiobiological evaluation models with cardiac mortality as the endpoints were used to evaluate the NTCP for heart, LV, and LAD. For the lungs, six possible endpoints available in the Eclipse TPS were used for radiobiological evaluation. Thus, the second study additionally provides optimum guidelines based on the NTCP of OAR to find the

most suitable techniques with respect to radiobiological evaluation of left-sided breast cancer treatment. Third, the dose to the skin surface of the SFB and PFB techniques was compared. The skin dose in breast cancer radiation treatment is an important factor in balancing the outcomes and cosmesis. Skin toxicity is often considered a dose-limiting factor, and the skin dose can be ignored in breast treatment and underdosing because it could cause recurrence. Thus, understanding the skin dose for each treatment technique help radiation oncologists in choosing the appropriate plan for treatment. In this study, therefore, the dose was evaluated from the surface to a depth of 5 mm for both prone and supine techniques. Additionally, two different grid calculation sizes of 1.0 mm and 2.5 mm were used to evaluate the influence of grid size on dose calculation in the superficial region for prone and supine techniques.

Evaluating the current treatment techniques for breast cancer enables health care providers to provide better disease control and care for these patients. To comprehensively evaluate the performance of these techniques, understanding and evaluating them dosimetrically, as well as radiologically, is important. Thus, the results of these three studies provide clinicians with a complete overview, knowledge, and comparison of the various techniques to make an informed decision on the best treatment technique for each patient undergoing RT for left-sided breast cancer. In this study, only the 3D tangent techniques were evaluated, and IMRT or VMAT treatment planning was not performed to evaluate the dose to OAR; these techniques must be evaluated for OAR doses. Further, we did not perform a physical measurement of the skin dose using trans-luminescent dosimeters (TLD) or diodes on the patient. This can be considered and evaluated in the future.

Chapter 4: Discussion²

4.1 First Study

The results of our first study suggest that the mean heart dose can be reduced by almost half using the SDIBH and PFB techniques compared with that using the SFB technique. When the patient takes a deep breath, the heart moves posteriorly and inferiorly because of lung expansion and diaphragmatic movements, consequently moving away from the chest wall. The moving of heart during SDIBH helps reduce the volume of heart in the treatment field, thereby reducing the dose to the heart and its components. The mean dose and all the dosimetric parameters were the lowest in PFB for the LV. It is believed that the dose to the LAD plays a crucial role in radiation-induced cardiac toxicity.^{51,52} The mean dose to the LAD in SDIBH and PFB was found to be similar, and the highest mean dose was observed in SFB. In a similar study,

Table 4.1 Dosimetry parameters (median values and quartiles) in supine free-breathing (SFB), supine deep inspiration breath-hold (SDIBH), prone free-breathing (PFB), and prone deep inspiration breath-hold (PDIBH) techniques for heart, left ventricle (LV), left anterior descending artery (LAD), and left lung. Please note that all dosimetric parameters are highest in SFB.

OAR	SFB	SDIBH	PFB
Heart	1.92 (1.42–2.76)	1.08 (0.84–1.36)	0.98 (0.83–1.15)
LV	3.19 (2.25–4.24)	1.50 (1.15–1.80)	1.34 (1.13–1.54)
LAD	21.73 (8.55–28.5)	6.30 (3.51–9.31)	6.57 (3.99–9.49)
Left lung	5.63 (4.23–6.86)	5.54 (4.29–6.42)	0.61 (0.47–0.80)

² This chapter is partially reproduced from work published in a peer reviewed journal. The author of this dissertation is the first author of the published work. See Appendix C,D,F,G for the published studies and permissions.

Verhoeven et al.¹⁹ concluded that PFB results in higher doses to the heart and LAD than the SFB and SDIBH techniques. However, the results of our study¹⁰ are different because both SDIBH and PFB result in lower heart and LAD doses than that in SFB, irrespective of the breast volume.

We found equivocal results related to the reduction of radiation doses to the heart in PFB in a literature study. However, all studies agree that the lung dose is drastically reduced in PFB compared with the doses in SFB and SDIBH.^{6-8,16-19} Similarly, in our study, we found that the lung doses are significantly lower in PFB than in SFB and SDIBH. The lung density of the irradiated lung volume decreases in SDIBH as well.^{7,19,21 10,15,30} A study has indicated that an opposite effect occurs in PFB, when the lungs are pushed downward by gravity, consequently increasing the lung density.¹⁹ However, PFB exhibits clear advantages over SFB and SDIBH in lowering lung doses and the values of most other dosimetric parameters compared with SFB in this study.

We could not find any other study in the literature that evaluates the heart, LV, LAD, and lung for V2.5, V5, V10, V20, and V30, and statistically compares the dosimetric parameters of the techniques and the dosimetric differences in OAR for SFB, SDIBH, and PFB with respect to the breast volume. The mean doses evaluated for each OAR increased in SFB and SDIBH in ascending order of small to large breast volumes of patients, as shown in Table 3. This can be attributed to the fact that, with the increase in breast volume, the separation between the fields increases, thus irradiating a larger volume to sufficiently cover the PTV. Further, a large breast volume requires wider beams to be covered, thereby radiating a larger volume in SFB and SDIBH, resulting in higher doses to the cardiac components and the lung.

An interesting observation is that differences between the doses and dosimetric parameters evaluated for SFB and SDIBH, and for SFB and PFB, increased in the order of small to large breast volumes of patients, as shown in Table 3. The dosimetric parameters are the lowest for PFB for patients with breast PTV volume $\geq 750 \text{ cm}^3$. Thus, the SDIBH and PFB techniques are more beneficial than SFB for patients with large breasts.

4.2 Second Study

In this study, we intended to find if the DIBH in the prone position produces additional benefits in sparing the heart and its components. The mean heart dose and mean LV dose in PDIBH are statistically and significantly lower than those in SFB, SDIBH, and PFB. The PDIBH exhibits a statistically significant reduction in mean LAD dose compared with SFB and PFB; however, no significant difference was found with respect to SDIBH. The PFB produces statistically and significantly lower mean heart and LAD doses compared with the SFB, which is in contrast with a study that concluded that PFB gives a higher dose. It has been reported that an increased risk of stenosis in the LAD exists for left-sided breast cancer patients.⁵²

Table 3.2 Mean dosimetric parameters (median values and quartiles) of OAR in SFB, SDIBH, and PFB based on breast PTV volume < 750 cm³ and ≥ 750 cm³. Please note that PFB has the lowest mean values for heart, LV, LAD, and lung for breast PTV volume ≥ 750 cm³.

Breast PTV volume < 750 cm ³	SFB	SDIBH	PFB
Mean heart dose (Gy)	1.65 (1.12–2.32)	0.87 (0.71–1.21)	0.90 (0.81–1.10)
Mean LV Dose (Gy)	2.93 (1.85–4.04)	1.30 (1.01–1.70)	1.32 (1.13–1.50)
Mean LAD dose (Gy)	19.86 (7.85–25.1)	5.97 (3.01–8.53)	6.5 (3.58–9.16)
Mean lung dose (Gy)	5.48 (3.93–6.52)	5.06 (4.09–6.38)	0.61(0.48–0.97)
Breast PTV volume ≥ 750 cm ³			
Mean heart dose (Gy)	2.59 (1.87–4.06)	1.36 (0.97–1.62)	1.07 (0.87–1.31)
Mean LV Dose (Gy)	3.61 (3.02–5.77)	1.72 (1.40–2.11)	1.2 (1.11–1.58)
Mean LAD dose (Gy)	24.74 (10.22–36.75)	7.05 (3.27–12.99)	6.7 (4.51–9.93)
Mean lung dose (Gy)	5.69 (4.77–7.08)	5.7 (5.23–7.06)	0.57 (0.36–0.68)

Higher LAD dose in PFB compared with the SDIBH could be attributed to the fact that the LAD falls close to mediastinum/chest wall because of gravity, which causes it to be closer to the treatment field; however, in PDIBH, it lowers because the deep inspiration pushes the proximity of LAD away from the treatment field. The QUANTEC group⁸¹ recommends that, for breast cancer patients, the irradiated heart volume should be minimized without compromising the target

coverage. Our results in Table 5 conclusively indicate that the PDIBH further reduces the dose to heart, LV, and LAD compared with SFB, SDIBH, and PFB.

The mean lung doses and other dosimetric parameters evaluated in PFB and PDIBH are statistically lower than those in SFB and SDIBH. In the prone position, the minimal beam propagates through the lung because of the pulling away from the breast from the chest wall and lung. Thus, the prone set up has a clear advantage over the supine set up in lowering the lung doses and the other dosimetric parameters calculated in this study, which are in agreement with those of several previous studies.^{6-10,16-18} However, similar to a study by Thomas et al.,¹¹ we found that the PFB administers a slightly lower lung dose than PDIBH, if the density correction caused by increased lung volume of PDIBH is not considered. This could be because the heart volume may have been replaced by the lung tissue in the irradiated volume; however, the increase in lung volume could compensate the increase in dose to a small volume.

Table 4.3 Dosimetry parameters (median values and quartiles) in supine free-breathing (SFB), supine deep inspiration breath-hold (SDIBH), prone free-breathing (PFB), and prone deep inspiration breath-hold (PDIBH) techniques for heart, left ventricle (LV), left anterior descending artery (LAD), and left lung.

OAR	SFB	SDIBH	PFB	PDIBH
Heart	1.88 (1.09–2.22)	0.97 (0.68–1.23)	0.85 (0.68–1.04)	0.77 (0.55–0.92)
LV	3.48 (2.21–4.60)	1.36 (0.97–2.32)	1.18 (0.98–1.34)	1.03 (0.80–1.22)
LAD	22.38 (5.34–26.19)	3.88 (2.59–7.98)	4.96 (3.45–6.56)	3.49 (2.30–5.12)
Left Lung	6.09 (4.89–7.86)	5.41 (4.80–6.75)	0.69 (0.47–0.87)	0.88 (0.62–1.31)

Further, although NTCP analysis is not currently used directly in radiotherapy plan evaluation, it is a very important tool for comparing the radiotherapy plans and methods. An NTCP analysis can also help find different methods to reduce radiotherapy-induced complication rates for patients undergoing RT treatment.^{56,57,81-85} Therefore, we performed a biological evaluation of each technique for the NTCP of OARs. Studies that compare the NTCP for OAR in SFB with

SDIBH exist in the literature.⁸²⁻⁸⁴ However, no study was found that compares the NTCP for heart, LV, LAD, and lung for supine and prone techniques. Moreover, our study is the first that calculates and compares the NTCP values of prone techniques with those of supine techniques in free-breathing and deep inspiration breath-hold. In addition, ours is the only study that calculates the NTCP for six endpoints of lung complications using the NTCP LKB model for each of the four techniques (Table 6).

Based on the biological evaluation of heart with cardiac morbidity, we found statistically and significantly lower NTCP for SDIBH, PFB, and PDIBH techniques compared with the SFB, which correlates with our result of lower dosimetry doses for heart for all techniques compared with the SFB technique. A study has concluded that the SDIBH, PFB, and PDIBH techniques significantly reduce the mean probability of both excessive cardiac mortality and lung complication compared with the SFB technique. Our results are similar to those of a few studies that concluded that the SDIBH significantly reduces the probability of heart and lung complication compared with SFB.⁸²⁻⁸⁴ In our study, we did not find any statistically significant difference in NTCP between the SDIBH, PFB, and PDIBH for heart, LAD, and LV. Both the prone techniques PFB and PDIBH showed that the NTCP of lung complication is statistically significant compared with the SFB and SDIBH, which correlates with the lower dosimetry dose in the lung between these techniques.

4.3 Third Study

Measuring the skin dose for tangential beams is difficult. Although skin dose has been studied relatively deeper, it could still be ignored. Most TPS is known to provide inaccurate dose estimates.^{71,86,87} Conventional model-based dose calculation algorithms have limitations at the buildup region because of the lack of electron equilibrium and incomplete scatter conditions close to the skin and air surface. This are caused by difficulties in modeling the contribution of dose from electrons originating from the primary photons interacting with a part of the LINAC, flattening filter, and collimators by the planning system. A study has concluded that the accuracy of AAA in a solid water phantom for tangential treatment plans is comparable to that of the Monte Carlo

method.⁸⁸ However, another study has concluded that the AAA algorithm cannot predict the dose reliably at depths less than 2 mm.⁸⁹ Panetti et al.⁹⁰ measured the calculation accuracy of AAA in the surface build region in tangential beam arrangements similar to that in breast treatment planning. It concluded that, for a 6 MV beam, using the AAA does not introduce clinically significant error in the buildup region for absorbed dose, particularly after the initial 2 mm of tissue.

Table 4.4 Calculated NTCP values (median values and quartiles) in supine free-breathing (SFB), supine deep inspiration breath-hold (SDIBH), prone free-breathing (PFB), and prone deep inspiration breath-hold (PDIBH) techniques with end-stage for heart, left ventricle (LV), left anterior descending artery (LAD), and the lung.

End point/Stage	Mean NTCP (%) SFB	Mean NTCP (%) SDIBH	Mean NTCP (%) PFB	Mean NTCP (%) PDIBH
Heart (Cardiac Mortality)	0.27 (0.01-0.55)	0 (0-0.01)	0 (0-0)	0 (0-0)
LV (Cardiac Mortality)	0.62 (0.023-1.98)	0 (0-0.038)	0 (0-0)	0 (0-0)
LAD (Cardiac Mortality)	4.23 (0-14.77)	0 (0-0.26)	0 (0-0.07)	0 (0-0)
Lung Pneumonitis (1), Grade >= 2	0.12 (0.1-0.188)	0.1 (0.082-0.13)	0.05 (0.05-0.05)	0.05 (0.05-0.05)
Lung Pneumonitis (2), Grade >= 2	0.69 (0.61-0.88)	0.62 (0.54-0.72)	0.36 (0.36-0.37)	0.37 (0.36-0.39)
Lung Symptomatic or Radiographic Pneumonitis (<= 6 months)	30.24 (28.11-34.52)	28.56 (25.20-30.97)	12.47 (11.95-14.40)	14.04 (12.51-16.79)
Lung Symptomatic Pneumonitis (< 6 months)	0.04 (0.03-0.073)	0.02 (0.02-0.04)	0.01 (0.01-0.01)	0.01 (0.01-0.01)
Lung Symptomatic or Radiographic Fibrosis (> 6 months)	15.09 (13.49-19.02)	13.85 (11.23-15.89)	3.2 (2.92-4.22)	4.26 (3.26-5.83)
Lung Symptomatic Fibrosis (> 6 months)	51.81 (48.95-54.64)	48.95 (45.96-51.52)	23.47 (19.99-28.48)	27.7 (22.58-34.01)
Lung composite	41.32 (38.21-47.41)	38.85 (33.95-42.36)	15.57 (14.82-18.30)	17.79 (15.75-21.76)

Many studies have evaluated various methods to verify the skin dose, but skin dose is not one of the parameters recorded—unlike OARs such as the heart and lungs.^{71,87,91} Skin dose, in addition to being energy-dependent, can be grid size-dependent as well. A study has indicated that a difference of up to 3% is observed in maximum and mean doses with a calculation grid.⁷¹

A limitation of our study is that the dose on the patient's surface during treatment was not measured using diodes or TLDs.

In this study, the superficial doses of 50 patients were compared in the prone and supine positions. The dose at depths of 3 mm, 4 mm, and 5 mm is statistically and significantly lower in the prone position than in the supine position. The doses at 3 mm, 4 mm, and 5 mm are similar for the prone position with calculation grid sizes of 1 mm and 2.5 mm; a similar observation is made for supine position for both grid sizes (Table 7). Thus, minimal effects of grid size are observed on dose at depths beyond 2 mm for prone and supine positions.

Table 4.5 Dose (median value and quartile range) in percentage from a depth of 0–5 mm for prone and supine techniques with grid sizes of 1.5 mm and 2.5 mm, respectively.

Technique (Grid size)	0 mm	1 mm	2 mm	3 mm	4 mm	5 mm
Prone (Grid size: 1.0 mm) dose in %	32.25 (29.48–33.92)	66.87 (63.77–68.11)	81.86 (80.26–82.91)	87.80 (86.47–88.90)	91.92 (90.90–92.97)	95.30 (93.77–96.00)
Supine (Grid size: 1.0 mm) dose in %	32.95 (30.55–36.82)	65.05 (63.35–67.99)	81.27 (79.50–82.75)	89.10 (87.23–90.36)	94.50 (92.57–95.62)	98.20 (96.6–99.51)
Prone (Grid size: 2.5 mm) dose in %	36.75 (33.3–39.32)	60.38 (56.90–64.08)	77.35 (74.55–80.37)	87.1 (85.20–88.31)	91.6 (90.27–92.76)	95.10 (93.74–96.00)
Supine (Grid size: 2.5 mm) dose in %	38.16 (32.82–42.32)	62.15 (57.27–67.50)	79.65 (76.77–81.75)	88.59 (86.68–90.14)	94.63 (92.85–95.34)	97.8 (96.71–99.44)

An optimum surface dose must realize the primary objective of treating breast cancer without excessive skin toxicity, such as erythema, desquamation, edema, and fibrosis. The dose beyond the depth of 2 mm is up to 3% lower in the prone technique compared with that in the supine technique. As mentioned earlier, the beam incidence angle is close to perpendicular in the prone technique, which may lead to lower superficial dose in the prone technique than supine technique. The inadequate superficial dose could lead to recurrence. Further, as indicated by

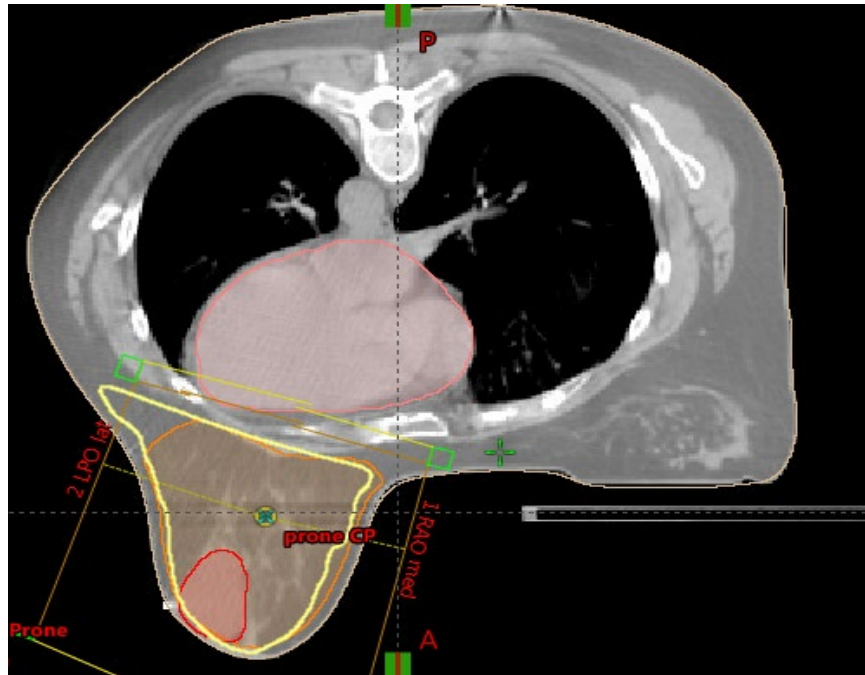
Katz et al.,⁶⁹ if a lumpectomy bed is close to the skin surface, it is important to consider the dose in case the clinician considers treating using the prone technique (Figure 4.1). A clinician should consider lumpectomy or tumor bed contouring, particularly for patients treated in the prone position, to evaluate the dose to the gross tumor volume. For such cases, boost treatment should be considered to deliver sufficient dose to the tumor bed; this prevents underdosing of the superficial tumor beds.

A statistically and significantly lower mean dose is delivered to all OAR in the prone position compared with the supine position (Table 8). The heart, LV, LAD, and left lung doses are significantly lower in the prone position. As mentioned earlier, the heart falls anteriorly in the prone position because the breast falls and elongates because of gravity; thus, the beam angles can be chosen to minimize the in-field heart, LV, and LAD doses. Similar to other studies, the largest dose reduction is seen in the left lung in the prone position compared with the supine position.^{6,8,10}

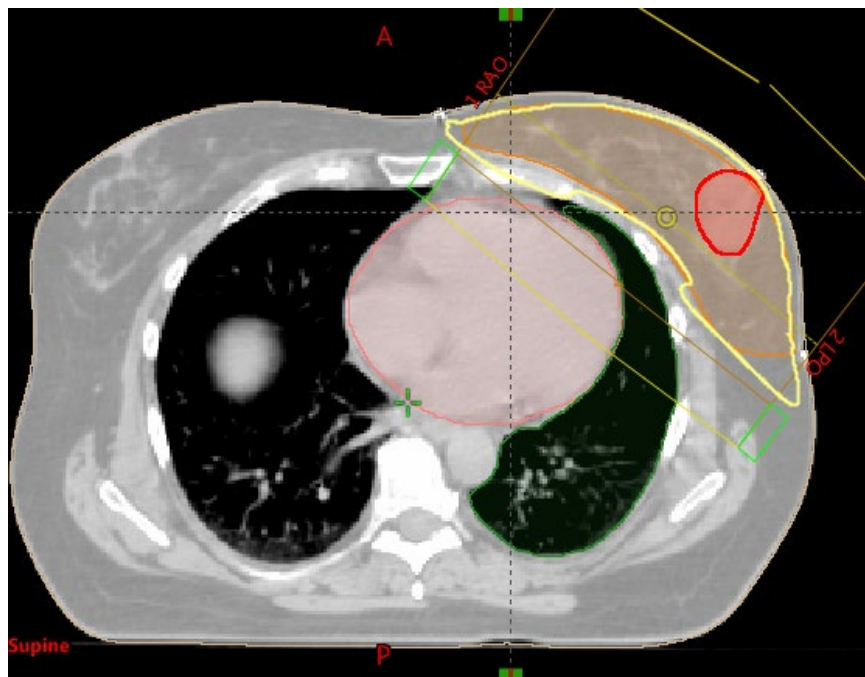
However, on the contrary to a study by Verhoeven et al.¹⁹ that concluded that LAD is higher in the prone position, we found a statistically significant dose reduction in LAD for the prone position compared with the supine position. Thus, we were able to reduce the dose to all the OAR in the prone position. Therefore, this is the only study that compares the skin dose in the prone and supine positions for the same patient, along with comparison of dose for OAR.

Table 4.6 Dose (median value and quartile range) in Gy for OAR in prone and supine positions.

Mean Dose for OAR	Prone Position	Supine Position
Heart Dose (Gy)	0.92 (0.72–1.11)	1.88 (1.42–2.58)
LV Dose (Gy)	1.31 (1.02–1.5)	3.24 (2.27–4.42)
LAD Dose (Gy)	5.81 (3.71–8.6)	21.76 (6.83–26.88)
Lung Dose (Gy)	0.65 (0.48–0.85)	5.74 (4.55–6.98)



(a)



(b)

Figure 4.1 (a) Prone and (b) Supine treatment techniques with 100% isodose line. Yellow line represents 100% isodose line, and orange, red, and pink contours represent breast PTV, lumpectomy, and heart, respectively.

Chapter 5: Conclusion³

We conclude that the radiation dose to the heart, LV, LAD, and left lung can be significantly reduced by selecting the appropriate technique. Based on the data of the first study, we can conclude that PFB is preferred dosimetrically over the SFB and SDIBH techniques. Although the first study analyzed the data based on the breast volume, we conclude that—irrespective of the breast volume—PFB is more beneficial than the SFB technique for OAR sparing. The SDIBH and PFB technique deliver lower doses to cardiac components than the SFB technique. The PFB technique delivers significantly lower lung doses than the SFB and SDIBH techniques. Thus, the PFB technique could be recommended for patients with pulmonary diseases.

In our second study, we included the PDIBH technique for evaluation, along with the SFB, SDIBH, and PFB techniques. Deep inspiration breath-hold in prone position has additional benefits in lowering heart, LV, and LAD doses compared with the SFB, SDIBH, and PFB techniques. The dosimetric findings are augmented with the NTCP for cardiac mortality, indicating that a substantial reduction can be achieved using SDIBH, PFB, and PDIBH compared with the SFB. The left Lung doses and composite NTCP for lung complications are statistically lower in the prone techniques than in the supine techniques. Thus, the PDIBH is more significantly beneficial in heart, LV, LAD, and lung sparing than the SDIBH. We conclude that a significant dose reduction can be achieved using the prone technique. Each clinic should not only evaluate the advantages and disadvantages of each technique but also consider the patient comfort level and breathing patterns when selecting the breast technique. Better integration of biological

³ This chapter is partially reproduced from work published in a peer reviewed journal. The author of this dissertation is the first author of the published work. See Appendix C,D,F,G for the published studies and permissions.

models in TPS with validated input parameters (α and β) for the OAR may facilitate adoption for clinical practice.

Our third study concluded that based on the same patient population in the prone and supine patients treated with a 6 MV beam, the dose to OAR is lower in the prone position, particularly for LAD and left lung. Further, the skin dose is lower in the prone position than the supine position, which could probably result in skin recurrence. The dose from the skin surface increases rapidly in both techniques to more than 95% at a depth of 5 mm. This confirms our hypothesis that the prone technique delivers a lower superficial dose than the supine technique, irrespective of the calculation grid size. Because the beam angle in the prone technique is almost perpendicular to the surface, this observation is accurate with physical parameters. The clinician should additionally consider routinely contouring the tumor bed, particularly for patients to be treated with prone positions, to evaluate the dose to the gross tumor volume; this helps avoid underdosing of superficial tumor beds. Thus, the prone position reduces the dose to the OAR; however, the dose to the skin may also be assessed in the prone technique, and if desired, the skin dose could be carefully augmented via a bolus or beam spoiler.

Based on these results and findings, we conclude that the PDIBH technique spares the heart and its components the most, whereas the PFB technique spares the lung the most in addition to adequately sparing the heart components. Furthermore, prone free-breathing techniques are the most suitable for patients with pulmonary issues. No statistically significant difference was found between the NTCP of SDIBH, PFB, and PDIBH techniques for heart, LV, and LAD. The PFB technique has a statistically and significantly lower lung NTCP than the SDIBH and PDIBH techniques. Thus, radio biologically, we conclude that prone free-breathing is the most suitable technique for sparing OAR.

However, recurrence could occur because of underdosing of skin. In cases where skin dose is a concern, such as when a tumor is close to the skin surface, physicians can use the SDIBH technique to spare the heart and its components. Furthermore, the prone technique can

be utilized with bolus or beam spoilers to increase the skin dose, if the lung function of the patient is compromised.

5.1 Future Work

Future work should include the IMRT and VMAT techniques in conjunction with the SDIBH and prone techniques for sparing of OAR, along with NTCP evaluation. In addition, the dose to the skin must be measured at various depths on the phantom to validate the dose calculated by the treatment planning system at a superficial depth. For future studies, the radiobiological model must be further evaluated, and the results should be clinically validated for clinical application on a regular basis. Further, radiobiological models with different α and β ratios need to be examined. Furthermore, these results must be confirmed by a long-term study on the effects on patients, after a few decades from the administration of the RT treatment.

References

1. American Cancer Society. Cancer Facts and Figures. 2019.
2. Mahmoudi R, Jabbari N, Aghdasi M, Khalkhali HR. Energy dependence of measured CT numbers on substituted materials used for CT number calibration of radiotherapy treatment planning systems. *PLoS One*. 2016;11(7):e0158828.
3. Emami B, Lyman J, Brown A, et al. Tolerance of normal tissue to therapeutic irradiation. *Int J Radiat Oncol Biol Phys*. 1991;21(1):109-122.
4. Korreman SS, Pedersen AN, Notttrup TJ, Specht L, Nystrom H. Breathing adapted radiotherapy for breast cancer: comparison of free breathing gating with the breath-hold technique. *Radiother Oncol*. 2005;76(3):311-318.
5. Korreman SS, Pedersen AN, Aarup LR, Notttrup TJ, Specht L, Nystrom H. Reduction of cardiac and pulmonary complication probabilities after breathing adapted radiotherapy for breast cancer. *Int J Radiat Oncol Biol Phys*. 2006;65(5):1375-1380.
6. Kirby AM, Evans PM, Donovan EM, Convery HM, Haviland JS, Yarnold JR. Prone versus supine positioning for whole and partial-breast radiotherapy: a comparison of non-target tissue dosimetry. *Radiother Oncol*. 2010;96(2):178-184.
7. Lymberis SC, deWyngaert JK, Parhar P, et al. Prospective assessment of optimal individual position (prone versus supine) for breast radiotherapy: volumetric and dosimetric correlations in 100 patients. *Int J Radiat Oncol Biol Phys*. 2012;84(4):902-909.
8. Ferrari A, Ivaldi G, Leonardi MC, Rondi E, Orecchia R. Prone breast radiotherapy in a patient with early stage breast cancer and a large pendulous breast. *Tumori*. 2009;95(3):394-397.
9. Buijsen J, Jager, J. J., Bovendeerd, J., Voncken, R., Borger, J. H., Boersma, L. J., Murrer, L. H., Lambin, P. Prone breast irradiation for pendulous breasts. *Radiother Oncol*. 2007;82(3):337-340.
10. Saini AS, Hwang CS, Biagioli MC, Das IJ. Evaluation of sparing organs at risk (OARs) in left-breast irradiation in the supine and prone positions and with deep inspiration breath-hold. *J Appl Clin Med Phys*. 2018;19(4):195-204.
11. Mulliez T, Veldeman L, Speleers B, et al. Heart dose reduction by prone deep inspiration breath hold in left-sided breast irradiation. *Radiother Oncol*. 2015;114(1):79-84.
12. Mulliez T, Speleers B, Mahjoubi K, et al. Prone left-sided whole-breast irradiation: significant heart dose reduction using end-inspiratory versus end-expiratory gating. *Cancer Radiotherapy*. 2014;18(7):672-677.
13. Junzo P, Chino LBM. Prone positioning causes the heart to be displaced anteriorly within the thorax: implications for breast cancer treatment. *Int J Radiat Oncol Biol Phys*. 2008;70(1):916-920.
14. Lymberis SC, Formenti SC. Prone-breast radiotherapy: too early for conclusions: in regard to Chino et Al. (*Int j radiat oncol biol phys* 2008;70:916-920). *Int J Radiat Oncol Biol Phys*. 2008;72(1):301-302; author reply 302.
15. Griem KL, Fetherston P, Kuznetsova M, Foster GS, Shott S, Chu J. Three-dimensional photon dosimetry: a comparison of treatment of the intact breast in the supine and prone position. *Int J Radiat Oncol Biol Phys*. 2003;57(3):891-899.

16. Varga Z, Hideghety K, Mezo T, Nikolenyi A, Thurzo L, Kahan Z. Individual positioning: a comparative study of adjuvant breast radiotherapy in the prone versus supine position. *Int J Radiat Oncol Biol Phys.* 2009;75(1):94-100.
17. Takahashi K, Morota M, Kagami Y, et al. Prospective study of postoperative whole breast radiotherapy for Japanese large-breasted women: a clinical and dosimetric comparisons between supine and prone positions and a dose measurement using a breast phantom. *BMC Cancer.* 2016;16(1):757.
18. Formenti SC, DeWyngaert JK, Jozsef G, Goldberg JD. Prone vs supine positioning for breast cancer radiotherapy. *JAMA.* 2012;308(9):861-863.
19. Verhoeven K, Sweldens C, Petillion S, et al. Breathing adapted radiation therapy in comparison with prone position to reduce the doses to the heart, left anterior descending coronary artery, and contralateral breast in whole breast radiation therapy. *Pract Radiat Oncol.* 2014;4(2):123-129.
20. Schubert LK, Gondi V, Sengbusch E, et al. Dosimetric comparison of left-sided whole breast irradiation with 3DCRT, forward-planned IMRT, inverse-planned IMRT, helical tomotherapy, and topotherapy. *Radiother Oncol.* 2011;100(2):241-246.
21. Yin Y, Chen J, Sun T, et al. Dosimetric research on intensity-modulated arc radiotherapy planning for left breast cancer after breast-preservation surgery. *Med Dosim.* 2012;37(3):287-292.
22. Saini AS, Das IJ, Hwang CS, Biagioli MC, Lee WE, 3rd. Biological indices evaluation of various treatment techniques for left-sided breast treatment. *Pract Radiat Oncol.* 2019;9(6):e579-e590.
23. Shah C, Badiyan S, Berry S, et al. Cardiac dose sparing and avoidance techniques in breast cancer radiotherapy. *Radiother Oncol.* 2014;112(1):9-16.
24. Yeung R, Conroy L, Long K, et al. Cardiac dose reduction with deep inspiration breath hold for left-sided breast cancer radiotherapy patients with and without regional nodal irradiation. *Radiat Oncol.* 2015;10:200.
25. Smyth LM, Knight KA, Aarons YK, Wasiak J. The cardiac dose-sparing benefits of deep inspiration breath-hold in left breast irradiation: a systematic review. *J Med Radiat Sci.* 2015;62(1):66-73.
26. Sakka M, Kunzelmann L, Metzger M, Grabenbauer GG. Cardiac dose-sparing effects of deep-inspiration breath-hold in left breast irradiation : Is IMRT more beneficial than VMAT? *Strahlenther Onkol.* 2017;193(10):800-811.
27. Hayden AJ, Rains M, Tiver K. Deep inspiration breath hold technique reduces heart dose from radiotherapy for left-sided breast cancer. *J Med Imaging Radiat Oncol.* 2012;56(4):464-472.
28. Nissen HD, Appelt AL. Improved heart, lung and target dose with deep inspiration breath hold in a large clinical series of breast cancer patients. *Radiother Oncol.* 2013;106(1):28-32.
29. Morrow NV, Stepaniak C, White J, Wilson JF, Li XA. Intra- and interfractional variations for prone breast irradiation: an indication for image-guided radiotherapy. *Int J Radiat Oncol Biol Phys.* 2007;69(3):910-917.
30. Guenzi M, Bosetti D, Lamanna G, et al. Novel 10-fraction breast irradiation in prone and supine position: technical, dosimetric and clinical evaluation. *Tumori.* 2015;101(2):154-160.
31. Bergom C, Currey A, Desai N, Tai A, Strauss JB. Deep inspiration breath hold: techniques and advantages for cardiac sparing during breast cancer irradiation. *Front Oncol.* 2018;8:87.
32. McIntosh A, Shoushtari AN, Benedict SH, Read PW, Wijesooriya K. Quantifying the reproducibility of heart position during treatment and corresponding delivered heart dose

- in voluntary deep inhalation breath hold for left breast cancer patients treated with external beam radiotherapy. *Int J Radiat Oncol Biol Phys*. 2011;81(4):e569-576.
33. van Haaren P, Claassen-Janssen F, van de Sande I, Boersma L, van der Sangen M, Hurkmans C. Heart position variability during voluntary moderate deep inspiration breath-hold radiotherapy for breast cancer determined by repeat CBCT scans. *Phys Med*. 2017;40:88-94.
 34. Wang W, Purdie TG, Rahman M, Marshall A, Liu FF, Fyles A. Rapid automated treatment planning process to select breast cancer patients for active breathing control to achieve cardiac dose reduction. *Int J Radiat Oncol Biol Phys*. 2012;82(1):386-393.
 35. Remouchamps VM, Letts N, Vicini FA, et al. Initial clinical experience with moderate deep-inspiration breath hold using an active breathing control device in the treatment of patients with left-sided breast cancer using external beam radiation therapy. *Int J Radiat Oncol Biol Phys*. 2003;56(3):704-715.
 36. Jaggi R, Moran JM, Kessler ML, Marsh RB, Balter JM, Pierce LJ. Respiratory motion of the heart and positional reproducibility under active breathing control. *Int J Radiat Oncol Biol Phys*. 2007;68(1):253-258.
 37. Ghoncheh M, Pournamdar Z, Salehiniya H. Incidence and mortality and epidemiology of breast cancer in the world. *Asian Pac J Cancer Prev*. 2016;17(S3):43-46.
 38. Satcher D, Thompson TG, Koplan JP. Women and smoking: a report of the Surgeon General. *Nicotine Tob Res*. 2002;4(1):7-20.
 39. Cronin KA, Lake AJ, Scott S, et al. Annual report to the nation on the status of cancer, part I: national cancer statistics. *Cancer*. 2018;124(13):2785-2800.
 40. Fisher B, Anderson S, Bryant J, et al. Twenty-year follow-up of a randomized trial comparing total mastectomy, lumpectomy, and lumpectomy plus irradiation for the treatment of invasive breast cancer. *N Engl J Med*. 2002;347(16):1233-1241.
 41. Fisher B, Jeong JH, Anderson S, Bryant J, Fisher ER, Wolmark N. Twenty-five-year follow-up of a randomized trial comparing radical mastectomy, total mastectomy, and total mastectomy followed by irradiation. *N Engl J Med*. 2002;347(8):567-575.
 42. Clarke M, Collins R, Darby S, et al. Effects of radiotherapy and of differences in the extent of surgery for early breast cancer on local recurrence and 15-year survival: an overview of the randomised trials. *Lancet*. 2005;366(9503):2087-2106.
 43. Darby SC, McGale P, Taylor CW, Peto R. Long-term mortality from heart disease and lung cancer after radiotherapy for early breast cancer: prospective cohort study of about 300,000 women in US SEER cancer registries. *Lancet Oncol*. 2005;6(8):557-565.
 44. Henson KE, McGale P, Taylor C, Darby SC. Radiation-related mortality from heart disease and lung cancer more than 20 years after radiotherapy for breast cancer. *Br J Cancer*. 2013;108(1):179-182.
 45. Taylor C, Correa C, Duane FK, et al. Estimating the risks of breast cancer radiotherapy: evidence from modern radiation doses to the lungs and heart and from previous randomized trials. *J Clin Oncol*. 2017;35(15):1641-1649.
 46. Darby SC, Ewertz M, McGale P, et al. Risk of ischemic heart disease in women after radiotherapy for breast cancer. *N Engl J Med*. 2013;368(11):987-998.
 47. Taylor CW, Nisbet A, McGale P, et al. Cardiac doses from Swedish breast cancer radiotherapy since the 1950s. *Radiother Oncol*. 2009;90(1):127-135.
 48. Taylor CW, Nisbet A, McGale P, Darby SC. Cardiac exposures in breast cancer radiotherapy: 1950s-1990s. *Int J Radiat Oncol Biol Phys*. 2007;69(5):1484-1495.
 49. Giordano SH, Kuo YF, Freeman JL, Buchholz TA, Hortobagyi GN, Goodwin JS. Risk of cardiac death after adjuvant radiotherapy for breast cancer. *J Natl Cancer Inst*. 2005;97(6):419-424.
 50. Hooning MJ, Botma A, Aleman BM, et al. Long-term risk of cardiovascular disease in 10-year survivors of breast cancer. *J Natl Cancer Inst*. 2007;99(5):365-375.

51. Correa CR, Litt HI, Hwang WT, Ferrari VA, Solin LJ, Harris EE. Coronary artery findings after left-sided compared with right-sided radiation treatment for early-stage breast cancer. *J Clin Oncol*. 2007;25(21):3031-3037.
52. Nilsson G, Holmberg L, Garmo H, et al. Distribution of coronary artery stenosis after radiation for breast cancer. *J Clin Oncol*. 2012;30(4):380-386.
53. Lind PA, Pagnanelli R, Marks LB, et al. Myocardial perfusion changes in patients irradiated for left-sided breast cancer and correlation with coronary artery distribution. *Int J Radiat Oncol Biol Phys*. 2003;55(4):914-920.
54. Marks LB, Yu X, Prosnitz RG, et al. The incidence and functional consequences of RT-associated cardiac perfusion defects. *Int J Radiat Oncol Biol Phys*. 2005;63(1):214-223.
55. Demirci S, Nam J, Hubbs JL, Nguyen T, Marks LB. Radiation-induced cardiac toxicity after therapy for breast cancer: interaction between treatment era and follow-up duration. *Int J Radiat Oncol Biol Phys*. 2009;73(4):980-987.
56. Gagliardi G, Bjohle J, Lax I, et al. Radiation pneumonitis after breast cancer irradiation: analysis of the complication probability using the relative seriality model. *Int J Radiat Oncol Biol Phys*. 2000;46(2):373-381.
57. Gagliardi G, Lax I, Ottolenghi A, Rutqvist LE. Long-term cardiac mortality after radiotherapy of breast cancer--application of the relative seriality model. *Br J Radiol*. 1996;69(825):839-846.
58. Dale RG. The application of the linear-quadratic dose-effect equation to fractionated and protracted radiotherapy. *Br J Radiol*. 1985;58(690):515-528.
59. Lee SP, Leu MY, Smathers JB, McBride WH, Parker RG, Withers HR. Biologically effective dose distribution based on the linear quadratic model and its clinical relevance. *Int J Radiat Oncol Biol Phys*. 1995;33(2):375-389.
60. Kim S, Liu CR, Zhu TC, Palta JR. Photon beam skin dose analyses for different clinical setups. *Med Phys*. 1998;25(6):860-866.
61. Chin MS, Siegel-Reamer L, FitzGerald GA, et al. Association between cumulative radiation dose, adverse skin reactions, and changes in surface hemoglobin among women undergoing breast conserving therapy. *Clin Transl Radiat Oncol*. 2017;4:15-23.
62. Kole AJ, Kole L, Moran MS. Acute radiation dermatitis in breast cancer patients: challenges and solutions. *Breast Cancer (Dove Med Press)*. 2017;9:313-323.
63. Osako T, Oguchi M, Kumada M, Nemoto K, Iwase T, Yamashita T. Acute radiation dermatitis and pneumonitis in Japanese breast cancer patients with whole breast hypofractionated radiotherapy compared to conventional radiotherapy. *Jpn J Clin Oncol*. 2008;38(5):334-338.
64. Habibollahi F, Mayles HM, Mayles WP, et al. Assessment of skin dose and its relation to cosmesis in the conservative treatment of early breast cancer. *Int J Radiat Oncol Biol Phys*. 1988;14(2):291-296.
65. Kulik A, Lyczek J, Kawczyn Ska M, Gruszczyn Ska E. Cosmetic effect in patients with early breast cancer treated with breast conserving therapy (BCT) and with HDR brachytherapy (HDR-BT) "boost". *J Contemp Brachytherapy*. 2009;1(2):77-86.
66. Beadle GF, Silver B, Botnick L, Hellman S, Harris JR. Cosmetic results following primary radiation therapy for early breast cancer. *Cancer*. 1984;54(12):2911-2918.
67. Dewar JA, Benhamou S, Benhamou E, et al. Cosmetic results following lumpectomy, axillary dissection and radiotherapy for small breast cancers. *Radiother Oncol*. 1988;12(4):273-280.
68. Liss AL, Ben-David MA, Jagsi R, et al. Decline of cosmetic outcomes following accelerated partial breast irradiation using intensity modulated radiation therapy: results of a single-institution prospective clinical trial. *Int J Radiat Oncol Biol Phys*. 2014;89(1):96-102.
69. Katz LM, Perez CA, Gerber NK, Purswani J, McCarthy A, Das IJ. Skin recurrence in radiation treatment of breast cancer. *And Radiat Oncol*. 2018;3(July/Sep):458-462.

70. Gerbi BJ, Meigooni AS, Khan FM. Dose buildup for obliquely incident photon beams. *Med Phys.* 1987;14(3):393-399.
71. Akino Y, Das IJ, Bartlett GK, Zhang H, Thompson E, Zook JE. Evaluation of superficial dosimetry between treatment planning system and measurement for several breast cancer treatment techniques. *Med Phys.* 2013;40(1):011714.
72. Duane F, Aznar MC, Bartlett F, et al. A cardiac contouring atlas for radiotherapy. *Radiother Oncol.* 2017;122(3):416-422.
73. Timothy J. Whelan BM, B.Ch., Jean-Philippe Pignol, M.D., Mark N. Levine, M.D., Jim A. Julian, Ph.D., Robert MacKenzie, M.D., Sameer Parpia, M.Sc., Wendy Shelley, M.D., Laval Grimard, M.D., Julie Bowen, M.D., Himu Lukka, M.D., Francisco Perera, M.D., Anthony Fyles, M.D., Ken Schneider, M.D., Sunil Gulavita, M.D., and Carolyn Freeman, M.D. Long-term results of hypofractionated radiation therapy for breast cancer. *N Eng J Med.* 2010;362:513-520.
74. Randomized phase III clinical trial evaluating post-mastectomy chestwall and regional nodal xrt and post-lumpectomy regional nodal xrt in patients with positive axillary nodes before neoadjuvant chemotherapy who convert to pathologically negative axillary nodes after neoadjuvant chemotherapy. *NSABP PROTOCOL B-51/RTOG PROTOCOL 1304.*
75. Kallman P, Agren A, Brahme A. Tumour and normal tissue responses to fractionated non-uniform dose delivery. *Int J Radiat Biol.* 1992;62(2):249-262.
76. Lyman JT. Complication probability as assessed from dose-volume histograms. *Radiat Res Suppl.* 1985;8:S13-19.
77. Kutcher GJ, Burman C, Brewster L, Goitein M, Mohan R. Histogram reduction method for calculating complication probabilities for three-dimensional treatment planning evaluations. *Int J Radiat Oncol Biol Phys.* 1991;21(1):137-146.
78. Seppenwoolde Y, Lebesque JV, de Jaeger K, et al. Comparing different NTCP models that predict the incidence of radiation pneumonitis. Normal tissue complication probability. *Int J Radiat Oncol Biol Phys.* 2003;55(3):724-735.
79. Kwa SL, Theuws JC, Wagenaar A, et al. Evaluation of two dose-volume histogram reduction models for the prediction of radiation pneumonitis. *Radiother Oncol.* 1998;48(1):61-69.
80. Moiseenko V, Craig T, Bezjak A, Van Dyk J. Dose-volume analysis of lung complications in the radiation treatment of malignant thymoma: a retrospective review. *Radiother Oncol.* 2003;67(3):265-274.
81. Gagliardi G, Constone LS, Moiseenko V, et al. Radiation dose-volume effects in the heart. *Int J Radiat Oncol Biol Phys.* 2010;76(3 Suppl):S77-85.
82. Utehina O, Popovs S, Purina D, et al. Analysis of cardiac and pulmonary complication probabilities after radiation therapy for patients with early-stage breast cancer. *Medicina (Kaunas).* 2009;45(4):276-285.
83. Korreman SS, Pedersen AN, Josipovic M, et al. Cardiac and pulmonary complication probabilities for breast cancer patients after routine end-inspiration gated radiotherapy. *Radiother Oncol.* 2006;80(2):257-262.
84. Edvardsson A, Nilsson MP, Amptoulach S, Ceberg S. Comparison of doses and NTCP to risk organs with enhanced inspiration gating and free breathing for left-sided breast cancer radiotherapy using the AAA algorithm. *Radiat Oncol.* 2015;10:84.
85. Gagliardi G, Lax I, Soderstrom S, Gyenes G, Rutqvist LE. Prediction of excess risk of long-term cardiac mortality after radiotherapy of stage I breast cancer. *Radiother Oncol.* 1998;46(1):63-71.
86. Almberg SS, Lindmo T, Frengen J. Superficial doses in breast cancer radiotherapy using conventional and IMRT techniques: a film-based phantom study. *Radiother Oncol.* 2011;100(2):259-264.

87. Soleymanifard S, Aledavood SA, Noghreiyani AV, Ghorbani M, Jamali F, Davenport D. In vivo skin dose measurement in breast conformal radiotherapy. *Contemp Oncol (Pozn)*. 2016;20(2):137-140.
88. Chakarova R, Gustafsson M, Back A, et al. Superficial dose distribution in breast for tangential radiation treatment, Monte Carlo evaluation of Eclipse algorithms in case of phantom and patient geometries. *Radiother Oncol*. 2012;102(1):102-107.
89. Chow JC, Jiang R, Leung MK. Dosimetry of oblique tangential photon beams calculated by superposition/convolution algorithms: a Monte Carlo evaluation. *J Appl Clin Med Phys*. 2010;12(1):3424.
90. Panettieri V, Barsoum P, Westermark M, Brualla L, Lax I. AAA and PBC calculation accuracy in the surface build-up region in tangential beam treatments. Phantom and breast case study with the Monte Carlo code PENELOPE. *Radiother Oncol*. 2009;93(1):94-101.
91. Dogan N, Glasgow GP. Surface and build-up region dosimetry for obliquely incident intensity modulated radiotherapy 6 MV x rays. *Med Phys*. 2003;30(12):3091-3096.
92. Early Breast Cancer Trialists' Collaborative G, Darby S, McGale P, et al. Effect of radiotherapy after breast-conserving surgery on 10-year recurrence and 15-year breast cancer death: meta-analysis of individual patient data for 10,801 women in 17 randomised trials. *Lancet*. 2011;378(9804):1707-1716.
93. Santiago RJ, Wu L, Harris E, et al. Fifteen-year results of breast-conserving surgery and definitive irradiation for Stage I and II breast carcinoma: the University of Pennsylvania experience. *Int J Radiat Oncol Biol Phys*. 2004;58(1):233-240.
94. Solin LJ, Kurtz J, Fourquet A, et al. Fifteen-year results of breast-conserving surgery and definitive breast irradiation for the treatment of ductal carcinoma in situ of the breast. *J Clin Oncol*. 1996;14(3):754-763.
95. Sardaro A, Petruzzelli MF, D'Errico MP, Grimaldi L, Pili G, Portaluri M. Radiation-induced cardiac damage in early left breast cancer patients: risk factors, biological mechanisms, radiobiology, and dosimetric constraints. *Radiother Oncol*. 2012;103(2):133-142.
96. Comsa D, Barnett E, Le K, et al. Introduction of moderate deep inspiration breath hold for radiation therapy of left breast: Initial experience of a regional cancer center. *Pract Radiat Oncol*. 2014;4(5):298-305.
97. Swanson T, Grills IS, Ye H, et al. Six-year experience routinely using moderate deep inspiration breath-hold for the reduction of cardiac dose in left-sided breast irradiation for patients with early-stage or locally advanced breast cancer. *Am J Clin Oncol*. 2013;36(1):24-30.
98. Formenti SC, Hsu H, Fenton-Kerimian M, et al. Prone accelerated partial breast irradiation after breast-conserving surgery: five-year results of 100 patients. *Int J Radiat Oncol Biol Phys*. 2012;84(3):606-611.
99. Huppert N, Jozsef G, DeWyngaert K, Formenti SC. The role of a prone setup in breast radiation therapy. *Front Oncol*. 2011;1 (October):31(31-38).
100. Taylor C, McGale P, Bronnum D, et al. Cardiac structure injury after radiotherapy for breast cancer: cross-sectional study with individual patient data. *J Clin Oncol*. 2018;36(22):2288-2296.
101. Stegman LD, Beal KP, Hunt MA, Fornier MN, McCormick B. Long-term clinical outcomes of whole-breast irradiation delivered in the prone position. *Int J Radiat Oncol Biol Phys*. 2007;68(1):73-81.
102. Gage I, Schnitt SJ, Recht A, et al. Skin recurrences after breast-conserving therapy for early-stage breast cancer. *J Clin Oncol*. 1998;16(2):480-486.
103. Cowen D, Houvenaeghel G, Jacquemier J, et al. [Local recurrences after conservative treatment of breast cancer: risk factors and influence on survival]. *Cancer Radiother*. 1998;2(5):460-468.

104. Boulle G, Saint-Martin C, De La Lande B, et al. Photons without bolus versus electrons with bolus after upfront mastectomy without immediate reconstruction in breast cancer patients. *Int J Radiat Oncol Biol Phys.* 2019;104(4):877-884.

Abbreviations

3D: Three-dimensional

AAA: Anisotropic Analytic Algorithm

ABC: Active Breathing Control

BC: Breast Cancer

BCS: Breast-Conserving Surgery

BEV: Beams Eye View

CT: Computed Tomography

CTV: Clinical Target Volume

DV: Dose Volume

DVH: Dose Volume Histogram

GTV: Gross Tumor Volume

HU: Hounsfield Unit

IMRT: Intensity Modulated Radiation Therapy

LAD: Left Anterior Descending Artery

LINAC: Linear Accelerator

LQ: Linear Quadratic

LV: Left Ventricle

MLC: Multi Leaf Collimator

MV: Mega Voltage

NTCP: Normal Tissue Complication Probability

OAR: Organs AT Risk

PDIBH: Prone Deep Inspiration Breath Hold

PFB: Prone Free Breathing

PTV: Planning Target Volume

RPM: Real Time Position Management

RT: Radiation Therapy

SDIBH: Supine Deep Inspiration Breath Hold

SFB: Supine Free Breathing

TCP: Tumor Control Probability

TPS: Treatment Planning System

TX: Treatment

V10: Volume of Organ Getting 10 Gy of Dose

V2.5: Volume of Organ Getting 2.5 Gy of Dose

V20: Volume of Organ Getting 20 Gy of Dose

V30: Volume of Organ Getting 30 Gy of Dose

V5: Volume of Organ Getting 5 Gy of Dose

VMAT: Volumetric Modulated Arc Therapy

CRT: Conformal Radiation Therapy

Appendix A: Lasers Based DIBH Procedure

A.1 Procedure 1: Computed Tomography (CT) Scan with Lasers Based DIBH

CT Scan in free-breathing and deep inspiration breath-hold using Lasers & cameras in the CT simulation room.

A.1.1 Prepare Patient

1. Bring the patient into room, explain the CT sim procedure.
2. Explain to the patient the DIBH procedure.
 - a. Two coaching sessions will be done to learn the extent of patients' ability to hold the breath for a sufficient period (usually 20 seconds or more) at a maximum inhalation point. (Deep inspiration breath should be to a higher-than-normal level. The patient should not be able to reach this higher level when breathing normally.)
 - b. Specific instructions will be given verbally to achieve deep inspiration breath-hold.
 - c. The first session occurs in the CT room where the patient is coached to follow the verbal commands and hold the breath for 20+ seconds.
 - d. The second session occurs using the free-breathing and breath-hold mark on the patient, where the consistent DIBH position will be determined.
3. Place patient on CT Table; for the supine position with both arms above head in Vac Lok, head turned to the unaffected side, knee sponge under knees; for prone position use prone board
4. Call the doctor into the wire scar and the breast.

5. Let patient breathe freely, once a patient is breathing normally, then place a mark on the patient with a sharpie where the isocenter of treatment lies during the free-breathing (2 lateral side marks and 1 mark anteriorly on the chest) with respect to fixed lasers
6. Instruct the patient to take in a deep breath and hold it, then place a mark on the patient with a sharpie where the iso lies during the breath-hold (2 lateral side marks and 1 mark anteriorly on the chest) with respect to lasers. Let the patient breath.
7. Please note down the distance between marks in free-breathing and breath-hold in anterior/posterior and superior/inferior directions.
8. Repeat Breath-hold after 2 minutes to ensure consistency of the breath-hold.
9. Ensure 2 dots of the patient are visible on an outside monitor attached to verify breath-hold during the scan. Adjust the camera if needed.
10. Ensure that lasers are on free-breathing marks with respect to lasers placed before free-breathing scan place marks and BB's on the patient.
11. Scan the patient with a free-breathing technique.
12. Begin in-room DIBH coaching first session.
13. Issue verbal commands
 - a. Relax and breathe normally
 - b. Take in a deep breath and (on my command), hold your breath
 - c. Breathe
14. Practice this with the patient, 2-3 times, aiming for a breath-hold of 20 seconds
 - a. Make sure patient marks are lined up and have the patient take a deep breath in and hold checking the breath-hold marks for consistency. Have the patient breath.
15. Ask the patient to take a deep breath and hold.
16. Scan the patient in breath-hold and ask the patient to breath as soon as the scan is over.
17. If the patient releases breath-hold or breath-hold drifts out of marked position w.r.t lasers, stop CT scan and repeat scan.

18. Have the patient relax and breathe normally.
19. If the patient is unable to hold the breath for 20 seconds, the patient may not be a candidate for DIBH. Consult with Physicians and Physics on how to proceed.
20. Take photos of set up and complete normal simulation tasks.
21. Explain to the patient that between now and when they return, they need to practice taking a deep breath in and holding it for 20-30 seconds several times a day. Let the patient dress. Explain that it takes approximately 1 week to complete the plan. And that we will call to schedule their first appointment as soon as the plan is complete and insurance authorizations are obtained.

A.2 Procedure 2: Treatment Procedure with Lasers Based DIBH

DIBH Treatment delivery using Lasers and High definition cameras installed in the treatment room with monitors located at the treatment console.

A.2.1 Prior to Bringing the Patient into the Treatment Room

1. Mode up the patient on Varian 4DITC.
2. Have the DIBH number paper printed with information on the distance between Free-breathing to DIBH marks on the patient along with the isocenter numbers.

A.2.2 Prepare Patient

1. Bring the patient into the room and give an overview as to what will occur during the new start procedure.
2. Review the DIBH procedure.
3. Position patient on the treatment table according to the simulation setup worksheet.
4. Align the patient to simulation marks.
5. Perform dosimetry shifts from the treatment plan. (Initial new Start)

6. Ensure that the High definition camera is on and zoom it to see the lasers on the free-breathing and the DIBH marks placed on the patient from outside. Adjust camera position if necessary.

A.2.3 Patient Coaching from Treatment Console

1. Prepare the HD camera and adjust so you can see the marks on the patient's skin clearly w.r.t lasers.
2. Coach patient on deep-inspiration-breath-hold via in-room speaker.
 - a. Allow the patient to relax
 - b. Give patient-specific instructions designed to achieve deep inspiration breath-hold
 - i. Relax and breathe normally.
 - ii. Take in a deep breath and (on my command), hold your breath.
 - iii. Verify using outside monitor attached to High definition cameras
 - iv. Confirm patient here at the breath-hold position for the required amount of time ~ 20 seconds.
 - v. Instruct the patient to breathe normally.
 - c. Repeat Step 2 a few times to determine patient can consistently achieve the DIBH position.

A.2.4 Perform Pretreatment Verification/Filming (KV)

1. Mode up KV field, move imager arms into position.
2. Give patient-specific instructions designed to achieve deep inspiration breath-hold.
 - a. Relax, breath normally.
 - b. Take in a deep breath and (on my command), hold your breath
 - c. Ensure that the patient achieves breath-hold position w.r.t marks on patients and lasers.
3. Press and hold footswitch/hand switch to acquire KV Image.

- a. (Press and hold the footswitch/hand switch several seconds before the beginning threshold is reached. This ensures that the tube is prepped in time for the X-Ray signal.)
4. Ask the patient to relax and breathe normally.
5. Repeat steps 2 through 5 for each image taken.

Note: When imaging is occurring, the image area displays the fluoroscopic image rather than the camera view.
6. Apply couch shifts at the Clinac Console.
7. Repeat KV images following steps 2 through 5 (based on the size of table shifts and Department protocol) and Step #8 if shifts are again applied.
8. Retract KV imager arms.

A.2.5 Perform Pretreatment Verification/Filming (MV)

1. Mode up MV image fields, move imager into position.
2. Turn on the Clinac key to Beam -On and the Clinac is in a green Ready State.
3. Give patient-specific instructions designed to achieve deep inspiration breath-hold.
 - a. Relax, breath normally.
 - b. Take in a deep breath and (on my command), hold your breath.
 - c. Ensure that the patient achieves breath-hold position w.r.t marks on patients and lasers.
4. While the patient is in breath-hold, Beam On.
5. Mode up 2nd portion of double image and Beam On while the patient remains in breath-hold state.
6. After a double exposure port completed, ask the patient to relax and breathe normally.
7. Repeat steps 1 thru 6 for each image taken.

(Note: When imaging is occurring, the image area displays the fluoroscopic image rather than the camera view.)

8. Apply couch shifts at the Clinac Console.
9. Repeat MV images following steps 1 through 6 (based on the size of table shifts and Department protocol) and Step #9 if shifts are again applied.
10. When imaging is complete click Stop. Do not enter Exam or Series #. Cancel.
11. Retract imager.

A.2.6 Begin Treatment

1. Mode up treatment field.
2. Give patient-specific instructions designed to achieve deep inspiration breath-hold.
 - a. Relax, breath normally.
 - b. Take in a deep breath and (on my command), hold your breath.
3. Ensure that the patient achieves breath-hold position w.r.t marks on patients and lasers.
4. While the patient is in breath-hold, Beam-on the treatment field.
8. Monitor the breath-hold using an HD camera
9. Mode up the next treatment field and follow steps 6 thru 8.
10. When all fields have been completed, click Stop.
11. Do not enter Exam or Series #, select Cancel.
12. Click Close Patient in the session panel.
13. Select Close in the Patient List dialog box and Exit program.
14. Turn the key in the gating switch box to the Disabled position to return the Clinac to non-gated operation.
15. Shutdown gating computer.
16. Turn off in the room camera.

Appendix B: Biological Evaluation Models and Parameters

Structure: Heart

Organ model

Tissue: Heart

Endpoint/Stage: Mortality (NTC)

Reference: Gagliardi, 1996

Volume: Whole

D50: 52.400 Gy

Y: 1.30

α/β : 3.000 Gy

Seriality: 1.00

Repair

Use parameters

T½ Long[h]: 4.00

T½ Short[h]: 0.30

Fraction with long repair time [%]: 50

OK Cancel

Figure B.1 Organ: heart; end point/stage: cardiac mortality; model: NTCP poisson-LQ.

Structure: Total_Lungs

Organ model

Tissue: Lung

Endpoint/Stage: Pneumonitis (1)

Reference: Kwa et al., Int. J.

Volume: Both lungs

D50: 30.500 Gy

α/β : 3.000 Gy

Parameter N: 1.00

Parameter M: 0.30

Repair

Use parameters

T $\frac{1}{2}$ Long[h]: 4.00

T $\frac{1}{2}$ Short[h]: 0.30

Fraction with long repair time [%]: 50

OK Cancel

Figure B.2 Organ: lung; end point/stage: pneumonitis (1) grade ≥ 2 ; model: NTCP lyman.

Structure: Total_Lungs

Organ model

Tissue: Lung

Endpoint/Stage: Pneumonitis (2)

Reference: Seppenwoolde et

Volume: Both lungs

D50: 30.800 Gy

α/β : 3.000 Gy

Parameter N: 0.99

Parameter M: 0.37

Repair

Use parameters

T $\frac{1}{2}$ Long[h]: 4.00

T $\frac{1}{2}$ Short[h]: 0.30

Fraction with long repair time [%]: 50

OK Cancel

Figure B.3 Organ: lung; end point/stage: pneumonitis (2) grade ≥ 2 ; model: NTCP lyman.

Structure: Total_Lungs

Organ model

Tissue: Lung

Endpoint/Stage: Symptomatic

Reference: Moiseenko et al.

Volume: Both lungs

D50: 21.900 Gy

α/β : 3.000 Gy

Parameter N: 0.37

Parameter M: 0.80

Repair

Use parameters

T $\frac{1}{2}$ Long[h]: 4.00

T $\frac{1}{2}$ Short[h]: 0.30

Fraction with long repair time [%]: 50

OK Cancel

Figure B.4 Organ: Lung; End point/stage: Symptomatic or Radiographic pneumonitis (≤ 6 months); Model: NTCP Lyman.

Structure: Total_Lungs

Organ model

Tissue: Lung

Endpoint/Stage: Symptomatic

Reference: Moiseenko et al.

Volume: Both lungs

D50: 21.000 Gy

α/β : 3.000 Gy

Parameter N: 1.02

Parameter M: 0.26

Repair

Use parameters

T $\frac{1}{2}$ Long[h]: 4.00

T $\frac{1}{2}$ Short[h]: 0.30

Fraction with long repair time [%]: 50

OK Cancel

Figure B.5 Organ: lung; end point/stage: symptomatic or radiographic pneumonitis (≤ 6 months); model: NTCP Lyman.

Add Function

Structure: Total_Lungs

Organ model

Tissue: Lung

Endpoint/Stage: Symptomatic

Reference: Moiseenko et al.

Volume: Both lungs

D50: 28.800 Gy

α/β : 3.000 Gy

Parameter N: 0.34

Parameter M: 0.50

Repair

Use parameters

T $\frac{1}{2}$ Long[h]: 4.00

T $\frac{1}{2}$ Short[h]: 0.30

Fraction with long repair time [%]: 50

OK Cancel

Figure B.6 Organ: lung; end point/stage: symptomatic or radiographic fibrosis; model: NTCP lyman

Add Function

Structure: Total_Lungs

Organ model

Tissue: Lung

Endpoint/Stage: Symptomatic

Reference: Moiseenko et al.

Volume: Both lungs

D50: 25.000 Gy

α/β : 3.000 Gy

Parameter N: 0.15

Parameter M: 0.85

Repair

Use parameters

T $\frac{1}{2}$ Long[h]: 4.00

T $\frac{1}{2}$ Short[h]: 0.30

Fraction with long repair time [%]: 50

OK Cancel

Figure B.7 Organ: lung; end point/stage: symptomatic fibrosis (>6 months); model: NTCP lyman

Appendix C: Published Study 1—Evaluation of Sparing Organs at Risk in Left-Sided Breast Irradiation in the Supine and Prone Positions with Deep Inspiration Breath Hold

Evaluation of sparing organs at risk (OARs) in left-breast irradiation in the supine and prone positions and with deep inspiration breath-hold

Amitpal Singh Saini^{1,2} | Catherine S. Hwang² | Matthew C. Biagioli² | Indra J. Das³

¹Department of Medical Engineering,
University of South Florida, Tampa, FL, USA

²Department of Radiation Oncology, Florida
Hospital Cancer Institute, Orlando, FL, USA

³Department of Radiation Oncology, NYU
Langone Medical Center, Laura and Isaac
Perlmutter Cancer Center, New York, NY,
USA

Author to whom correspondence should be
addressed: Amitpal Singh Saini
E-mail: amitpal.saini@fhsop.org

Abstract

Purpose: To compare doses to organs at risk (OARs) for left-sided whole-breast radiation therapy with comparable planning target volume (PTV) coverage using three techniques: free breathing in a supine position (SFB), deep inspirational breath-hold in a supine position (SDIBH), and free breathing in prone position (PFB).

Materials and methods: Thirty-three patients with left-sided early-stage breast cancer underwent CT simulation following SFB, SDIBH, and PFB protocols for whole-breast radiation therapy. One radiation oncologist contoured the breast PTV, heart, left ventricle (LV), and left anterior descending artery (LAD). Treatment plans were optimized using field-in-field technique with the AAA algorithm. Each plan was optimized to provide identical coverage to the PTV such that a reasonable comparison for OAR dosimetry could be evaluated. All plans were prescribed 42.56 Gy in 16 fractions to the left-breast PTV.

Results: The mean dose in SFB for the heart, LV, and LAD was 1.92, 3.19, and 21.73 Gy, respectively, which were significantly higher than the mean dose in SDIBH for the heart (1.08 Gy, $P \leq 0.0001$), LV (1.50 Gy, $P \leq 0.0001$), and LAD (6.3 Gy, $P \leq 0.0001$) and in PFB for the heart (0.98 Gy, $P \leq 0.0001$), LV (1.34 Gy, $P \leq 0.0001$), and LAD (6.57 Gy, $P \leq 0.0001$). Similar findings were noted for the cardiac components in SFB for V2.5, V5, V10, V20, and V30 compared with values in SDIBH and PFB. The mean dose for the left lung in PFB was 0.61 Gy that was significantly lower than in SFB (5.63 Gy, $P \leq 0.0001$) and SDIBH (5.54 Gy, $P \leq 0.0001$). Mean dose and dosimetric values for each OAR increased in SFB and SDIBH for patients with a large breast volume compared with values for patients with a small breast volume.

Conclusions: SFB results in higher heart, LAD, and LV doses than the other techniques. Both PFB and SDIBH are more advantageous for these OARs irrespective of breast volume. PFB results in significantly lower lung doses than SFB and SDIBH. PFB always provided better results than SFB for the heart, LV, LAD, and lung. This conclusion contrasts with some published studies concluding that the prone position has no benefit for heart sparing.

This is an open access article under the terms of the Creative Commons Attribution License, which permits use, distribution and reproduction in any medium, provided the original work is properly cited.

© 2018 The Authors. *Journal of Applied Clinical Medical Physics* published by Wiley Periodicals, Inc. on behalf of American Association of Physicists in Medicine

J Appl Clin Med Phys 2018; 19:4:195–204

wileyonlinelibrary.com/journal/jacmp | 195

PACS

87.55.D, 87.55.de, 87.55.dk, 87.55.GH, 87.55.kh, 87.55.ne

KEY WORDS

cardiac toxicity, deep inspiration breath-hold, heart dose, LAD dose, left ventricle dose, Lt breast radiation, lung dose, prone position, supine position

1 | INTRODUCTION

Lumpectomy followed by whole-breast radiation therapy is considered the standard of care for the treatment of early-stage breast cancer.¹ While radiation therapy reduces the risk of local recurrence by 26% at 5 yr and improves overall survival by 5% at 15 yr, it is also associated with increased toxicity.²

Treatment of left-sided breast cancers, in particular, results in increased risks of cardiac diseases and ischemic heart events,²⁻⁵ and radiation doses delivered to the heart, left anterior descending artery (LAD), and lungs when patients are in a supine position remain significant.⁶⁻⁸ Darby et al.² reported that an increase of 1 Gy to the mean dose to the heart results in a 7.4% relative increase in the risks of major coronary events. Another study demonstrated a significant increase in nonbreast-cancer-related mortality from heart disease with relative risk (RR, 1.27) and lung cancer (RR, 1.78) associated with breast radiation.² However, these results are based on data using older radiation techniques and treatment modalities.

Modern radiation techniques, such as 3-dimensional conformal radiation therapy (3DCRT), intensity-modulated radiation therapy (IMRT), and volumetric-modulated arc therapy (VMAT), are considered to decrease cardiac and pulmonary doses, while providing excellent coverage to the target volume with proper optimization.^{5,9-11}

With advances in cancer diagnosis and management techniques, patients are diagnosed early and live longer and are, therefore, at increased risk of developing long-term complications from the treatment. Different techniques are used to reduce doses to organs at risk (OARs) without compromising coverage of the target volume. Deep inspiration breath-hold (DIBH) is one such technique that has been shown to reduce cardiac doses.^{12,13} Breast radiation while in a prone position is another technique that is utilized to minimize the dose to the heart and underlying lung.¹⁴⁻¹⁷ However, no consensus has been reached in terms of the best treatment strategy between techniques utilizing free breathing in a supine position and in a prone position.^{13,16,18-23}

The aim of this study is to compare dosimetric parameters of various OARs in three different treatment positions for the same patient during left-sided whole-breast radiation therapy: a standard free-breathing supine position (SFB), a supine position with a deep inspiration breath-hold (SDIBH), and a free-breathing prone position (PFB). In addition, dosimetric parameters were also evaluated and compared for three positions with respect to the breast volume of the patients.

2 | MATERIALS AND METHODS

Between August 2015 and July 2016, 33 patients underwent whole-breast radiation therapy for early-stage left-breast cancer (pathologic T1-2N0 disease) were included in this retrospective study with approval from the institutional review board (IRB). Eligibility was not restricted based on the size or volume of the breast or the whole-breast planning target volume (PTV). Only those patients who could follow instructions and hold their breath for a minimum of 25 s were considered suitable to be included in this study. A Vac-Lock positioning cushion was used to immobilize patients in the supine position. A Bionix prone-positioning breast board and Vac-Lock cushion were used to immobilize patients in the prone position. Prior to scanning, the radiation oncologist marked the borders of the breast with a radio-opaque wire. All scans were performed with a GE light speed RT scanner, model no 2266521.

The patients were first CT scanned in the SFB position, the second CT scan was done according to the SDIBH protocol established in our institution, and the third CT scan was done following the PFB protocol. Our SDIBH protocol entailed marking the patient in the medial and lateral directions with respect to CT lasers while breathing freely. Patients were then coached to take deep breath and hold it. New positions in the medial and lateral directions were marked on the patient's skin. Patients were again asked to take deep breath so that the CT simulation therapist could verify the consistency of the breath with respect to the lasers. Audio coaching was used to guide the patients through the breath-holding process. High-definition cameras were installed in the treatment room to clearly observe the marks made during the SDIBH procedure from outside. These cameras were also used to check the position of the patients during treatment with respect to the lasers. Table 1 presents the SDIBH simulation data sheet used during CT simulation to record positional shifts with respect to laser marks during the SFB protocol. After CT simulation following the SDIBH protocol, a third CT scan was taken following the PFB protocol. Figs 1(a)-1(c) shows typical scans and beam placement on a patient indicating anatomy and locations in various techniques.

TABLE 1 Table for recording SDIBH measurements.

Voluntary breath-hold details
Max breath-hold achieved (sec)
Anterior FB bb and BH bb, distance (mm)
Lateral FB bb and BH bb, distance (mm)

After the CT scans were obtained, images were transferred to the treatment planning system (TPS). At our institute (Florida Hospital Cancer Center), we use Eclipse TPS (Varian Medical System, version 11, Palo Alto, CA, USA). One radiation oncologist who specializes in breast contoured the breast PTV, heart, LV, LAD, and contralateral breast of each patient using the RTOG-1304²⁴ guidelines and RTOG Breast Cancer Atlas for planning (<https://www.rtog.org/CoreLab/ContouringAtlases/BreastCancerAtlas.aspx>). According to the atlas, breast was defined as all apparent CT glandular breast tissue, while taking into account the RTOG consensus definition of anatomical borders. Cranial border was defined at the second rib insertion. Caudal border was defined as the loss of CT apparent breast tissue. Anterior boundary was defined as the skin. Posterior boundary was the anterior aspect of the pectoralis muscles. Medial border was the sternal-rib junction and lateral border was at the mid-axillary line. The LAD was defined as the vessel that descended anteriolaterally from the anterior interventricular groove down to the apex of the heart.²⁵ Cardiac contouring started superior at the level of the great vessel insertion into the heart and extended inferior to the apex of the heart. Contours were drawn by one physician for consistency. The lungs were contoured using an automatic segmentation tool available in Eclipse TPS, and lung contours were manually edited by physician as needed. Breast PTVs were cropped 5 mm from the skin surface for planning purposes as dosimetry in the buildup region is not well defined.²⁶ The contralateral breast was not cropped from the skin surface.

Treatments for all patients were planned with a field-in-field (FIF) tangential beam technique, and no wedges were used in any plan. Only a 6-MV beam was used for all three techniques. Treatments for all patients were planned using a hypofractionated fractionation scheme as defined by Whelan et al.²⁷ Doses were prescribed as a total dose of 42.56 Gy in 16 fractions. Dose calculations were performed using the Anisotropic Analytical Algorithm (AAA Version 11.0.31) with a grid size of $0.25 \times 0.25 \text{ cm}^2$. Treatment plans were normalized to an isocenter placed in the PTV. As per the RTOG-1304 protocol, a 7-mm margin was added to the PTV to form the field shapes using MLC.²⁴ All plans were optimized according to specified constraints to ensure that the data were comparable, and 95% of the PTV was prescribed to receive 100% of the prescribed dose while achieving maximum sparing of OARs. Dose-volume histograms were used to analyze the dosimetry in PTV, dose homogeneity, and doses to OARs. Dosimetric values for the mean dose, V2.5, V5, V10, V20 and V30, were recorded and evaluated for all OARs. In addition, dosimetric parameters were also evaluated within each technique with respect to a small and large breast volume.

2.A | Statistical analysis

The mean dose, V2.5, V5, V10, V20, and V30, was compared between SFB and SDIBH, SFB and PFB, and SDIBH and PFB plans. All the dosimetry parameters for the heart, LV, LAD, and left lung were determined using a Wilcoxon signed-rank test for related

sample with SPSS statistical software, version 23.0, as data had a non-normal distribution. Data were considered statistically significant at a P value ≤ 0.05 .

3 | RESULTS

3.A | Volume analysis

Heart volume was smallest in PFB and largest in SFB. Mean heart volume was 592.4 cm^3 (range, $380\text{--}967 \text{ cm}^3$), 554 cm^3 (range, $370\text{--}712 \text{ cm}^3$), and 544 cm^3 (range, $354\text{--}756 \text{ cm}^3$) for SFB, SDIBH, and PFB, respectively. Whole-breast PTV volumes ranged between 330 and 1723 cm^3 . Mean whole-breast PTV volume was 654.2 cm^3 (range, $299.8\text{--}1641 \text{ cm}^3$), 660.6 cm^3 (range, $253.2\text{--}1650.1 \text{ cm}^3$), and 685.9 cm^3 (range, $302\text{--}1723 \text{ cm}^3$) for SFB, SDIBH, and PFB, respectively. Thus, mean whole-breast PTV volume was highest in PFB and lowest in SFB.

Based on a literature search, a breast volume of 750 cm^3 was chosen to divide the patients into two groups: patients with a small breast volume and patients with a large breast volume in this study.^{22,23} Patients with a breast PTV $< 750 \text{ cm}^3$ were considered to have small breasts, and patients with a breast PTV $\geq 750 \text{ cm}^3$ were considered to have large breasts. From the 33 patients evaluated in this study, 21 were considered to have small breasts, and 12 patients were considered to have large breasts.

3.B | Dosimetric analysis

The mean dose to the heart was reduced by 50% in SDIBH and PFB as compared with the dose in SFB. The mean dose to heart in SFB was 1.92 Gy, compared with 1.11 Gy in SDIBH and 0.98 Gy in PFB, as shown in Fig. 2(a). Statistically significant differences were found for mean doses to the heart between SFB and SDIBH ($P \leq 0.0001$) and between SFB and PFB ($P \leq 0.0001$); however, no statistically significant difference was found between SDIBH and PFB ($P = 0.114$). Out of 33 patients, only one patient has higher mean heart dose in PFB as compared with SFB. All other dosimetric values were higher in SFB than in SDIBH and PFB, as shown in Table 2(a).

Mean LV dose was reduced by 47% in SDIBH and PFB compared with the dose in SFB. The LV received the largest mean dose, 3.19 Gy in SFB and received doses of 1.5 Gy in SDIBH and 1.34 Gy in PFB, as shown in Fig. 2(b). The mean dose to the LV was significantly reduced between SFB and SDIBH ($P \leq 0.0001$) and between SFB and PFB ($P \leq 0.0001$), but no statistically significant difference was found between SDIBH and PFB ($P = 0.137$). Out of 33 patients, only one patient has higher mean LV dose in PFB as compared with SFB. The LV dosimetry values were also found to be higher in SFB than in SDIBH and PFB. A marginally lower dosimetric values in PFB was observed compared with SDIBH, as shown in Table 2(b).

The mean LAD dose was highest, 21.73 Gy, in SFB and was 6.30 Gy in SDIBH and 6.57 Gy in PFB, as shown in Fig. 2(c). SDIBH and PFB resulted in a 70% reduction in the mean LAD

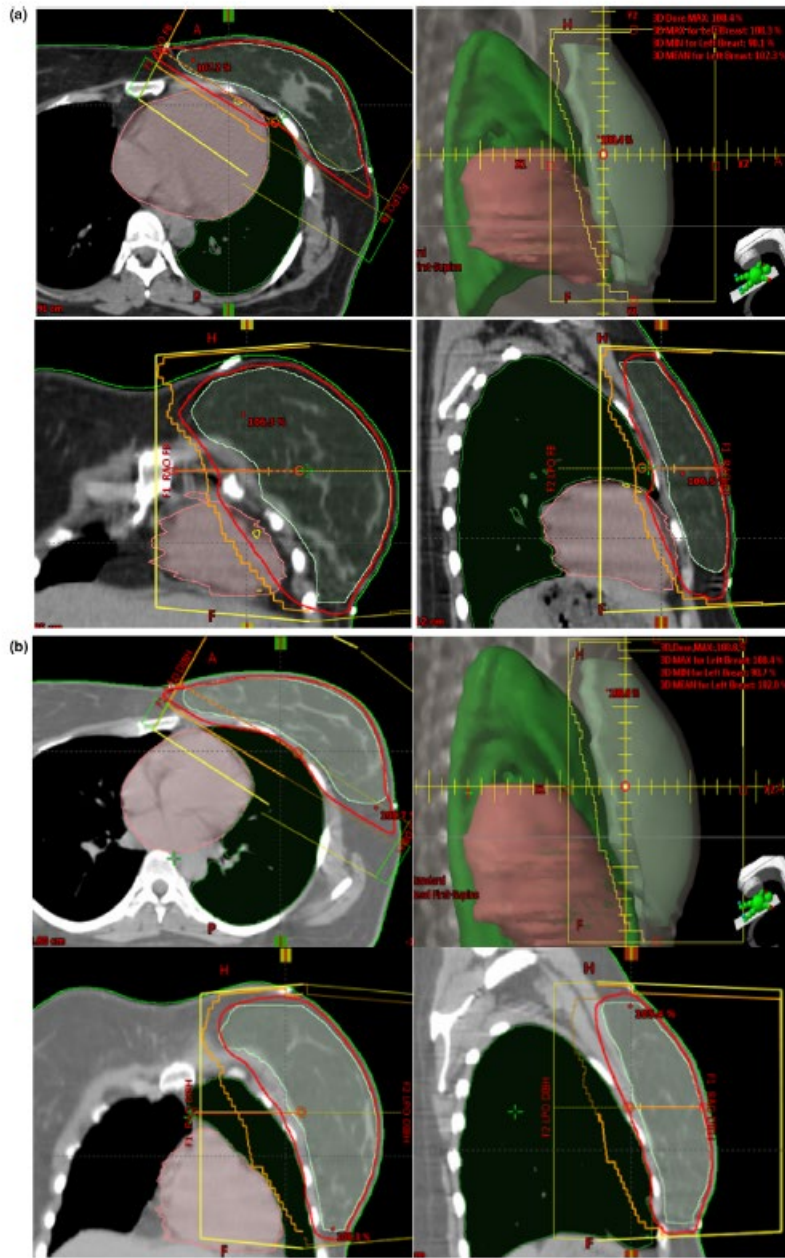


FIG. 1. Clockwise, axial, beam's eye view, sagittal, and coronal images. Green line indicates PTV, red indicates 95% isodose line, orange indicates MLC field shape, and yellow indicates beam outline. Heart and lung volumes are also shown. (a) Supine free breathing (SFB), (b) supine deep inspirational breath-hold (SDIBH) and (c) prone-free breathing (PFB). Note the heart and lung positions in three techniques with respect to beam geometry.

dose compared with the dose in SFB. The mean dose for LAD was significantly reduced between SFB and SDIBH ($P \leq 0.0001$) and between SFB and PFB ($P \leq 0.0001$), but no statistically significant reduction in dose was found between SDIBH and PFB ($P = 0.122$). Out of 33 patients, six patients had higher mean LAD dose in PFB as compared with SFB. The LAD dosimetric parameters were also higher in SFB than in SDIBH and PFB, as shown in Table 2(c).

The mean dose to the lung was reduced by 89% in PFB compared with doses in SFB and SDIBH. The lung received 5.63 Gy in SFB, 5.54 Gy in SDIBH, and 0.61 Gy in PFB, as shown in Fig. 2(d). Differences in mean doses to the lung were not statistically significant between SFB and SDIBH ($P = 0.964$), but doses were significantly different between SFB and PFB ($P \leq 0.0001$) and between SDIBH and PFB ($P \leq 0.0001$). All other dosimetric values for the lung were also the lowest in PFB, as shown in Table 2(d).

The P values were also calculated for all the OARs and for all dosimetric parameters to identify statistically significant differences between the techniques, as shown in Table 3. SDIBH and PFB were significantly better than SFB according to all the dosimetric parameters for the heart, LV, and LAD, but there was no significant difference between SDIBH and PFB, except in V5 for the LAD. The left lung was significantly less at risk in PFB than in SFB and SDIBH for all the dosimetric parameters evaluated in this study.

3.C | Dosimetric analysis based on breast volume

Mean doses to all OARs in patients based on breast PTV are shown in Table 4. Differences for all dosimetric parameters between all three techniques with respect to small and large breast volumes are shown in Table 5. Doses to the heart, LV, LAD, and lung in SFB and

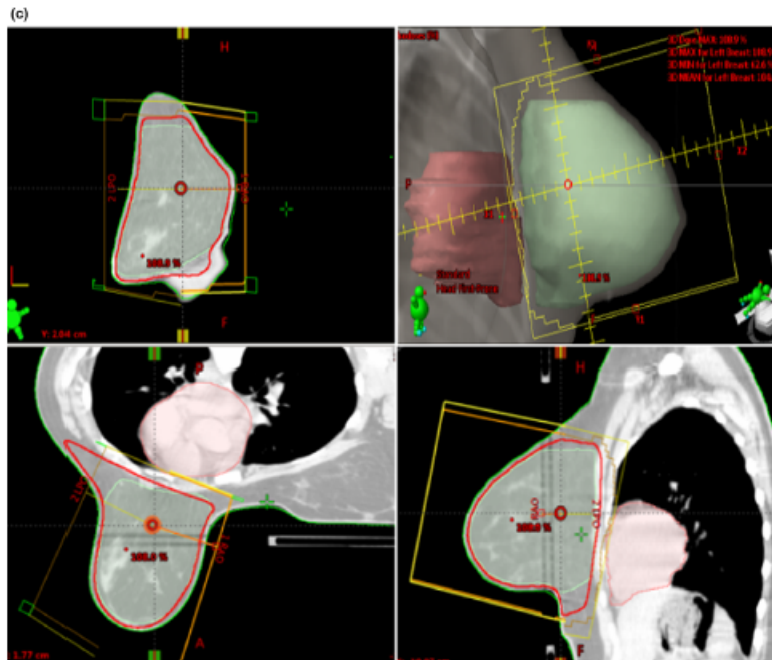


FIG. 1b. Continued.

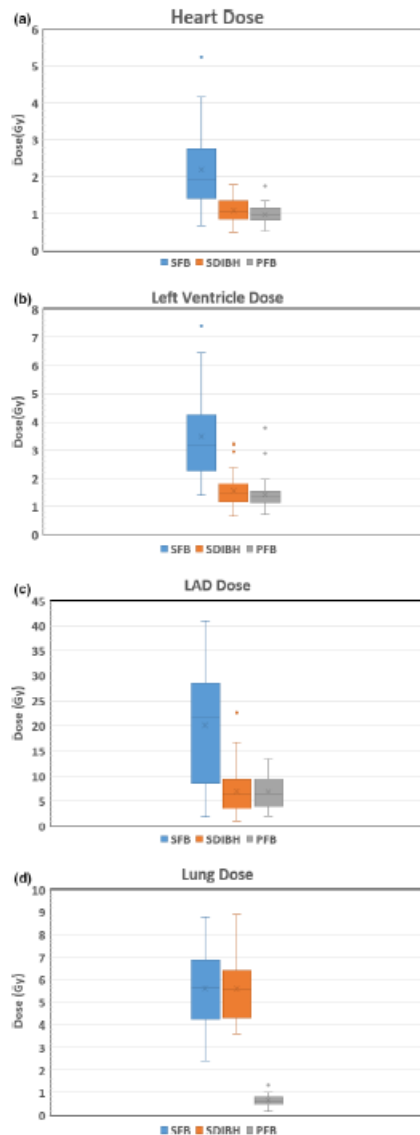


FIG. 2. Box-whisker plot of dose with error bars in supine free breathing (SFB), supine deep inspiration breath-hold (SDIBH), and prone free-breathing (PFB) techniques. Outlier data are shown if they existed for (a) heart, (b) left ventricle (LV), (c) left anterior descending artery (LAD), and (d) lung.

SDIBH are higher for large-volume breasts than for small-volume breasts. In contrast, in PFB, most of the dosimetric values for all of the OARs were lower for patients with large breasts.

4 | DISCUSSION

Radiation-induced cardiac toxicity and injury after radiation therapy treatment for left-sided breast cancers are well documented in the literature.^{2-5,26} The rate of major coronary events increases linearly with mean radiation doses to the heart without any threshold.^{3,5,28} Thus, it is important to find treatment techniques that will lower the dose to cardiac components without compromising the target coverage.

Das et al.²⁹ provided an analytical approach correlating lung and heart doses to pulmonary and cardiac complication rates. Therefore, it is also important to reduce doses to OARs such as the left lung and contralateral breast to reduce the risk of pneumonitis, lung fibrosis, and secondary cancers, especially in patients who are expected to have long-life expectancies.²⁻⁴

The PFB uses gravity to pull the treated breast away from the heart and lung, thus resulting in dose reduction to OARs. Also, in PFB, with careful planning, one can minimize the treatment fields going through the heart without compromising PTV coverage. A literature search yielded mixed results on the benefits of PFB for heart sparing. Some studies have reported that the prone position reduces heart doses,^{15,23} but other studies have concluded that this position is only beneficial for patients with a large breast volumes.^{14,16,22} It has been reported that in some patients, heart doses in the prone position increase because of the proximity of the heart to the treated area.^{14,20} A few studies have indicated that PFB provides no benefits for sparing the heart.^{21,30} Formenti et al.²³ reported that the benefits of PFB are statistically significant compared with the results of SFB when breast volume is larger than 750 cm³.

Our results suggest that the mean heart dose can be reduced by almost half using SDIBH and PFB compared with using SFB. When the patient takes a deep breath, the heart moves posteriorly and inferiorly due to lung expansion and diaphragmatic movements. Thus, the heart moves away from the chest wall. Moving of heart during SDIBH helps in reducing the volume of the heart in the treatment field, reducing the dose to the heart. The mean dose and values for all the dosimetric parameters were lowest in PFB for the LV. It is believed that the dose to the LAD plays a vital role in radiation-induced cardiac toxicity.³¹⁻³³ The mean dose to the LAD was found to be similar for SDIBH and PFB, and highest mean dose was in SFB. In a similar study, Venhoven et al.³⁰ concluded that PFB results in higher doses to the heart and LAD than the SFB and SDIBH techniques, but the results of our study are different as both SDIBH and PFB led to lower heart and LAD doses than SFB, irrespective of the breast volume. A significant reduction in V2.5, V5, V10, V20 and V30 for the heart, LV and LAD in SDIBH and PFB was observed compared with values in SFB.

Table 2 Dosimetry parameters (median values and quartiles) in supine free breathing (SFB), supine deep inspiration breath-hold (SDIBH), and prone free-breathing (PFB) techniques. (a) Heart, (b) left ventricle (LV), (c) left anterior descending artery (LAD), and (d) left lung.

	SFB	SDIBH	PFB
(a) Heart dose (Gy)			
Mean dose	1.92 (1.42–2.76)	1.08 (0.84–1.36)	0.98 (0.83–1.15)
V2.5	14.60 (9.27–22.34)	7.20 (3.98–11.46)	6.30 (4.47–8.89)
V5	4.81 (2.73–7.35)	0.90 (0.22–1.92)	0.80 (0.275–1.61)
V10	2.66 (1.43–4.58)	0.11 (0.00–0.86)	0.10 (0.01–0.47)
V20	1.74 (0.79–3.21)	0.00 (0.00–0.20)	0.00 (0.00–0.12)
V30	1.15 (0.23–2.34)	0.00 (0.00–0.17)	0.00 (0.00–0.00)
(b) Left ventricle dose (Gy)			
Mean dose	3.19 (2.25–4.24)	1.50 (1.15–1.80)	1.34 (1.13–1.54)
V2.5	30.00 (18.84–39.00)	11.54 (7.46–19.08)	8.92 (6.01–12)
V5	9.23 (5.24–14.23)	1.05 (0.38–3.29)	0.92 (0.43–1.88)
V10	5.01 (2.34–9.65)	0.00 (0.00–1.05)	0.30 (0.00–0.55)
V20	3.10 (1.29–6.27)	0.00 (0.00–0.19)	0.00 (0.00–0.15)
V30	2.04 (0.27–4.61)	0.00 (0.00–0.00)	0.00 (0.00–0.00)
(c) LAD dose (Gy)			
Mean dose	21.73 (8.55–28.5)	6.30 (3.51–9.31)	6.57 (3.99–9.49)
V2.5	95.70 (85.32–99.37)	84.62 (68.90–90.65)	87.50 (74.83–93.93)
V5	74.91 (55.86–93.16)	39.52 (11.12–61.87)	54.46 (27.45–66.70)
V10	61.50 (27.79–81.50)	12.66 (0.03–40.45)	19.50 (4.28–35.25)
V20	48.90 (13.30–73.27)	0.00 (0.00–9.02)	0.96 (0.00–9.49)
V30	36.33 (0.91–58.80)	0.00 (0.00–0.19)	0.00 (0.00–0.23)
(d) Left lung dose (Gy)			
Mean dose	5.63 (4.23–6.86)	5.54 (4.29–6.42)	0.61 (0.47–0.80)
V2.5	30.60 (25.75–38.3)	34.90 (28.04–39.21)	2.52 (1.85–4.49)
V5	19.99 (15.97–25.00)	21.23 (16.30–25.25)	0.95 (0.34–1.61)
V10	13.27 (9.76–17.16)	13.14 (9.84–16.37)	0.38 (0.05–0.865)
V20	9.84 (6.39–12.98)	9.34 (6.79–11.73)	0.10 (0.0–0.32)
V30	7.54 (4.78–10.26)	7.15 (4.81–8.79)	0.01 (0.0–0.13)

We found equivocal results related to the reduction of radiation doses to the heart in PFB in the literature search. However, all studies agree that lung dose are dramatically reduced in PFB compared with doses in SFB and SDIBH.^{14–17,21–23,30} Lung doses are significantly lower in PFB than in SFB and SDIBH. The lung density of the irradiated lung volume decreases also in SDIBH.^{10,15,30} One study mentioned that the opposite occurs in PFB, as the lungs are pushed downward by gravity and consequently lung density may increase.³⁰ However, PFB showed clear advantages over SFB and SDIBH for lowering lung doses and the values of most other dosimetric parameters compared with SFB in this study.

We did not find any other study in literature search that has evaluated the heart, LV, LAD, and lung for V2.5, V5, V10, V20, V30 and statistically compared each dosimetric parameter between the techniques and that has also compared dosimetric differences in OARs for SFB, SDIBH, and PFB with respect to breast volume. Mean doses evaluated for each OAR increased in SFB and SDIBH

going from patients with small to large breast volumes, as shown in Table 4. This is because as breast volume increases, the separation between fields also increases, thus irradiating a larger volume to cover the PTV adequately. A large breast volume also requires wider beams to cover it, thus radiating a larger volume in SFB and SDIBH and leading to higher doses to cardiac components and the lung.

An interesting observation is that differences in doses and in dosimetric parameters evaluated between SFB and SDIBH and between SFB and PFB increased from patient with small to large breast volumes, as shown in Table 5. Thus, SDIBH and PFB are even more beneficial than SFB for patients with large breasts.

5 | CONCLUSION

It is concluded that radiation dose can be significantly reduced to the heart, LV, LAD, and lung with the selection of the proper

TABLE 3 P value between PFB and SDIBH, PFB and SFB, PFB and SDIBH for all the dosimetric parameters of heart, LV, LAD, and lung. Please note that P values for heart, LV, LAD are statistically significant between SDIBH and SFB, and PFB and SFB. P values ≤ 0.05 were considered statistically significant.

Dose/volume	Technique	Heart	LV	LAD	Lung
Mean	SDIBH and SFB	0.000	0.000	0.000	0.964
	PFB and SFB	0.000	0.000	0.000	0.000
	PFB and SDIBH	0.114	0.137	0.122	0.000
V2.5	SDIBH and SFB	0.000	0.000	0.000	0.0080
	PFB and SFB	0.000	0.000	0.034	0.0000
	PFB and SDIBH	0.242	0.055	0.211	0.0000
V5	SDIBH and SFB	0.000	0.000	0.000	0.0560
	PFB and SFB	0.000	0.000	0.000	0.0000
	PFB and SDIBH	0.936	0.335	0.007	0.0000
V10	SDIBH and SFB	0.000	0.000	0.000	0.7791
	PFB and SFB	0.000	0.000	0.000	0.0000
	PFB and SDIBH	0.765	0.746	0.153	0.0000
V20	SDIBH and SFB	0.000	0.000	0.000	0.6739
	PFB and SFB	0.000	0.000	0.000	0.0000
	PFB and SDIBH	0.932	0.935	0.627	0.0000
V30	SDIBH and SFB	0.000	0.000	0.000	0.5143
	PFB and SFB	0.000	0.000	0.000	0.0000
	PFB and SDIBH	0.569	0.311	0.955	0.0000

TABLE 4 Dosimetric parameters (median values and quartiles) of OARs in SFB, SDIBH, and PFB based on breast PTV volume $<750 \text{ cm}^3$ and $\geq 750 \text{ cm}^3$. Please note that PFB has the lowest mean values for heart, LV, LAD, and lung for breast PTV volume $\geq 750 \text{ cm}^3$.

Breast PTV volume $<750 \text{ cm}^3$	SFB	SDIBH	PFB
Mean heart dose (Gy)	1.65 (1.12–2.32)	0.87 (0.71–1.21)	0.90 (0.81–1.10)
Mean LV dose (Gy)	2.93 (1.85–4.04)	1.30 (1.01–1.70)	1.32 (1.13–1.50)
Mean LAD dose (Gy)	19.86 (7.85–25.1)	5.97 (3.01–8.53)	6.5 (3.58–9.16)
Mean lung dose (Gy)	5.48 (3.93–6.52)	5.06 (4.09–6.38)	0.61 (0.48–0.97)
Breast PTV volume $\geq 750 \text{ cm}^3$			
Mean heart dose (Gy)	2.59 (1.87–4.06)	1.36 (0.97–1.62)	1.07 (0.87–1.31)
Mean LV dose (Gy)	3.61 (3.02–5.77)	1.72 (1.40–2.11)	1.2 (1.11–1.58)
Mean LAD dose (Gy)	24.74 (10.22–36.75)	7.05 (3.27–12.99)	6.7 (4.51–9.93)
Mean lung dose (Gy)	5.69 (4.77–7.08)	5.7 (5.23–7.06)	0.57 (0.36–0.68)

TABLE 5 Dosimetric differences of median values between each technique, that is, SFB-SDIBH, SFB-PFB, SDIBH-PFB, based on breast PTV volume

Breast PTV volume $<750 \text{ cm}^3$	SFB-SDIBH	SFB-PFB	SDIBH-PFB
Mean heart dose (Gy)	0.78	0.75	-0.03
Mean LV dose (Gy)	1.63	1.61	-0.02
Mean LAD dose (Gy)	13.96	13.36	-0.6
Mean lung dose (Gy)	0.42	4.87	4.45
Breast PTV volume $\geq 750 \text{ cm}^3$			
Mean heart dose (Gy)	1.235	1.525	0.29
Mean LV dose (Gy)	1.89	2.415	0.525
Mean LAD dose (Gy)	17.695	18.045	0.35
Mean lung dose (Gy)	-0.005	5.12	5.125

technique. PFB is obviously preferred dosimetrically over SFB and SDIBH. PFB is more beneficial than SFB for OARs sparing irrespective of breast volumes. SDIBH and PFB deliver lower doses to cardiac components than SFB. PFB delivers significantly lower lung doses than SFB and SDIBH. Thus, PFB could be the treatment of choice for patients with underlying pulmonary diseases. In addition, a patient-specific analysis, patient anatomy, patient comfort, selection of beam arrangements, and breathing patterns should be given consideration in the selection process of techniques to treat breast cancer.

ACKNOWLEDGMENTS

Authors acknowledge the radiation therapist of Florida hospital cancer institute at Altamonte Springs for assistance in CT simulation using three techniques and SDIBH set up of patients in treatment room.

CONFLICT OF INTEREST

No conflict of interest to declare.

REFERENCES

- Fisher B, Anderson S, Bryant J, et al. Twenty-year follow-up of a randomized trial comparing total mastectomy, lumpectomy, and lumpectomy plus irradiation for the treatment of invasive breast cancer. *N Engl J Med*. 2002;347:1233-1241.
- Clarke M, Collins R, Darby S, et al. Effects of radiotherapy and of differences in the extent of surgery for early breast cancer on local recurrence and 15-year survival: an overview of the randomised trials. *Lancet*. 2005;366:2087-2106.
- Darby SC, McGale P, Taylor CW, Peto R. Long-term mortality from heart disease and lung cancer after radiotherapy for early breast cancer: prospective cohort study of about 300,000 women in US SEER cancer registries. *Lancet Oncol*. 2005;6:557-565.
- Henson KE, McGale P, Taylor C, Darby SC. Radiation-related mortality from heart disease and lung cancer more than 20 years after radiotherapy for breast cancer. *Br J Cancer*. 2013;108:179-182.
- Taylor CW, Povall JM, McGale P, et al. Cardiac dose from tangential breast cancer radiotherapy in the year 2006. *Int J Radiat Oncol Biol Phys*. 2008;72:501-507.
- Ares C, Khan S, Macartain AM, et al. Postoperative proton radiotherapy for localized and locoregional breast cancer: potential for clinically relevant improvements? *Int J Radiat Oncol Biol Phys*. 2010;76:685-697.
- Hayden AJ, Rains M, Tiver K. Deep inspiration breath hold technique reduces heart dose from radiotherapy for left-sided breast cancer. *J Med Imaging Radiat Oncol*. 2012;56:464-472.
- Grantzau T, Thomsen MS, Vaeth M, Overgaard J. Risk of second primary lung cancer in women after radiotherapy for breast cancer. *Radiother Oncol*. 2014;111:366-373.
- Schubert LK, Gondi V, Sengbusch E, et al. Dosimetric comparison of left-sided whole breast irradiation with 3DCRT, forward-planned IMRT, inverse-planned IMRT, helical tomotherapy, and tomotherapy. *Radiother Oncol*. 2011;100:241-246.
- Yin Y, Chen J, Sun T, et al. Dosimetric research on intensity-modulated arc radiotherapy planning for left breast cancer after breast-preservation surgery. *Med Dosim*. 2012;37:287-292.
- Muren LP, Maurstad G, Hafslund R, Anker G, Dahl O. Cardiac and pulmonary doses and complication probabilities in standard and conformal tangential irradiation in conservative management of breast cancer. *Radiother Oncol*. 2002;62:173-183.
- Korreman SS, Pedersen AN, Aarup LR, Notttrup TJ, Specht L, Nystrom H. Reduction of cardiac and pulmonary complication probabilities after breathing adapted radiotherapy for breast cancer. *Int J Radiat Oncol Biol Phys*. 2006;65:1375-1380.
- Korreman SS, Pedersen AN, Notttrup TJ, Specht L, Nystrom H. Breathing adapted radiotherapy for breast cancer: comparison of free breathing gating with the breath-hold technique. *Radiother Oncol*. 2005;76:311-318.
- Kirby AM, Evans PM, Donovan EM, Convery HM, Haviland JS, Yarnold JR. Prone versus supine positioning for whole and partial-breast radiotherapy: a comparison of non-target tissue dosimetry. *Radiother Oncol*. 2010;96:178-184.
- Lymberis SC, deWyngaert JK, Parhar P, et al. Prospective assessment of optimal individual position (prone versus supine) for breast radiotherapy: volumetric and dosimetric correlations in 100 patients. *Int J Radiat Oncol Biol Phys*. 2012;84:902-909.
- Ferrari A, Valdi G, Leonardi MC, et al. Prone breast radiotherapy in a patient with early stage breast cancer and a large pendulous breast. *Tumori*. 2009;95:394-397.
- Bujsen J, Jager JJ, Bovendeerd J, et al. Prone breast irradiation for pendulous breasts. *Radiother Oncol*. 2007;82:337-340.
- Chino JP, Marke LB. Prone positioning causes the heart to be displaced anteriorly within the thorax: implications for breast cancer treatment. *Int J Radiat Oncol Biol Phys*. 2008;70:916-920.
- Lymberis SC, Formenti SC. Prone-breast radiotherapy: too early for conclusions: in regard to Chino et al. (*Int j radiat oncol biol phys* 2008;70:916-920). *Int J Radiat Oncol Biol Phys*. 2008; 72:301-302; author reply 302.
- Griem KL, Fetherston P, Kuznetsova M, et al. Three-dimensional photon dosimetry: a comparison of treatment of the intact breast in the supine and prone position. *Int J Radiat Oncol Biol Phys*. 2003;57:891-899.
- Varga Z, Hideghety K, Mezo T, et al. Individual positioning: a comparative study of adjuvant breast radiotherapy in the prone versus supine position. *Int J Radiat Oncol Biol Phys*. 2009;75:94-100.
- Takahashi K, Moroto M, Kagami Y, et al. Prospective study of post-operative whole breast radiotherapy for Japanese large-breasted women: a clinical and dosimetric comparisons between supine and prone positions and a dose measurement using a breast phantom. *BMC Cancer*. 2016;16:757.
- Formenti SC, DeWyngaert JK, Jozsef G, et al. Prone vs supine positioning for breast cancer radiotherapy. *JAMA*. 2012;308:861-863.
- The Radiation Therapy Oncology Group. RTOG 1304/NSABP B-51/Endorsed Study: A Randomized Phase III Clinical Trial Evaluating Post-Mastectomy Chestwall and Regional Nodal XRT and Post-Lumpectomy Regional Nodal XRT in Patients with Positive Axillary Nodes Before Neoadjuvant Chemotherapy who Convert to Pathologically Negative Axillary Nodes After Neoadjuvant Chemotherapy.
- Duane F, Aznar MC, Cutter DJ, et al. A cardiac contouring atlas for radiotherapy. *Radiother Oncol*. 2017;122:416-422.
- Akino Y, Das IJ, Bartlett GK, Zhang H, Thompson E, Zook JE. Evaluation of superficial dosimetry between treatment planning system and measurement for several breast cancer. *Med Phys*. 2013;40:011714.
- Whelan TJ, Pignol JP, Levine MN, et al. Long-term results of hypofractionated radiation therapy for breast cancer. *N Engl J Med*. 2010;362:513-520.
- Darby SC, Ewertz M, McGale P, et al. Risk of ischemic heart disease in women after radiotherapy for breast cancer. *N Engl J Med*. 2013;368:987-998.

29. Das UJ, Andrews JZ, Cao M, Johnstone PA. Correlation of 2D parameters to lung and heart dose-volume in radiation treatment of breast cancer. *Acta Oncol*. 2013;52:178-183.
30. Verhoeven K, Sweldens C, Petillon S, et al. Breathing adapted radiation therapy in comparison with prone position to reduce the doses to the heart, left anterior descending coronary artery, and contralateral breast in whole breast radiation therapy. *Pract Radiat Oncol*. 2014;4:123-129.
31. Taylor CW, Nisbet A, McGale P, Darby SC. Cardiac exposures in breast cancer radiotherapy: 1950s-1990s. *Int J Radiat Oncol Biol Phys*. 2007;69:1484-1495.
32. Taylor CW, Nisbet A, McGale P, et al. Cardiac doses from Swedish breast cancer radiotherapy since the 1950s. *Radiother Oncol*. 2009;90:127-135.
33. Nilsson G, Holmberg L, Garmo H, et al. Distribution of coronary artery stenosis after radiation for breast cancer. *J Clin Oncol*. 2012;30:380-386.

**Appendix D: Published Study 2—Biological Indices Evaluation of Various Treatment
Techniques for Left-Sided Breast Treatment**

Basic Original Report

Biological Indices Evaluation of Various Treatment Techniques for Left-Sided Breast Treatment



Amitpal Singh Saini, MS,^{a,b,*} Indra J. Das, PhD,^c
Catherine S. Hwang, MD,^a Matthew C. Biagioli, MD, MS,^a and
William E. Lee III, PhD^d

^aDepartment of Radiation Oncology, Advent Health Cancer Institute, Orlando, Florida; ^bDepartment of Medical Engineering, University of South Florida, Tampa, Florida; ^cDepartment of Radiation Oncology, NYU Langone School of Medicine & Laura and Isaac Perlmutter Cancer Center, New York, New York; and ^dDepartment of Chemical & Biomedical Engineering, University of South Florida, Tampa, Florida

Received 10 January 2019; revised 20 June 2019; accepted 28 June 2019

Abstract

Purpose: To compare dose to organs at risk (OARs) and biological evaluation using normal tissue complication probability (NTCP) for left-sided breast radiation therapy in 4 techniques: supine free breathing (SFB), supine deep inspiration breath hold (SDIBH), prone free breathing (PFB), and prone deep inspiration breath hold (PDIBH).

Methods and Materials: Twenty-five patients with left-sided breast cancer suitable for this study underwent a computed tomography scan using SFB, SDIBH, PFB, and PDIBH. One radiation oncologist contoured the planning target volume and OAR (cardiac components). Dose-volume histograms and NTCPs for the heart, left ventricle (LV), left anterior descending artery (LAD), and left lung were calculated for all 4 techniques.

Results: The mean heart dose in PDIBH is 0.77 Gy, which is statistically significantly lower than in SFB (1.88 Gy, $P < .0001$), SDIBH (0.97 Gy, $P < .001$), and PFB (0.85 Gy, $P < .001$). The mean left lung dose is 0.69 Gy in PFB and 0.88 Gy in PDIBH. PFB and PDIBH have statistically significantly lower doses compared with SFB (6.09 Gy, $P < .0001$) and SDIBH (5.41 Gy, $P < .0001$). The mean NTCP in SFB for the heart, LV, and LAD is 0.27%, 0.62%, and 4.23%, respectively, and it is negligible for other techniques.

Conclusions: We found that PDIBH had a dosimetrically lower mean dose for the heart and LV compared with the other 3 techniques. In addition, SDIBH, PFB and PDIBH had statistically significantly lower NTCP for the heart, LV, and LAD compared with SFB. NTCP for the left lung was statistically significantly lower for prone techniques compared with supine techniques. Therefore we concluded that, compared with SDIBH, PDIBH provides the added benefit of sparing the heart while keeping the benefit of sparing the lung as in the prone technique.

© 2019 American Society for Radiation Oncology. Published by Elsevier Inc. All rights reserved.

Sources of support: This work had no specific funding.

Disclosures: none.

* Corresponding author: Amitpal Singh Saini, MS; E-mail: amitpal97@gmail.com

<https://doi.org/10.1016/j.prro.2019.06.020>

1879-8500/© 2019 American Society for Radiation Oncology. Published by Elsevier Inc. All rights reserved.

Introduction

Radiation therapy has become an integral part of the combined treatment modality for the management of early breast cancer. It is well documented that radiation therapy for breast cancer significantly increases the overall survival rate.^{1,2} However, left-sided breast cancer radiation therapy has also been associated with higher cardiac and pulmonary toxicity with increased risk of secondary cancer.¹⁻⁸ It has also been reported that there is a significant increase in the rate of ischemic heart disease after exposure of the heart to ionizing radiation during radiation therapy for breast cancer.⁶ Clarke et al² compared a group of irradiated patients with nonirradiated patients and found a significant increase in mortality rate, mainly for the heart disease (rate ratio, 1.27) and lung cancer (rate ratio, 1.78).²

Some studies suggest that arteries are especially sensitive to radiation, and radiation-induced damage to the left anterior descending artery (LAD) is one of the components responsible for the ischemic heart disease.^{6,9} It is also recommended that radiation dose to the heart and LAD be minimized as a priority until there is evidence that there is a threshold dose below which there is no extra risk of cardiac morbidity and mortality.¹⁰ In addition to cardiac complications, it is well known that the increase in lung dose also leads to an increase in the incidences of lung complications, including radiation pneumonitis.^{3,11} Mortality as a result of ipsilateral lung cancer is reportedly higher compared with contralateral lung cancer for those women undergoing breast radiation therapy.³

Lung and cardiac doses are well documented for left breast radiation treatment.⁵⁻⁷ Many techniques have been evaluated to reduce the dose to cardiac components, such as deep inspiration breath hold (DIBH)^{12,13} and prone position,¹⁴⁻¹⁸ but consensus has not been reached as to which treatment strategy is superior.^{16,19-24} One study compared 3 techniques, supine free breathing (SFB), supine DIBH (SDIBH), and prone free breathing (PFB), to evaluate doses to the organs at risk (OARs).¹⁸

Recently, biological evaluation tools have become available in many treatment planning systems. Normal tissue complication probability (NTCP) tools could be used to biologically evaluate the treatment plan along with dose-volume histogram (DVH)-based evaluation for OARs.^{11,25} Previous studies have found that biological parameters applied to these biological models help predict the biological effects on normal tissues and have more direct correlations with treatment outcome than DVH-based parameters.^{26,27}

The aim of this study is to retrospectively compare DVH and biological (NTCP) dose metrics for 4 different treatment techniques used for radiation therapy to the left breast: SFB, SDIBH, PFB, and prone DIBH (PDIBH).

Methods and Materials

Twenty-five patients with early-stage left-sided breast cancer (pathologic T1-2N0 disease) undergoing whole breast radiation therapy between January 2017 and March 2018 were selected for this retrospective study, which was approved by the institutional review board. Patients who could follow instructions to hold their breath for a minimum of 25 seconds in supine and prone positions were considered for this study. All computed tomography (CT) scans were performed with a GE Lightspeed RT scanner (model number 2266521). Before the scan, a radiation oncologist marked the borders of the breast tissue with a radio-opaque wire. Four scans were performed on each patient in SFB, SDIBH, PFB, and PDIBH positions. The radiation oncologist evaluated each CT scan to decide the optimal treatment technique for a patient. Audio coaching was used to guide the patients for breath holds. In this study a commercial gating system was not used; instead, an in-house technique was developed by using high-definition cameras to observe the position of in-room lasers with respect to skin marks and tattoos to confirm the position of the patient during a breath hold treatment.

The CT images were transferred to the Eclipse (Varian Medical Systems Inc, Version 13.7) treatment planning system (TPS). One radiation oncologist was responsible for contouring all OARs and target volumes. The breast planning target volume (PTV), heart, left ventricle (LV), and LAD of each patient were contoured using the RTOG-1304²⁸ guidelines and the RTOG Breast Cancer Atlas²⁸ (<https://www.rtog.org/CoreLab/ContouringAtlases/BreastCancerAtlas.aspx>) in the Eclipse TPS. The breast clinical target volume was defined as all apparent CT glandular breast tissue, along with considering RTOG consensus definition of anatomic borders. The cranial border was defined at the second rib insertion, whereas the caudal border was 2 cm inferior to the apparent breast tissue. The anterior aspect of the breast was defined as the skin, and the posterior aspect was at the anterior aspect of the pectoralis muscles. The medial border was the sternal-rib junction, and the lateral border was at the midaxillary line. The heart was contoured starting superiorly at the level of the great vessel insertion into the heart, and the inferior border was defined by the apex of the heart. The LAD was defined as the vessel that descended anterolaterally from the anterior interventricular groove down to the apex of the heart.²⁹ The lungs are contoured using an automatic segmentation tool available in the TPS and manually edited as needed by the physician. Because the dosimetry in the buildup region is not well modeled by the TPS dose calculation algorithm, the left breast PTVs were cropped 5 mm from the skin surface for treatment planning.³⁰ Figure 1a to 1d shows typical scans and beam placement on the same patient for each technique. The

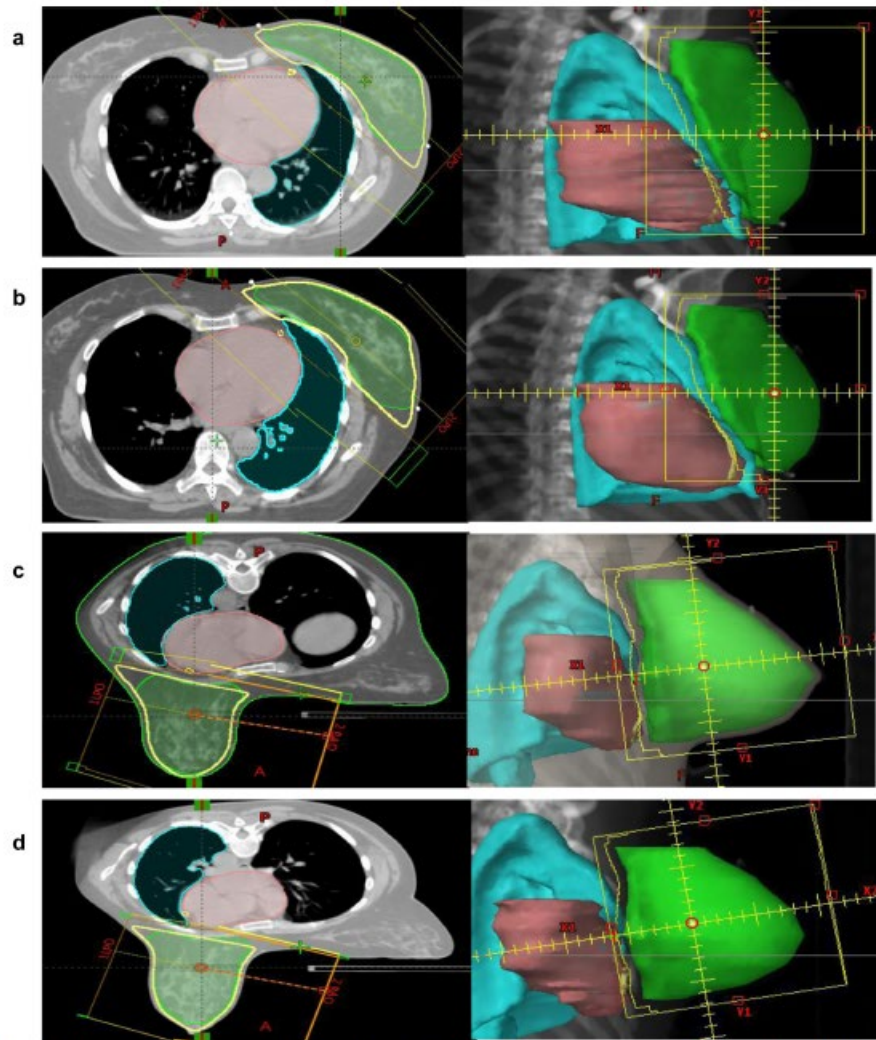


Figure 1 Axial and beam's eye view (BEV) image. The green line indicates planning target volume; yellow line, 100% isodose line; orange, multileaf collimator field shape and yellow-beam outline. The heart and left lung volumes are also shown in various techniques: (a) SFB, (b) SDIBH, (c) PFB, and (d) PDIBH. Note the heart and left lung positions in these techniques with respect to beam geometry. *Abbreviations:* PDIBH = prone deep inspiration breath hold; PFB = prone free breathing; SDIBH = supine deep inspiration breath hold; SFB = supine free breathing.

Table 1 NTCP parameters for models used to evaluate OAR with specific end stage

Structure	Organ model	Model	Endpoint/stage	D50 (Gy)	Y	α/β	Seriality	Parameter N	Parameter M	References
Heart	Heart	NTCP Poisson-LQ	Mortality	52.4	1.3	3.0	1	NA	NA	Gagliardi et al ²⁵
LV	Heart	NTCP Poisson-LQ	Mortality	52.4	1.3	3.0	1	NA	NA	Gagliardi et al ²⁵
LAD	Heart	NTCP Poisson-LQ	Mortality	52.4	1.3	3.0	1	NA	NA	Gagliardi et al ²⁵
Lung	Lung	NTCP Lyman	Pneumonitis (1), grade ≥ 2	30.5	NA	3.0	NA	1	0.3	Kwa et al ³⁵
Lung	Lung	NTCP Lyman	Pneumonitis (2), grade ≥ 2	30.8	NA	3.0	NA	0.99	0.37	Seppenwoolde et al ³⁴
Lung	Lung	NTCP Lyman	Symptomatic or Radiographic pneumonitis (≤ 6 mo)	21.9	NA	3.0	NA	0.37	0.8	Moiseenko et al ³⁶
Lung	Lung	NTCP Lyman	Symptomatic pneumonitis (≤ 6 mo)	21.0	NA	3.0	NA	1.02	0.26	Moiseenko et al ³⁶
Lung	Lung	NTCP Lyman	Symptomatic or radiographic fibrosis (>6 mo)	28.8	NA	3.0	NA	0.34	0.5	Moiseenko et al ³⁶
Lung	Lung	NTCP Lyman	Symptomatic fibrosis (>6 mo)	25.0	NA	3.0	NA	0.15	0.85	Moiseenko et al ³⁶

Abbreviations: LAD = left anterior descending artery; LV = left ventricle; NA = not applicable; NTCP = normal tissue complication probability; OAR = organ at risk.

prescription dose for all cases was 42.66 Gy in 16 fractions with a 6 MV photon beam using the field-in-field technique for planning. Anisotropic Analytical Algorithm Version 13.7.14 with a grid size of $0.25 \times 0.25 \text{ cm}^2$ was used to perform calculations. Additionally, a 7-mm margin was added to conform treatment fields around the PTV, as recommended by the RTOG-1304 protocol.²⁸ All plans were optimized to accomplish maximum sparing of OARs while achieving the PTV coverage goals ($\geq 95\%$ of the PTV receives 100% of the prescribed dose with less than 107% hot spot). The DVHs were used to evaluate PTV coverage and to record the mean dose, V2.5 Gy, V5 Gy, V10 Gy, V20 Gy, and V30 Gy for all OARs. In this present work, data of more than 100 treatment plans (4 plans/patient) were analyzed.

Two NTCP models, NTCP-Poisson LQ and NTCP-LKB, are available in the Eclipse TPS. The user can select a specific endpoint for the NTCP calculations.³¹⁻³³ Treatment plans were exported to the Eclipse biological evaluation module, and the NTCP were calculated from DVH. The NTCP-Poisson LQ function was used for calculation of the NTCP of the heart, LV, and LAD with cardiac mortality as the endpoint.²⁵ NTCP-LKB model of the lung with all the available endpoints in the Eclipse TPS was used for calculation of the lung NTCP.³⁴⁻³⁶ The NTCP input factors and associated endpoints for each OAR for the NTCP calculations are shown in Table 1.

Statistical analysis

The dosimetric parameters for the heart, LV, LAD, and left lung as well the calculated OAR NTCP for all 4 breast treatment techniques were compared using a Wilcoxon signed-rank test for the related sample with SPSS statistical software (version 24.0). Data were considered statistically significant at a P value $\leq .05$.

Results

Volume analysis

Figure 1 shows the setup of all 4 techniques and indicates variability in the position of the tissue volume. Mean whole breast PTV was 632.98 cm^3 (range, 236.13-1350.8 cm^3) for SFB, 626.62 cm^3 (range, 221.97-1277.62 cm^3) for SDIBH, 654.15 cm^3 (range, 217.1-1372.55 cm^3) for PFB, and 648.57 cm^3 (range, 224.6-1364.64 cm^3) for PDIBH. Thus the mean whole breast PTV was higher in prone positions, possibly because breast tissue elongates as a result of gravity. The mean heart volume was 548.2 cm^3 (range, 469-768 cm^3) for SFB, 507 cm^3 (range, 370-609 cm^3) for SDIBH, 501 cm^3 (range, 443-717 cm^3) for PFB, and 470 cm^3 (range, 360.6-600 cm^3) for PDIBH. Variability in the heart volumes can be due to physiological changes;

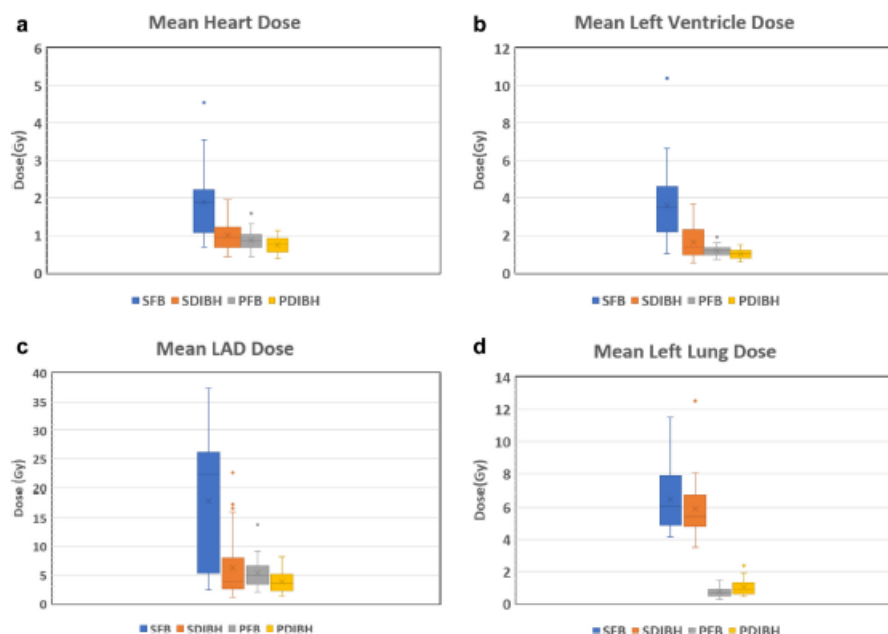


Figure 2 Box-whisker plot of mean doses with error bars in SFB, SDIBH, PFB, and PDIBH. Outlier data are shown if they existed for (a) heart, (b) LV, (c) LAD, and (d) left lung. *Abbreviations:* LAD = left anterior descending artery; LV = left ventricle; PDIBH = prone deep inspiration breath hold; PFB = prone free breathing; SDIBH = supine deep inspiration breath hold; SFB = supine free breathing.

during DIBH, the air in the lung pushes and likely contracts the heart, which leads to relatively lower heart volume compared with free breathing. Heart volume was largest in SFB and smallest in PDIBH, which implies that prone positions provide the lowest heart dose. The mean left lung volume was 1198 cm³ (range, 952-1548 cm³) for SFB, 1876 cm³ (range, 1745-2214 cm³) for SDIBH, 1404 cm³ (range, 1255-1599 cm³) for PFB, and 1840 cm³ (range, 1621-2197 cm³) for PDIBH. The left lung volume was smallest in PFB and largest in SDIBH.

Dosimetric analysis

Mean dose to the heart was 1.88 Gy, 0.97 Gy, 0.85 Gy and 0.77 Gy for SFB, SDIBH, PFB, and PDIBH, respectively. The data are also shown in Figure 2a and Table 2 and indicate the dosimetric parameters were highest for the heart in SFB and lowest in PDIBH. It is shown that SDIBH, PFB, and PDIBH produced a statistically significant reduction in the mean heart dose compared with SFB. For all the patients, SDIBH, PFB, and PDIBH techniques have lower mean heart doses

compared with SFB. The LV mean doses are 3.47 Gy, 1.36 Gy, 1.18 Gy, and 1.03 Gy in SFB, SDIBH, PFB, and PDIBH, respectively. These are also shown in Figure 2b. The dosimetric parameters are statistically lowest for PDIBH, as shown in Table 2. The LAD mean doses are 22.38 Gy, 3.88 Gy, 4.96 Gy, and 3.49 Gy in SFB, SDIBH, PFB, and PDIBH, respectively, as shown in Figure 2c. For LAD, other dosimetric parameters are shown in Table 2.

The mean dose reduction for the heart is statistically significant between PDIBH and SFB ($P < .001$), PDIBH and SDIBH ($P < .001$), and PDIBH and PFB ($P < .001$). The mean dose reduction for LV is also statistically significant between PDIBH and SFB ($P < .001$), PDIBH and SDIBH ($P < .001$), and PDIBH and PFB ($P < .001$). Additionally, the mean dose reduction for LAD is statistically significant between PDIBH and SFB ($P < .001$) and PDIBH and PFB ($P < .0001$). However, no statistically significant difference was identified between PDIBH and SDIBH, as indicated by the P value ($P < .194$).

Mean dose to the left lung was 6.09 Gy, 5.41 Gy, 0.69 Gy, and 0.88 Gy for SFB, SDIBH, PFB, and PDIBH,

Table 2 Dosimetry parameters (mean values and quartiles) in SFB, SDIBH, PFB, and PDIBH

	SFB	SDIBH	PFB	PDIBH
Heart				
Mean dose (Gy)	1.88 (1.09-2.22)	0.97 (0.68-1.23)	0.85 (0.68-1.04)	0.77 (0.55-0.92)
V2.5 Gy (%)	13.72 (6.93-18.32)	4.77 (2.06-10.54)	3.61 (1.77-6.16)	2.98 (1.02-4.99)
V5 Gy (%)	4.53 (1.84-5.55)	0.30 (0.01-2.50)	0.24 (0.09-0.85)	0.15 (0.01-0.44)
V10 Gy (%)	2.46 (0.68-3.37)	0.001 (0.00-0.74)	0.02 (0.00-0.26)	0.003 (0.00-0.09)
V20 Gy (%)	1.53 (0.17-2.36)	0.00 (0.00-0.24)	0.00 (0.00-0.04)	0.0 (0.00-0.018)
V30 Gy (%)	0.91 (0.09-1.74)	0.00 (0.00-0.16)	0.00 (0.00-0.00)	0.00 (0.00-0.00)
Left ventricle				
Mean dose (Gy)	3.47 (2.21-4.60)	1.36 (0.97-2.32)	1.18 (0.98-1.34)	1.03 (0.80-1.22)
V2.5 Gy (%)	27.52 (18.25-40.6)	10.78 (4.22-22.90)	6.12 (2.96-8.88)	3.00 (0.89-6.54)
V5 Gy (%)	10.29 (4.52-15.03)	0.93 (0.03-6.16)	0.39 (0.04-1.22)	0.00 (0.00-0.80)
V10 Gy (%)	5.86 (2.01-8.80)	0.00 (0.00-2.38)	0.00 (0.00-0.25)	0.00 (0.00-0.18)
V20 Gy (%)	3.80 (0.72-6.25)	0.00 (0.0-0.91)	0.00 (0.00-0.007)	0.00 (0.00-0.00)
V30 Gy (%)	2.27 (0.29-4.54)	0.00 (0.00-0.19)	0.00 (0.00-0.00)	0.00 (0.00-0.00)
LAD				
Mean dose (Gy)	22.38 (5.34-26.19)	3.88 (2.59-7.98)	4.96 (3.45-6.56)	3.49 (2.30-5.12)
V2.5 Gy (%)	96.9 (73.59-99.89)	79.2 (52.34-96.81)	80.27 (56.95-91.03)	74.8 (38.3-88.1)
V5 Gy (%)	76.03 (39.27-87.48)	19.7 (1.00-52.54)	36.78 (17.13-56.21)	12.28 (0.28-41.73)
V10 Gy (%)	55.65 (6.46-71.00)	0.03 (0.00-6.24)	7.76 (0.76-17.58)	2.33 (0.00-8.07)
V20 Gy (%)	53.85 (0.01-66.22)	0.00 (0.00-6.21)	0.13 (0.00-1.52)	0.00 (0.00-0.02)
V30 Gy (%)	41.63 (0.00-56.37)	0.00 (0.00-0.29)	0.00 (0.00-0.00)	0.00 (0.00-0.00)
Left lung				
Mean dose (Gy)	6.09 (4.89-7.86)	5.41 (4.80-6.75)	0.69 (0.47-0.87)	0.88 (0.62-1.31)
V2.5 Gy (%)	34.35 (30.73-42.09)	33.90 (29.53-39.63)	3.98 (2.06-5.70)	6.03 (3.29-9.08)
V5 Gy (%)	21.9 (18.43-23.32)	21.12 (18.38-25.00)	1.26 (0.52-1.90)	2.03 (1.06-4.25)
V10 Gy (%)	14.7 (11.5-19.43)	13.24 (11.18-16.16)	0.48 (0.16-0.99)	0.91 (0.39-2.05)
V20 Gy (%)	10.94 (8.17-14.69)	9.50 (7.58-12.15)	0.16 (0.04-0.50)	0.49 (0.09-1.19)
V30 Gy (%)	8.78 (6.27-11.83)	7.39 (5.39-9.62)	0.07 (0.00-0.21)	0.16 (0.01-0.70)

Abbreviations: LAD = left anterior descending artery; LV = left ventricle; PDIBH = prone deep inspiration breath hold; PFB = prone free breathing; SDIBH = supine deep inspiration breath hold; SFB = supine free breathing.

respectively, as shown in Figure 2d. The mean dose reduction for left lung is statistically significant between PDIBH and SFB ($P < .0001$) and PDIBH and SDIBH ($P < .0001$). Mean left lung dose in PFB was statistically lower than in PDIBH ($P < .001$). Other dosimetric parameters for left lung doses are shown in Table 2. All the statistical values of various OARs in the SFB, SDIBH, and PFB with respect to PDIBH are shown in Table 3.

Biological evaluation

Cardiac mortality as an endpoint with the NTCP-Poisson LQ model was used for the calculation of the NTCP for the heart, LV, and LAD. Mean NTCP in SFB is 0.27% for the heart, 0.62% for the LV, and 4.23% for the LAD, whereas it is negligible for other 3 treatment techniques, as shown in Figure 3a, 3b, and 3c, respectively. The NTCP for the left lung was calculated for all the NTCP-LKB models available in the Eclipse TPS with different endpoints, as shown in Table 1. The mean composite NTCP was also generated using a function available in the Eclipse TPS for the 3 left lung

endpoints: pneumonitis (2) grade ≥ 2 , symptomatic or radiographic pneumonitis (≤ 6 months), and symptomatic or radiographic fibrosis (> 6 months). These 3 NTCP endpoints were chosen because they cover a broad range of left lung complications. The calculated composite NTCP of the left lung is 41.32% for SFB, 38.85% for SDIBH, 15.57% for PFB, and 17.79% for PDIBH, as shown in Figure 3d. The NTCP for the left lung with various techniques is shown in Figure 3e to 3j. The NTCP for all available endpoints for the left lung and the composite NTCP for the left lung are shown in Table 4.

There was a statistically significant reduction in mean NTCP value of the heart, LV, and LAD for SDIBH, PFB, and PDIBH compared with SFB: SDIBH and SFB ($P < .0001$); PFB and SFB ($P < .0001$), and PDIBH and SFB ($P < .0001$). There was a statistically significant reduction between the mean composite NTCP values of the left lung compared with SFB: SDIBH and SFB ($P < .004$), PFB and SFB ($P < .0001$), and PDIBH and SFB ($P < .0001$); and compared with SDIBH: PFB and SDIBH ($P < .0001$) and PDIBH and SDIBH ($P < .0001$). However, PFB has statistically lower left lung doses

Table 3 P value between various combinations, PDIBH and SFB, PDIBH and SDIBH, and PDIBH and PFB, for the dosimetric parameters of the heart, LV, LAD, and left lung

	Technique	Heart	LV	LAD	Lung
Mean dose	PDIBH & SFB	≤.001 ↓	≤.001 ↓	≤.001 ↓	≤.001 ↓
	PDIBH & SDIBH	≤.001 ↓	≤.001 ↓	≤.194	≤.001 ↓
	PDIBH & PFB	≤.001 ↓	≤.001 ↓	≤.001 ↓	≤.001 ↑
V2.5 Gy	PDIBH & SFB	≤.001 ↓	≤.001 ↓	≤.001 ↓	≤.001 ↓
	PDIBH & SDIBH	≤.001 ↓	≤.001 ↓	≤.732	≤.001 ↓
	PDIBH & PFB	≤.002 ↓	≤.001 ↓	≤.045 ↓	≤.001 ↑
V5 Gy	PDIBH & SFB	≤.001 ↓	≤.001 ↓	≤.001 ↓	≤.001 ↓
	PDIBH & SDIBH	≤.013 ↓	≤.001 ↓	≤.023 ↓	≤.001 ↓
	PDIBH & PFB	≤.017 ↓	≤.002 ↓	≤.001 ↓	≤.001 ↑
V10 Gy	PDIBH & SFB	≤.001 ↓	≤.001 ↓	≤.001 ↓	≤.001 ↓
	PDIBH & SDIBH	≤.036 ↓	≤.016 ↓	≤.501	≤.001 ↓
	PDIBH & PFB	≤.049 ↓	≤.064	≤.001 ↓	≤.001 ↑
V20 Gy	PDIBH & SFB	≤.001 ↓	≤.001 ↓	≤.001 ↓	≤.001 ↓
	PDIBH & SDIBH	≤.021 ↓	≤.010 ↓	≤.047 ↓	≤.001 ↓
	PDIBH & PFB	≤.306	≤.441	≤.002 ↓	≤.001 ↑
V30 Gy	PDIBH & SFB	≤.001 ↓	≤.001 ↓	≤.001 ↓	≤.001 ↓
	PDIBH & SDIBH	≤.037 ↓	≤.011 ↓	≤.028 ↓	≤.001 ↓
	PDIBH & PFB	≤.345	≤.593	≤.068	≤.002 ↑

Abbreviations: LAD = left anterior descending artery; LV = left ventricle; NTCP = normal tissue complication probability; PDIBH = prone deep inspiration breath hold; PFB = prone free breathing; SDIBH = supine deep inspiration breath hold; SFB = supine free breathing. Note that P values for the heart and LV are statistically significantly reduced for PDIBH compared with SFB, SDIBH, and PFB. P values ≤ .05 were considered statistically significant. Up and down arrows depict if P values represent an increase or decrease in dose in each position with regard to PDIBH.

compared with PDIBH; PDIBH and PFB ($P < .0001$). Statistical values of NTCP calculated for OAR in each technique are shown in Table 5.

Discussion

Cardiac injuries such as cardiac mortality, coronary heart disease, or myocardial infarction after breast radiation therapy are well discussed in literature.^{1-4,6} The risk of injury arises a few years after radiation, but it has the potential to continue for decades. There is no evidence to date of a threshold dose for injury caused by radiation; thus, it is imperative to minimize doses to cardiac components.¹⁻⁴ Das et al³⁷ provided a technique to correlate the left lung and the heart doses with pulmonary and cardiac complication rates. Thus it is important to find the techniques that can lower the heart dose and spare left lung because of the risk of pneumonitis, left lung fibrosis, and cancer induction.

Mean heart dose quartile range was 1.09 to 2.21 Gy for SFB, 0.68 to 1.23 Gy for SDIBH, 0.68 to 1.04 Gy for PFB, and 0.55 to 0.92 Gy for PDIBH. Darby et al⁶

estimated that a 1 Gy increase in the mean heart dose leads to a 7.4% increase in the rate of major coronary events. Thus the mean heart dose quartile range will lead to an increase in the rate of major coronary events of between 8.07% and 16.35% for SFB, 5.03% and 9.10% for SDIBH, 5.03% and 7.69% for PFB, and 4.07% and 6.81% for PDIBH above baseline risk levels. Sardora et al³⁸ estimated that 1 Gy increases in the mean heart dose lead to a 4% increase in the long-term risk of late heart disease from baseline; thus, the mean heart dose range calculated in this study will increase long-term risk of late heart disease by between 4.36% to 8.88% for SFB, 2.72% and 4.92% for SDIBH, 2.72% and 4.16% for PFB, and 2.20% and 3.68% for PDIBH above baseline risk level. Hence, SDIBH, PFB, and PDIBH lead to a lower risk of late heart diseases and a lower rate of major coronary events compared with SFB. PDIBH leads to the lowest increase in risk estimate above baseline risk among all the techniques.

In DIBH the heart can be pushed away from the chest wall by inflating the left lung; therefore it is away from treatment fields, which leads to lower heart dose. Prone setup can reduce the dose to the heart and left lung

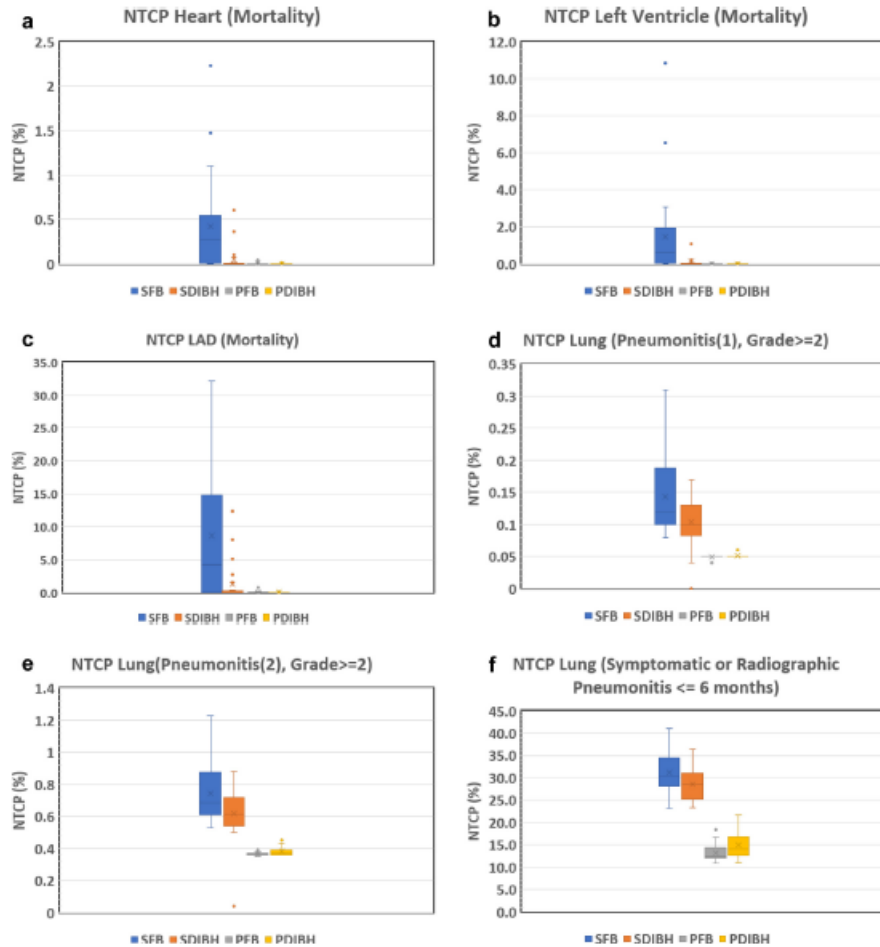


Figure 3 Box-whisker plot of mean NTCP values with error bars in SFB, SDIBH, PFB, and PDIBH. Outlier data are shown if they existed for (a) heart, (b) LV, (c) LAD, and (d) composite left lung; (e) symptomatic pneumonitis (≤ 6 months) of left lung; (f) symptomatic or radiographic pneumonitis (≤ 6 months) of left lungs; (g) symptomatic fibrosis (>6 months) of left lungs; (h) symptomatic or radiographic fibrosis (>6 months) of left lungs; (i) pneumonitis (1), grade ≥ 2 , of left lungs; and (j) pneumonitis (2), grade ≥ 2 , of left lungs. *Abbreviations:* LAD = left anterior descending artery; LV = left ventricle; NTCP = normal tissue complication probability; PDIBH = prone deep inspiration breath hold; PFB = prone free breathing; SDIBH = supine deep inspiration breath hold; SFB = supine free breathing.

because gravity pulls the left breast away from the chest wall, thus minimizing the treatment fields going through the heart and lung. Although it is widely recognized that the heart can also be pulled anteriorly by gravity, this

study consistently found that PFB and PDIBH always deliver lower heart doses compared with SFB. Some studies have reported that the prone position reduces the heart doses^{15,18,24}; however, a few studies have also

Table 5 P value of calculated NTCP with specific end stage of the heart, LV, LAD, and left lung between each technique

Structure	Endpoint/stage	SDIBH & SFB	PFB & SFB	PDIBH & SFB	PDIBH & SDIBH	PDIBH & PFB	PFB & SDIBH
Heart	Mortality	.0001	.0001	.0001	.034	.236	.138
LV	Mortality	.0001	.0001	.0001	.012	.317	.028
LAD	Mortality	.0001	.0001	.0001	.036	.029	.286
Lung	Pneumonitis (1), grade ≥ 2	.003	.0001	.0001	.0001	.014	.001
Lung	Pneumonitis (2), grade ≥ 2	.004	.0001	.0001	.0001	.0001	.0001
Lung	Symptomatic or radiographic pneumonitis (≤ 6 mo)	.003	.0001	.0001	.0001	.0001	.0001
Lung	Symptomatic pneumonitis (≤ 6 mo)	.012	.0001	.0001	.0001	1.000	.0001
Lung	Symptomatic or radiographic fibrosis (> 6 mo)	.003	.0001	.0001	.0001	.0001	.0001
Lung	Symptomatic fibrosis (> 6 mo)	.002	.0001	.0001	.0001	.0001	.0001
Lung	Composite NTCP	.004	.0001	.0001	.0001	.0001	.0001

Abbreviations: LAD = left anterior descending artery; LV = left ventricle; NTCP = normal tissue complication probability; PDIBH = prone deep inspiration breath hold; PFB = prone free breathing; SDIBH = supine deep inspiration breath hold; SFB = supine free breathing. P values $\leq .05$ were considered statistically significant.

statistically significant difference was found with respect to SDIBH. PFB gives statistically significantly lower mean heart and LAD dose compared with SFB, which is in contrast to one study that concluded that PFB gives a higher dose.³⁹ It is reported that there is increased risk of stenosis in the LAD for patients with left-sided breast cancer.⁹ Higher LAD dose in PFB compared with SDIBH may be because LAD falls close to the mediastinum/chest wall because of gravity placing it closer to the treatment field, but in PDIBH it is lower because deep inspiration pushes the LAD away from the treatment field. The QUANTEC group⁴³ recommends that for patients with breast cancer, the irradiated heart volume should be minimized without compromising target coverage. From our results, it can be concluded that PDIBH further reduces the mean dose to the heart and LV compared with SFB, SDIBH, and PFB. PDIBH also reduces the mean dose to the LAD compared with SFB and PFB.

The mean left lung doses are statistically significantly lower in prone setup. The mean left lung doses and other dosimetric parameters evaluated in PFB and PDIBH are statistically lower compared with SFB and SDIBH. This could be attributed to the geometry in prone position: the minimal beam passes through the left lung because of the pulling away of the breast from the chest wall and left lung. Thus, a prone setup has a clear advantage over a supine setup for lowering left lung doses and other dosimetric parameters calculated in this study, which is in agreement with several previous studies.^{14,18,22-24} However, similar to a study by Mulliez et al,⁴² this study also found that PFB gives a slightly lower left lung dose compared with PDIBH. The difference in the mean left lung doses between PFB and PDIBH will be further reduced if density correction

is applied to the left lung because of its increased volume in PDIBH.

NTCP analysis can assist in finding new ways to reduce radiation therapy-induced complication rates.^{11,25,43-47} In the literature there are studies comparing NTCP for OARs in SFB with SDIBH.⁴⁵⁻⁴⁷ A literature search did not yield any study that has compared NTCP for the heart, LV, LAD, and left lung with the supine and prone techniques. This is the only study that calculates and compares NTCP values of prone techniques with those of supine techniques in free breathing and DIBH. In addition, this is the only study that has calculated NTCP for 6 endpoints of left lung complications using an NTCP-LKB model for each of the 4 techniques.

Based on the biological evaluation of the heart with cardiac morbidity as an end result, this study found statistically significantly lower NTCP for SDIBH, PFB, and PDIBH compared with SFB, which correlates with results of lower dosimetry doses for the heart for all techniques compared with the SFB technique. This study concludes that SDIBH, PFB, and PDIBH techniques statistically significantly reduce the mean probability of excessive cardiac mortality and of left lung complications compared with SFB. These results are similar to those of a few previous studies that also concluded that SDIBH leads to a significant reduction in the heart and left lung complication probability compared with SFB.⁴⁵⁻⁴⁷ The present study did not find any statistically significant difference in the NTCP among SDIBH, PFB, and PDIBH for the heart, LAD, and LV.

For both prone techniques (PFB and PDIBH), the reduction of the NTCP for left lung complications was statistically significant compared with SFB and SDIBH, which correlates with lower dosimetry dose in the left lung between these techniques.

Conclusions

This study found that radiation dose can be reduced to the heart, LV, LAD, and left lung with the selection of a proper technique. The PDIBH technique does have added benefits in lowering the mean doses to heart, LV, and LAD compared with SFB, SDIBH, and PFB techniques. The dosimetric findings are augmented with the NTCP for cardiac mortality, indicating that substantial reduction can be achieved by using SDIBH, PFB, and PDIBH compared with SFB. Left lung doses and composite NTCP for the left lung complications are statistically significantly lower in prone techniques compared with supine techniques. Thus, PDIBH does provide the benefit of the heart, LV, and left lung sparing statistically significantly better than SDIBH. This study concludes that statistically significant dose reduction in the left lung can be achieved by using prone techniques. The PDIBH seems to be an optimal technique for minimizing doses to cardiac components while adequately sparing left lung if the patient can comfortably perform breath holding. The PFB can be the optimal technique for OAR sparing for patients unable to hold their breath. Each clinic should evaluate the pros and cons of each technique while maintaining the patient's comfort level and breathing patterns. Better integration of biological models in the TPS with validated input parameters (α and β) for the OAR may facilitate adoption in clinical practices.

Acknowledgments

The authors would like to thank Chief Medical Physicist Steven Harrell (Advent Health) for his continuous support, encouragement, and motivation to complete this work. The readiness and cooperation from the radiation oncologists, radiation therapist, and dosimetrist at Advent Health Cancer Institute to participate in this study is greatly appreciated. Authors would also like to thank Ron Phillips (Varian Medical Systems) for his support and help to provide access to biological evaluation software used in this study. Thanks to Varian Medical Systems, Palo Alto, CA for giving access to biological evaluation software to do the biological evaluation for this study.

References

- Fisher B, Anderson S, Bryant J, et al. Twenty-year follow-up of a randomized trial comparing total mastectomy, lumpectomy, and lumpectomy plus irradiation for the treatment of invasive breast cancer. *N Engl J Med*. 2002;347:1233-1241.
- Clarke M, Collins R, Darby S, et al. Effects of radiotherapy and of differences in the extent of surgery for early breast cancer on local recurrence and 15-year survival: An overview of the randomised trials. *Lancet*. 2005;366:2087-2106.
- Darby SC, McGale P, Taylor CW, Peto R. Long-term mortality from heart disease and left lung cancer after radiotherapy for early breast cancer: Prospective cohort study of about 300,000 women in US SEER cancer registries. *Lancet Oncol*. 2005;6:557-565.
- Henson KE, McGale P, Taylor C, Darby SC. Radiation-related mortality from heart disease and left lung cancer more than 20 years after radiotherapy for breast cancer. *Br J Cancer*. 2013;108:179-182.
- Taylor CW, Povall JM, McGale P, et al. Cardiac dose from tangential breast cancer radiotherapy in the year 2006. *Int J Radiat Oncol Biol Phys*. 2008;72:501-507.
- Darby SC, Ewertz M, McGale P, et al. Risk of ischemic heart disease in women after radiotherapy for breast cancer. *N Engl J Med*. 2013;368:987-998.
- Hayden AJ, Rains M, Tiver K. Deep inspiration breath hold technique reduces heart dose from radiotherapy for left-sided breast cancer. *J Med Imag Radiat Oncol*. 2012;56:464-472.
- Grantzau T, Thomsen MS, Vaeth M, Overgaard J. Risk of second primary left lung cancer in women after radiotherapy for breast cancer. *Radiother Oncol*. 2014;111:366-373.
- Nilsson G, Holmberg L, Garmo H, et al. Distribution of coronary artery stenosis after radiation for breast cancer. *J Clin Oncol*. 2012;30:380-386.
- Demirci S, Nam J, Hubbs JL, Nguyen T, Marks LB. Radiation-induced cardiac toxicity after therapy for breast cancer: Interaction between treatment era and follow-up duration. *Int J Radiat Oncol Biol Phys*. 2009;73:980-987.
- Gagliardi G, Bjohle J, Lax I, et al. Radiation pneumonitis after breast cancer irradiation: Analysis of the complication probability using the relative seriality model. *Int J Radiat Oncol Biol Phys*. 2000;46:373-381.
- Korreman SS, Pedersen AN, Aarup LR, et al. Reduction of cardiac and pulmonary complication probabilities after breathing adapted radiotherapy for breast cancer. *Int J Radiat Oncol Biol Phys*. 2006;65:1375-1380.
- Korreman SS, Pedersen AN, Nottrup TJ, et al. Breathing adapted radiotherapy for breast cancer: comparison of free breathing gating with the breath-hold technique. *Radiother Oncol*. 2005;76:311-318.
- Kirby AM, Evans PM, Donovan EM, et al. Prone versus supine positioning for whole and partial-breast radiotherapy: A comparison of non-target tissue dosimetry. *Radiother Oncol*. 2010;96:178-184.
- Lymberis SC, deWyngaert JK, Parfitt P, et al. Prospective assessment of optimal individual position (prone versus supine) for breast radiotherapy: Volumetric and dosimetric correlations in 100 patients. *Int J Radiat Oncol Biol Phys*. 2012;84:902-909.
- Ferrari A, Ivaldi G, Leonardi MC, et al. Prone breast radiotherapy in a patient with early stage breast cancer and a large pendulous breast. *Tumori*. 2009;95:394-397.
- Buijssen J, Jager JJ, Bovendeerd J, et al. Prone breast irradiation for pendulous breasts. *Radiother Oncol*. 2007;82:337-340.
- Saini AS, Hwang CS, Biagioli MC, Das IJ. Evaluation of sparing organs at risk (OARs) in left-breast irradiation in the supine and prone positions and with deep inspiration breath-hold. *J Appl Clin Med Phys*. 2018;19:195-204.
- Junzo P, Chino LBM. Prone positioning causes the heart to be displaced anteriorly within the thorax: Implications for breast cancer treatment. *Int J Radiat Oncol Biol Phys*. 2008;70:916-920.
- Lymberis SC, Formenti SC. Prone-breast radiotherapy: Too early for conclusions: In regard to Chino et al. (*Int J Radiat Oncol Biol Phys* 2008;70:916-920). *Int J Radiat Oncol Biol Phys*. 2008;72:301-302. author reply 302.
- Griem KL, Fethenston P, Kuznetsova M, et al. Three-dimensional photon dosimetry: A comparison of treatment of the intact breast in the supine and prone position. *Int J Radiat Oncol Biol Phys*. 2003;57:891-899.
- Varga Z, Hkleghty K, Mezo T, et al. Individual positioning: A comparative study of adjuvant breast radiotherapy in the prone

- versus supine position. *Int J Radiat Oncol Biol Phys.* 2009;75:94-100.
23. Takahashi K, Morota M, Kagami Y, et al. Prospective study of postoperative whole breast radiotherapy for Japanese large-breasted women: A clinical and dosimetric comparisons between supine and prone positions and a dose measurement using a breast phantom. *BMC Cancer.* 2016;16:757.
 24. Formenti SC, DeWynngaert JK, Jozsef G, Goldberg JD. Prone vs supine positioning for breast cancer radiotherapy. *JAMA.* 2012;308:861-863.
 25. Gagliardi G, Lax I, Ottolenghi A, Rutqvist LE. Long-term cardiac mortality after radiotherapy of breast cancer—application of the relative seriality model. *Br J Radiol.* 1996;69:839-846.
 26. Dale RG. The application of the linear-quadratic dose-effect equation to fractionated and protracted radiotherapy. *Br J Radiol.* 1985;58:515-528.
 27. Lee SP, Leu MY, Smathers JB, et al. Biologically effective dose distribution based on the linear quadratic model and its clinical relevance. *Int J Radiat Oncol Biol Phys.* 1995;33:375-389.
 28. Randomized phase III clinical trial evaluating post-mastectomy chestwall and regional nodal XRT and post-lumpectomy regional nodal XRT in patients with positive axillary nodes before neoadjuvant chemotherapy who convert to pathologically negative axillary nodes after neoadjuvant chemotherapy. NSABP Protocol B-51/RT0G Protocol 1304. Available at: https://ascopubs.org/doi/abs/10.1200/JCO.2017.35.15_suppl.TP5589
 29. Duane F, Aznar MC, Bartlett F, et al. A cardiac contouring atlas for radiotherapy. *Radiother Oncol.* 2017;122:416-422.
 30. Akino Y, Das U, Bartlett GK, et al. Evaluation of superficial dosimetry between treatment planning system and measurement for several breast cancer. *MedPhys.* 2013;40:011714.
 31. Kallman P, Agren A, Brahmé A. Tumour and normal tissue responses to fractionated non-uniform dose delivery. *Int J Radiat Biol.* 1992;62:249-262.
 32. Lyman JT. Complication probability as assessed from dose-volume histograms. *Radiat Res Suppl.* 1985;8:S13-19.
 33. Kutcher GJ, Burman C, Bawster L, et al. Histogram reduction method for calculating complication probabilities for three-dimensional treatment planning evaluations. *Int J Radiat Oncol Biol Phys.* 1991;21:137-146.
 34. Seppenwoolde Y, Lebesque JV, de Jaeger K, et al. Comparing different NTCP models that predict the incidence of radiation pneumonitis. Normal tissue complication probability. *Int J Radiat Oncol Biol Phys.* 2003;55:724-735.
 35. Kwa SL, Theuvs JC, Wagenaar A, et al. Evaluation of two dose-volume histogram reduction models for the prediction of radiation pneumonitis. *Radiother Oncol.* 1998;48:61-69.
 36. Moiseenko V, Craig T, Bezjak A, Van Dyk J. Dose-volume analysis of left lung complications in the radiation treatment of malignant thymoma: A retrospective review. *Radiother Oncol.* 2003;67:265-274.
 37. Das U, Andrews JZ, Cao M, et al. Correlation of 2D parameters to left lung and heart dose-volume in radiation treatment of breast cancer. *Acta Oncol.* 2013;52:178-183.
 38. Sardaro A, Petruzzelli MF, D'Errico MP, et al. Radiation-induced cardiac damage in early left breast cancer patients: Risk factors, biological mechanisms, radiobiology, and dosimetric constraints. *Radiother Oncol.* 2012;103:133-142.
 39. Verhoeven K, Sweldens C, Petillion S, et al. Breathing adapted radiation therapy in comparison with prone position to reduce the doses to the heart, left anterior descending coronary artery, and contralateral breast in whole breast radiation therapy. *Pract Radiat Oncol.* 2014;4:123-129.
 40. Siegman LD, Beal KP, Hunt MA, et al. Long-term clinical outcomes of whole-breast irradiation delivered in the prone position. *Int J Radiat Oncol Biol Phys.* 2007;68:73-81.
 41. Morrow NV, Stepaniak C, White J, et al. Intra- and interfraction variations for prone breast irradiation: An indication for image-guided radiotherapy. *Int J Radiat Oncol Biol Phys.* 2007;69:910-917.
 42. Mulliez T, Vekleman L, Speleers B, et al. Heart dose reduction by prone deep inspiration breath hold in left-sided breast irradiation. *Radiother Oncol.* 2015;114:79-84.
 43. Gagliardi G, Constine LS, Moiseenko V, et al. Radiation dose-volume effects in the heart. *Int J Radiat Oncol Biol Phys.* 2010;76:S77-85.
 44. Gagliardi G, Lax I, Soderstrom S, et al. Prediction of excess risk of long-term cardiac mortality after radiotherapy of stage I breast cancer. *Radiother Oncol.* 1998;46:63-71.
 45. Uehina O, Popovs S, Purina D, et al. Analysis of cardiac and pulmonary complication probabilities after radiation therapy for patients with early-stage breast cancer. *Medicina (Kaunas).* 2009;45:276-285.
 46. Korreman SS, Pedersen AN, Josipovic M, et al. Cardiac and pulmonary complication probabilities for breast cancer patients after routine end-inspiration gated radiotherapy. *Radiother Oncol.* 2006;80:257-262.
 47. Edvardsson A, Nilsson MP, Amptoulach S, Ceberg S. Comparison of doses and NTCP to risk organs with enhanced inspiration gating and free breathing for left-sided breast cancer radiotherapy using the AAA algorithm. *Radiat Oncol.* 2015;10:84.

**Appendix E: Submitted Study 3—Skin Dose in Radiation Treatment of Left Breast:
Analysis in the Context of Prone Versus Supine Treatment Techniques**

Skin Dose in Radiation Treatment of Left Breast: Analysis in the Context of Prone Versus Supine Treatment Technique

Amitpal Singh Saini, MS,^{a,b,*} Indra J. Das, PhD,^c

Catherine S. Hwang, MD,^a Matthew C. Biagioli, MD, MS,^a

And William E. Lee III, PhD^d

^aDepartment of Radiation Oncology, Advent Health Cancer Institute, Orlando, Florida;

^bDepartment of Medical Engineering, University of South Florida, Tampa, Florida;

^cDepartment of Radiation Oncology, NYU Langone School of Medicine & Laura and

Isaac Perlmutter Cancer Center, New York, New York; and ^dDepartment of Chemical &

Biomedical Engineering, University of South Florida, Tampa, Florida

Abstract

Introduction: The skin dose in radiation treatment for breast cancer is an important consideration in terms of not only the outcomes but also cosmesis. However, an inadequate skin dose can lead to skin recurrence. This study was undertaken to analyze how the skin dose varies in patients treated in the prone and supine positions.

Methods: Fifty patients were scanned in the prone and supine positions. A radiation treatment plan was created for the left breast, using a 6-MV beam for a prescribed dose of 42.66 Gy in 16 fractions. The dose was calculated using 1- and 2.5-mm calculation grid sizes.

Results: The mean dose difference between the prone and supine techniques was statistically significant from a 3- to 5-mm depth for both grid sizes. For the 1-mm calculation grid size, the doses at 3-, 4-, and 5-mm depths in the prone and supine techniques were 87.80% and 89.10% ($P<0.003$), 91.92% and 94.50% ($P<0.00$), and 95.30% and 98.20% ($P<0.00$), respectively; for the 2.5-mm grid size, the respective doses were 87.10% and 88.59% ($P<0.00$), 91.60% and 94.63% ($P<0.00$), and 95.10% and 97.80% ($P<0.00$), respectively. The median angles relative to the skin surface were 8 and 52 degrees for treatment in the prone and supine positions, respectively.

Conclusions: Based on the same patient population, this study demonstrates that the prone technique facilitates a lower skin dose than does the supine technique, probably because of the beam angles. The beam is more perpendicular to the skin surface in the prone technique, whereas it is more tangential in the supine technique, thus delivering a higher skin dose. Thus, dose to the skin may also be assessed in the prone technique and if desired, the skin dose should be carefully augmented via a bolus or beam spoiler.

Introduction

Most women with early-stage breast cancer undergo combined treatment with radiation as part of their cancer management [1, 2]. Treatment for breast cancer includes surgery, radiation therapy, chemotherapy, and hormone therapy. Radiation therapy after breast-conserving surgery is associated with improvement in local control and is equivalent to mastectomy in terms of overall survival [1-5]. This combined multimodality treatment has improved the outcome for early-stage breast cancer to its highest level. However, as these patients live longer, they are now experiencing and reporting the associated radiation-induced complications. Several studies have demonstrated that the treatment of left breast cancer has the risk of significantly higher radiation mortality than does the treatment of right breast cancer [1-5]. Other studies have shown that there is an increased risk of death due to cardiac events, as well as of developing ipsilateral lung disease in patients with left breast cancer who are treated with radiation therapy [6, 7]. Darby et al. [6] showed that cardiac toxicity has no threshold dose, and that cardiac toxicity increases

linearly with the radiation dose, at a slope of 7.4%/Gy.

Typically, most patients with breast cancer are treated in the supine position using tangential radiation fields. The treatment field for left breast irradiation includes the heart and left lung. These organs are also partially irradiated along with the breast planning target volume (PTV). Various strategies, such as deep inspiration breath hold (DIBH) [8-10], moderate inspiration breath hold [11-13], and prone breast [14-16], have been successfully implemented to reduce the dose delivered to cardiac components, including the left ventricle (LV) and left anterior descending artery (LAD). A recent study by Taylor et al. indicated that an increase in radiation-related injuries is seen in the LV and LAD in patients undergoing left-sided breast radiation therapy [17]. A higher incidence of LAD stenosis has also been reported for left-sided breast radiation therapy [18, 19].

The clinical implementation of radiation treatment in the prone position has been well analyzed. The prone breast treatment technique utilizes gravity, which pulls the breast tissue away from the heart

and lung. This geometry helps to reduce the radiation dose to the cardiac structures and lungs. This technique also improves dose distribution in the breast, while additionally reducing the dose delivered to the organs at risk (OAR).

The skin dose in breast cancer radiation treatment is an important factor when considering the balance between cosmesis and outcome. Often, skin toxicity is considered as a dose limiting factor [20, 21]. Radiation dermatitis has consistently been a concern of radiation oncologists when using high-dose treatments [22, 23]. Skin dose toxicity has an impact on the tolerance of treatment and on the cosmetic outcomes in patients with breast cancer [24-28]. Breast recurrences are relatively rare, either with the prone or supine treatment. The outcomes are reported to be similar with both techniques [29]. However, a recent study by Katz et al. [30] described a case report of inadequate skin dose that led to skin recurrence when treated using the prone treatment technique. Thus, it is important to determine the dose delivered to the skin during breast radiation therapy to avoid underdosing tumors near the surface and prevent possible recurrence. Moreover, determining the skin dose for

each treatment technique will help radiation oncologists choose an appropriate plan for treatment.

In general, the surface/skin dose depends on the incident beam angle, field size, source to skin distance, beam energy, and beam modifying devices. The beam incidence angle is less oblique in the prone position, which may lead to a lower superficial dose, than in the supine position, where the breast is treated at an angle ranging between 45-55 degrees. Such a steep angle produces a bigger surface dose based on the obliquity factor defined by Gerbi et al. [31]. Additionally, the TPSs are unable to adequately compute the dose in the superficial/buildup region due to voxel size averaging [32]. In our clinic, we regularly use a 2.5-mm grid size for 3D dose calculations. Das et al. [32] showed that a smaller grid size can lead to a more accurate dose calculation in the buildup region. The smallest grid size available in Eclipse version 13.7 is 1 mm; therefore, we chose grid sizes of 1 mm and 2.5 mm to evaluate the skin dose.

This study was undertaken to analyze the skin dose in a cohort of patients who underwent treatment

planning with both techniques (prone and supine treatments). The study was further extended to assess the impact of varying the calculation grid size on the skin dose, in the same patient population.

Materials and methods

Fifty patients who exhibited early-stage left breast cancer with a pathological stage of T1-2N0 and underwent computed tomography (CT) scanning in both the prone and supine positions between August 2017 and March 2018 were included in this retrospective study. The study was approved by the AdventHealth Institutional Review Board (Orlando, FL; reference no #1430). All CT scans were performed using the GE lightspeed RT scanner, at 2.5-mm slice thickness. In the supine set up, the patient's head was turned away to the right. The prone board (CIVCO, Kalona, USA) was used for the prone set up, with both arms above the head and the hands holding a hand-bar to reduce rotation of the body, to ensure a more reproducible setup. The radiation oncologist marked the borders of the breast tissue before the CT scan. CT scan images were transferred to the Eclipse (Varian Medical Systems Inc., Version 13.7) treatment planning

system (TPS). The breast PTV, heart, LV, LAD, and contralateral breast of each patient were contoured by the same radiation oncologist, using RTOG-1304 [33] guidelines in the Eclipse TPS. The external body and left lung were contoured using the automatic contouring function, which was verified by a physicist for accuracy. The breast PTV was pulled 5 mm from the skin surface for both scans.

Radiation treatment was planned for the whole left breast with 6-MV beams, using a hypo-fractioned schedule for the prescribed dose of 42.66 Gy, in 16 fractions. The calculation was performed in the Eclipse TPS using the Anisotropic Analytical Algorithm (AAA; Version 13.7) for 1- and 2.5-mm calculation grid sizes. Two opposing tangential fields were used to cover the breast PTV in both prone and supine positions. The beam's eye view was used to find optimal gantry angles to maximize the distance between the breast PTV and cardiac components to minimize the dose to the OAR without compromising the breast PTV coverage. The treatment field was formed by adding a 7-mm margin to the breast PTV, as recommended in RTOG-1304 protocol [33]. The breast PTV had an identical coverage both in the prone and supine

position, with at least 95% of the PTV receiving 100% of the dose, and with a maximum dose of 108%. A dose-volume histogram (DVH) was used to evaluate the PTV coverage and doses to the OAR. The gantry angles of the treatment beams were recorded in each technique to assess the frequency distribution of the beam angle in this patient population, as shown in Figure 1a, using isodose lines, as shown in Figure 1b. The skin dose was measured perpendicular to the skin surface at the central axis of the beam. Point dosage from the skin surface to a depth of 5 mm was recorded for analysis. The mean dose values for the heart, LV, LAD, and left lung were also recorded and compared between prone and supine positions for treatment plans using the 2.5-mm calculation grid size.

Data between two groups were compared using Wilcoxon signed-rank test for related samples. All statistical analyses were performed using SPSS, version 24.0. Data were considered statistically significant at a P-value ≤ 0.05 .

Results

For the prone position, the median angle of the medial beam relative to the skin surface at the central axis was 8 degrees (3.45-12 degrees); for the supine position, it was 52.5 degrees (48-55.25 degrees). The medial beam angle relative to the skin surface was nearly perpendicular in the prone position but was tangential in the supine position, as shown in the scatter plot in Figure 2.

The median breast PTV volume of the patient was 519.9 cm³ (range, 354.4-756.4 cm³) in the prone position and 544.8 cm³ (range 380.4-796.2 cm³) in the supine position; thus, these two populations had similar breast volumes. The mean dose for the prone vs supine position for the 1-mm calculation grid size was 32.25% vs 32.95% (P <0.62) at the surface, 66.87% vs 65.05% (P <0.86) at 1-mm depth, 81.86% vs 81.27% (P <0.26) at 2-mm depth, 87.80% vs 89.10% (P <0.003) at 3-mm depth, 91.92% vs 94.50% (P <0.00) at 4-mm depth, and 95.30% vs 98.20% (P <0.00) at 5-mm depth. The mean dose for the prone vs supine position for the 2.5-mm calculation grid size was 36.75% vs 38.16% (P <0.34) at the surface, 60.38% vs 62.15% (P

<0.14), 77.35% vs 79.65% (P <0.02), 87.10% vs 88.59% (P <0.00), 91.60% vs 94.63% (P <0.01), and 95.10% vs 97.80% (P <0.01) at 1-, 2-, 3-, 4-, and at 5-mm depth, respectively (Figure 3a-3b and Table 1). The statistical comparisons using P values are shown in Table 2.

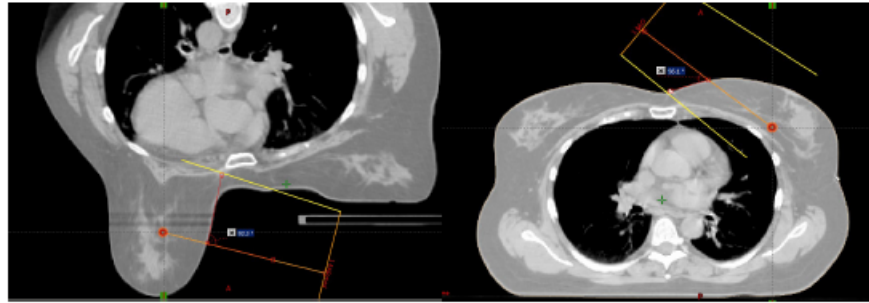
In addition, the doses to heart, LV, LAD, and left lung were analyzed in the supine and prone positions. The median dose in the prone position was 0.92 Gy (0.72–1.11 Gy) for the heart, 1.31 Gy (1.02–1.5 Gy) for the LV, 5.81 Gy (3.71–8.6 Gy) for the LAD, and 0.65 Gy (0.48–0.85 Gy) for the left lung. In the supine position, the respective median doses were 1.88 Gy (1.42–2.58 Gy), 3.24 Gy (2.27–4.42 Gy), 21.76 Gy (6.83–26.88 Gy), and 5.74 Gy (4.55–6.98 Gy). The results for all OAR using both techniques are shown in Figure 4a-4d.

Discussion

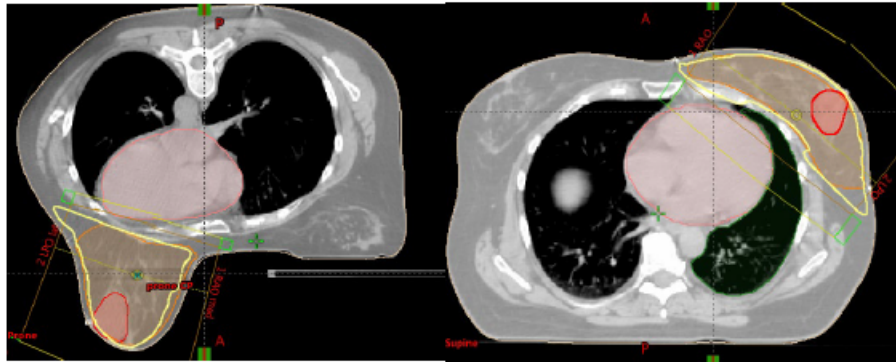
Skin recurrence is relatively rare in breast cancer and is usually associated with specific clinical and pathological factors [30, 34, 35]. In high-energy megavoltage beams, the dose builds up to a maximum dose at a certain depth below the skin, which may potentially underdose the skin. The skin

dose in breast radiation treatment plans is dependent upon many parameters, including the energy, source to skin distance, field size, beam modifying devices, and beam angles. Furthermore, it is dependent upon the bolus in photon and electron beam treatments.

Bouille et al. [36] presented skin recurrence after chest wall treatments in a population of 807 patients and concluded that photon treatment without bolus has a much higher recurrence. An optimum surface dose is required to achieve the primary goal of treating breast cancer without excessive skin toxicity, such as erythema, desquamation, edema, and fibrosis. Skin-sparing is required to avoid unfavorable cosmetic outcomes; however, inadequate skin dose may lead to skin recurrence, as shown by Katz et al [30]. Thus, clinicians should also consider tumor bed contouring, especially for patients who will be treated in the prone position, to evaluate the dose to the gross tumor volume. For such cases, boost treatment should be considered to deliver an adequate dose to the tumor bed. This will prevent underdosing of the superficial tumor beds. The skin dose, in addition to being energy-dependent, can also be grid size-dependent. One study mentioned that differences up to 3% are observed between the maximum and mean doses



1(a)



1(b)

Fig 1 (a): Typical beam angle and beam placement in the prone and supine treatment positions. (b): Typical beam placement in the prone and supine treatment techniques with a 100% isodose line. The yellow line represents the 100% isodose line; orange, red, and pink color contours represent breast PTV lumpectomy, and heart, respectively. PTV, planning target volume.

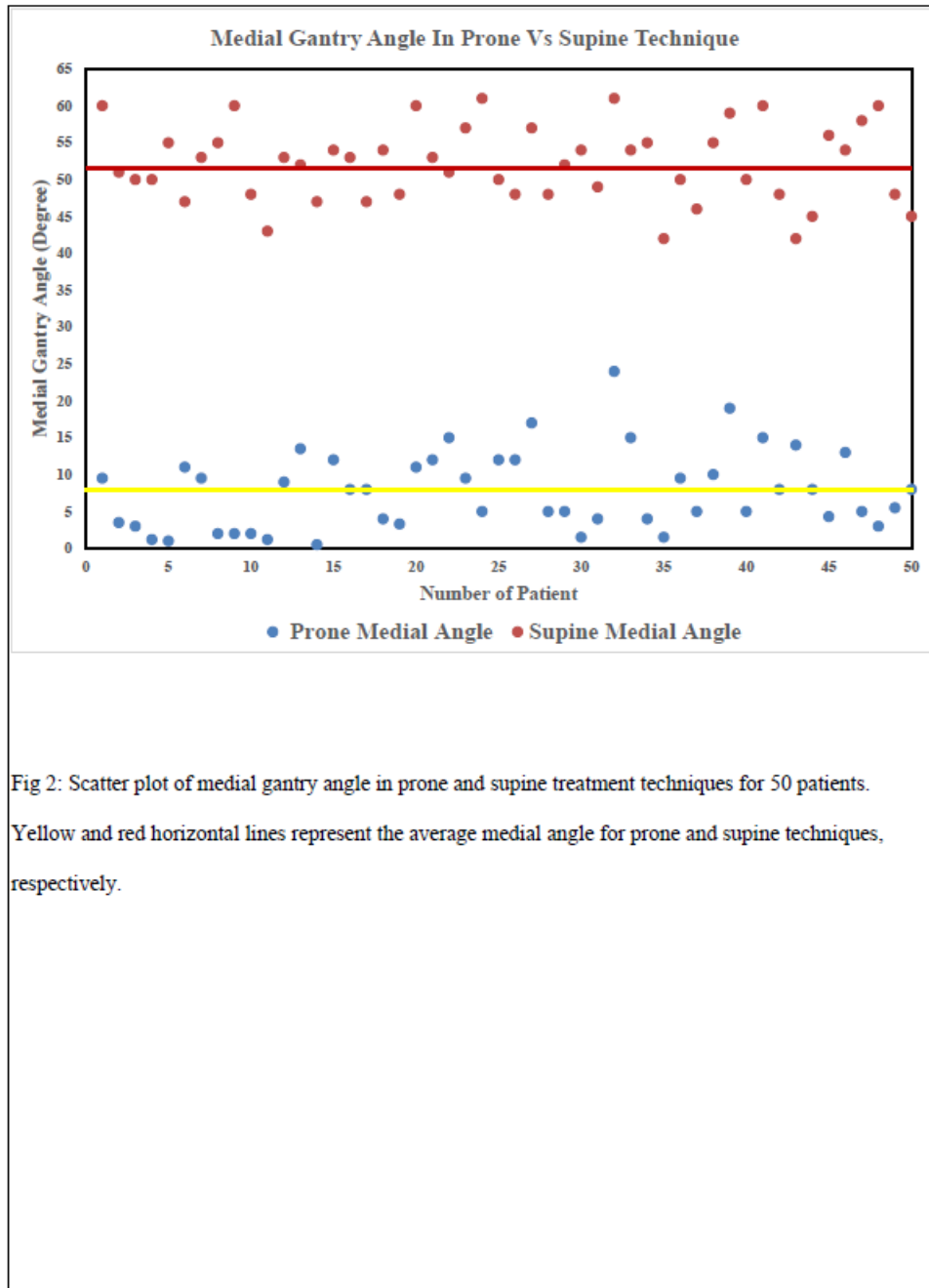


Fig 2: Scatter plot of medial gantry angle in prone and supine treatment techniques for 50 patients. Yellow and red horizontal lines represent the average medial angle for prone and supine techniques, respectively.

Table 1: Percent skin dose (median value and quartile range) from 0-5-mm depth using the supine and prone treatment techniques and a grid size of 1.5 or 2.5 mm

Depth	0 mm	1 mm	2 mm	3 mm	4 mm	5 mm
Prone (1.0-mm grid size) dose in %	32.25(29.48-33.92)	66.87(63.77-68.11)	81.86(80.26-82.91)	87.80(86.47-88.90)	91.92(90.90-92.97)	95.30(93.77-96.00)
Supine (1.0-mm grid size) dose in %	32.95(30.55-36.82)	65.05(63.35-67.99)	81.27(79.50-82.75)	89.10(87.23-90.36)	94.50(92.57-95.62)	98.20(96.6-99.51)
Prone (2.5-mm grid size) dose in %	36.75(33.3-39.32)	60.38(56.90-64.08)	77.35(74.55-80.37)	87.1(85.20-88.31)	91.6(90.27-92.76)	95.10(93.74-96.00)
Supine (2.5-mm grid size) dose in %	38.16(32.82-42.32)	62.15(57.27-67.50)	79.65(76.77-81.75)	88.59(86.68-90.14)	94.63(92.85-95.34)	97.8(96.71-99.44)

Table2: P values in supine vs prone techniques for a grid size of 2.5 or 1 mm, at a depth of 0 to 5 mm. P-values ≤ 0.05 are considered statistically significant

Depth	0 mm	1 mm	2 mm	3 mm	4 mm	5 mm
P value (1.0-mm grid size)	≤ 0.013	≤ 0.862	≤ 0.257	≤ 0.003	≤ 0.001	≤ 0.001
P value (2.5-mm grid size)	≤ 0.342	≤ 0.142	≤ 0.017	≤ 0.001	≤ 0.001	≤ 0.001

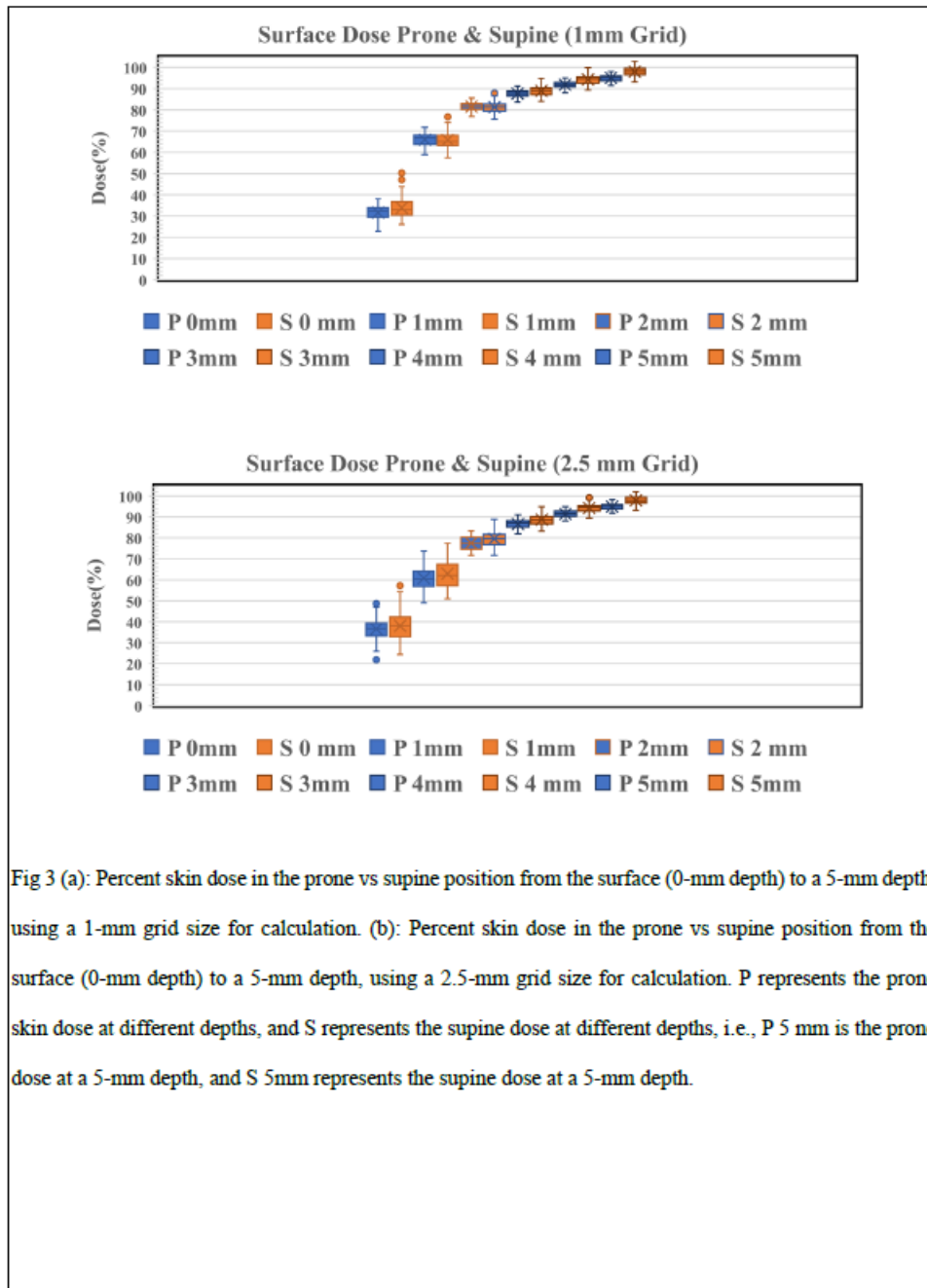


Fig 3 (a): Percent skin dose in the prone vs supine position from the surface (0-mm depth) to a 5-mm depth, using a 1-mm grid size for calculation. (b): Percent skin dose in the prone vs supine position from the surface (0-mm depth) to a 5-mm depth, using a 2.5-mm grid size for calculation. P represents the prone skin dose at different depths, and S represents the supine dose at different depths, i.e., P 5 mm is the prone dose at a 5-mm depth, and S 5mm represents the supine dose at a 5-mm depth.

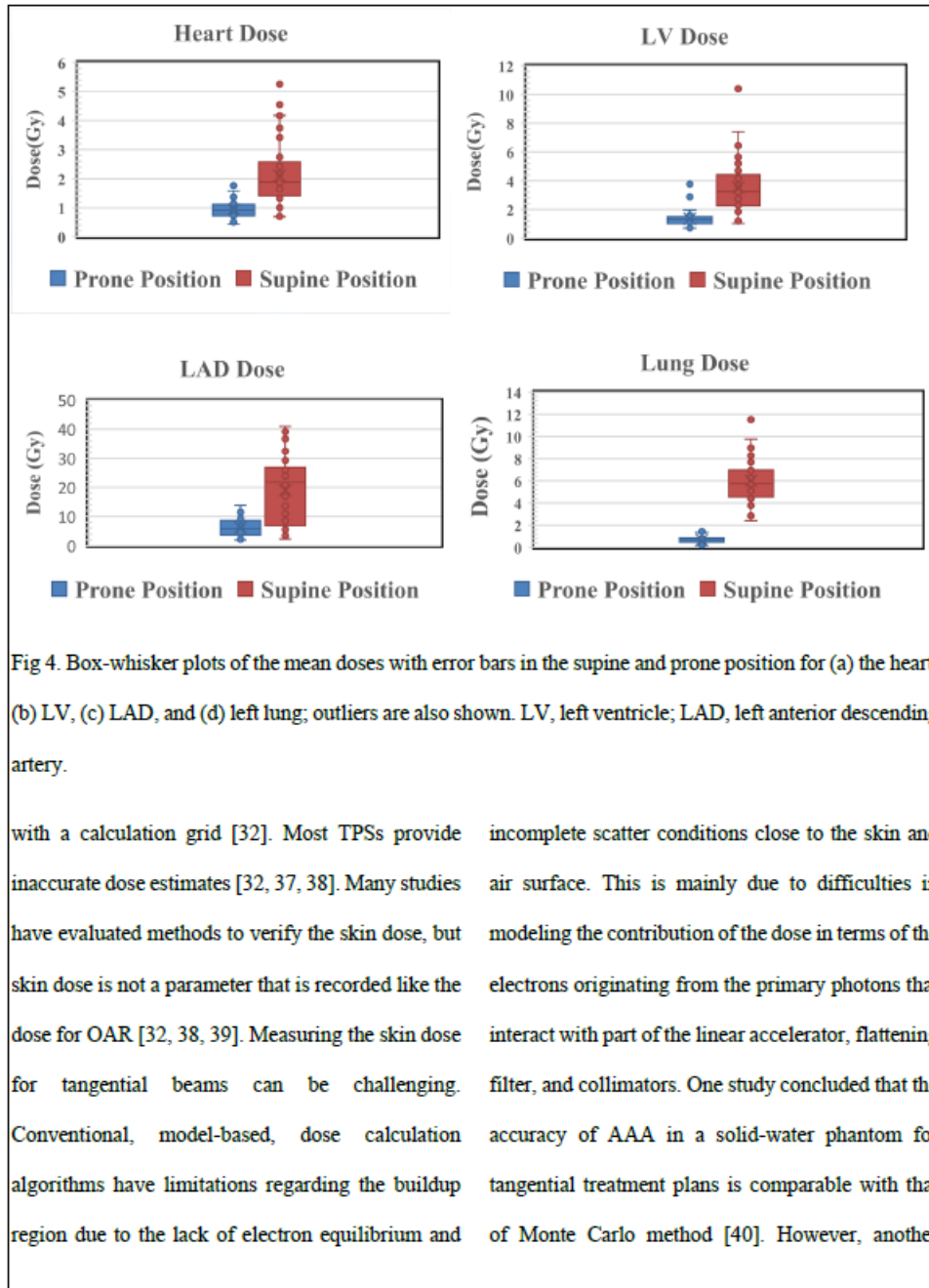


Fig 4. Box-whisker plots of the mean doses with error bars in the supine and prone position for (a) the heart, (b) LV, (c) LAD, and (d) left lung; outliers are also shown. LV, left ventricle; LAD, left anterior descending artery.

with a calculation grid [32]. Most TPSs provide inaccurate dose estimates [32, 37, 38]. Many studies have evaluated methods to verify the skin dose, but skin dose is not a parameter that is recorded like the dose for OAR [32, 38, 39]. Measuring the skin dose for tangential beams can be challenging. Conventional, model-based, dose calculation algorithms have limitations regarding the buildup region due to the lack of electron equilibrium and

incomplete scatter conditions close to the skin and air surface. This is mainly due to difficulties in modeling the contribution of the dose in terms of the electrons originating from the primary photons that interact with part of the linear accelerator, flattening filter, and collimators. One study concluded that the accuracy of AAA in a solid-water phantom for tangential treatment plans is comparable with that of Monte Carlo method [40]. However, another

study concluded that the AAA algorithm cannot reliably predict the dose at a depth less than 2 mm [41]. Panetti et al. [42] measured the calculation accuracy of AAA in the surface build region in tangential beam arrangements similar to those used for breast treatment planning. The authors concluded that, for a 6-MV beam, the use of AAA will not introduce clinically significant errors in the buildup region for the absorbed dose, especially after the first 2 mm of tissue. One limitation of our study is that the dose on the patient's skin surface was not measured.

In this study, doses at depths of 3, 4, and 5 mm were statistically significantly lower in the prone position than in the supine position, irrespective of the grid size used, as shown in Table 1. These doses in the prone position were identical between grid sizes of 1 and 2.5 mm, and similar observations were made for the supine position. Thus, we found minimal effects of the grid size on the dose at a depth beyond 2 mm for both positions. Our data indicate that a depth dose reduction of up to 3% can be possible in the prone position compared to the supine position at 5 mm. This is because the median angle in the prone positions was only 8 degrees, and thus the

beam was almost perpendicular to the skin surface; in contrast, the median angle in the supine position was 52.5 degrees.

Further, we found that a statistically significantly lower mean dose is delivered to all OAR when in the prone position than the supine position using a grid size of 2.5 mm. The heart, LV, LAD, and left lung doses were significantly lower in the prone position. Although the heart falls anteriorly in the prone position, since the breast also falls and elongates due to gravity, beam angles can be chosen so as to minimize in-field heart, LV, and LAD doses. Similarly to other studies, the largest dose reduction was seen in the left lung in the prone position [8, 43, 44]. However, contrary to a study by Verhoeven et al. [16], which concluded that LAD is higher in the prone position, we found statistically significantly lower dose to the LAD in the prone position than in the supine position. Thus, the prone position seems to reduce the dose to all OAR.

Conclusions

Based on the same patient population treated in the prone and supine positions with 6-MV beams, this study established that the dose to the OAR is lower in the prone position than in the supine position,

especially for the LAD and left lung. The grid size had a minimal effect on the dose calculated by the treatment planning system in superficial regions. Notably, the skin dose was also lower in the prone position than in the supine position. In both techniques, the dose rapidly increased to more than 95% beyond a 5-mm depth from the skin surface. This validates our hypothesis that the prone technique allows for a lower superficial dose than

does the supine technique. This observation is consistent with physical parameters, as the beam angle is almost perpendicular to the surface in the prone technique. Thus, the prone position reduces the dose to the OAR, however dose to the skin may also be assessed in the prone technique and if desired, the skin dose should be carefully augmented via a bolus or beam spoiler.

References

1. Fisher B, Anderson S, Bryant J, Margolese RG, Deutsch M, Fisher ER, et al. Twenty-year follow-up of a randomized trial comparing total mastectomy, lumpectomy, and lumpectomy plus irradiation for the treatment of invasive breast cancer. *N Engl J Med.* 2002;347(16):1233-41. doi: 10.1056/NEJMoa022152. PubMed PMID: 12393820.
2. Clarke M, Collins R, Darby S, Davies C, Elphinstone P, Evans V, et al. Effects of radiotherapy and of differences in the extent of surgery for early breast cancer on local recurrence and 15-year survival: an overview of the randomised trials. *Lancet.* 2005;366(9503):2087-106. doi: 10.1016/S0140-6736(05)67887-7. PubMed PMID: 16360786.
3. Early Breast Cancer Trialists' Collaborative G, Darby S, McGale P, Correa C, Taylor C, Arriagada R, et al. Effect of radiotherapy after breast-conserving surgery on 10-year recurrence and 15-year breast cancer death: meta-analysis of individual patient data for 10,801 women in 17 randomised trials. *Lancet.* 2011;378(9804):1707-16. doi: 10.1016/S0140-6736(11)61629-2. PubMed PMID: 22019144; PubMed Central PMCID: PMC3254252.
4. Santiago RJ, Wu L, Harris E, Fox K, Schultz D, Glick J, et al. Fifteen-year results of breast-conserving surgery and definitive irradiation for Stage I and II breast carcinoma: the University of Pennsylvania experience. *Int J Radiat Oncol Biol Phys.* 2004;58(1):233-40. PubMed PMID: 14697443.
5. Solin LJ, Kurtz J, Fourquet A, Amalric R, Recht A, Bornstein BA, et al. Fifteen-year results of breast-conserving surgery and definitive breast irradiation for the treatment of ductal carcinoma in situ of the breast. *J Clin Oncol.* 1996;14(3):754-63. doi: 10.1200/JCO.1996.14.3.754. PubMed PMID: 8622021.
6. Darby SC, Ewertz M, McGale P, Bennet AM, Blom-Goldman U, Bronnum D, et al. Risk of ischemic heart disease in women after radiotherapy for breast cancer. *N Engl J Med.* 2013;368(11):987-98. doi: 10.1056/NEJMoa1209825. PubMed PMID: 23484825.
7. Sardaro A, Petruzzelli MF, D'Errico MP, Grimaldi L, Pili G, Portaluri M. Radiation-induced cardiac damage in early left breast cancer patients: risk factors, biological mechanisms, radiobiology, and dosimetric constraints. *Radiother Oncol.* 2012;103(2):133-42. doi: 10.1016/j.radonc.2012.02.008. PubMed PMID: 22391054.
8. Saini AS, Hwang CS, Biagioli MC, Das JJ. Evaluation of sparing organs at risk (OARs) in left-breast irradiation in the supine and prone positions and with deep inspiration breath-hold. *J Appl Clin Med Phys.* 2018;19(4):195-204. doi: 10.1002/acm2.12382. PubMed PMID: 29927027; PubMed Central PMCID: PMC6036360.
9. Smyth LM, Knight KA, Aarons YK, Wasiak J. The cardiac dose-sparing benefits of deep inspiration breath-hold in left breast irradiation: a systematic review. *J Med Radiat Sci.* 2015;62(1):66-73. doi:

- 10.1002/jmrs.89. PubMed PMID: 26229669; PubMed Central PMCID: PMC4364808.
10. Hayden AJ, Rains M, Tiver K. Deep inspiration breath hold technique reduces heart dose from radiotherapy for left-sided breast cancer. *J Med Imaging Radiat Oncol.* 2012;56(4):464-72. doi: 10.1111/j.1754-9485.2012.02405.x. PubMed PMID: 22883657.
 11. Comsa D, Barnett E, Le K, Mohamoud G, Zaremski D, Fenkell L, et al. Introduction of moderate deep inspiration breath hold for radiation therapy of left breast: Initial experience of a regional cancer center. *Pract Radiat Oncol.* 2014;4(5):298-305. doi: 10.1016/j.prro.2013.10.006. PubMed PMID: 25194098.
 12. Swanson T, Grills IS, Ye H, Entwistle A, Teahan M, Letts N, et al. Six-year experience routinely using moderate deep inspiration breath-hold for the reduction of cardiac dose in left-sided breast irradiation for patients with early-stage or locally advanced breast cancer. *Am J Clin Oncol.* 2013;36(1):24-30. doi: 10.1097/COC.0b013e31823fe481. PubMed PMID: 22270108; PubMed Central PMCID: PMC3375337.
 13. van Haaren P, Claassen-Janssen F, van de Sande I, Boersma L, van der Sangen M, Hurlkmans C. Heart position variability during voluntary moderate deep inspiration breath-hold radiotherapy for breast cancer determined by repeat CBCT scans. *Phys Med.* 2017;40:88-94. doi: 10.1016/j.ejmp.2017.07.014. PubMed PMID: 28743616.
 14. Formenti SC, Hsu H, Fenton-Kerimian M, Roses D, Guth A, Jozsef G, et al. Prone accelerated partial breast irradiation after breast-conserving surgery: five-year results of 100 patients. *Int J Radiat Oncol Biol Phys.* 2012;84(3):606-11. Epub 2012/04/13. doi: 10.1016/j.ijrobp.2012.01.039. PubMed PMID: 22494589; PubMed Central PMCID: PMC3714845.
 15. Huppert N, Jozsef G, DeWynngaert K, Formenti SC. The role of a prone setup in breast radiation therapy. *Front Oncol.* 2011;1 (October):31(1-8).
 16. Verhoeven K, Sweldens C, Petillion S, Laenen A, Peeters S, Janssen H, et al. Breathing adapted radiation therapy in comparison with prone position to reduce the doses to the heart, left anterior descending coronary artery, and contralateral breast in whole breast radiation therapy. *Pract Radiat Oncol.* 2014;4(2):123-9. doi: 10.1016/j.prro.2013.07.005. PubMed PMID: 24890353.
 17. Taylor C, McGale P, Bronnum D, Correa C, Cutter D, Duane FK, et al. Cardiac structure injury after radiotherapy for breast cancer: cross-sectional study with individual patient data. *J Clin Oncol.* 2018;36(22):2288-96. doi: 10.1200/JCO.2017.77.6351. PubMed PMID: 29791285; PubMed Central PMCID: PMC6067799.
 18. Correa CR, Litt HI, Hwang WT, Ferrari VA, Solin LJ, Harris EE. Coronary artery findings after left-sided compared with right-sided radiation treatment for early-stage breast cancer. *J Clin Oncol.* 2007;25(21):3031-7. doi: 10.1200/JCO.2006.08.6595. PubMed PMID: 17634481.
 19. Nilsson G, Holmberg L, Garmo H, Duvernoy O, Sjogren I, Lagerqvist B, et al. Distribution of coronary artery stenosis after radiation for breast cancer. *J Clin Oncol.* 2012;30(4):380-6. doi: 10.1200/JCO.2011.34.5900. PubMed PMID: 22203772.
 20. Kim S, Liu CR, Zhu TC, Palta JR. Photon beam skin dose analyses for different clinical setups. *Med Phys.* 1998;25(6):860-6. doi: 10.1118/1.598261. PubMed PMID: 9650173.
 21. Chin MS, Siegel-Reamer L, FitzGerald GA, Wyman A, Connor NM, Lo YC, et al. Association between cumulative radiation dose, adverse skin reactions, and changes in surface hemoglobin among women undergoing breast conserving therapy. *Clin Transl Radiat Oncol.* 2017;4:15-23. doi: 10.1016/j.ctro.2017.03.003. PubMed PMID: 29594203; PubMed Central PMCID: PMC5833900.
 22. Kole AJ, Kole L, Moran MS. Acute radiation dermatitis in breast cancer patients: challenges and solutions. *Breast Cancer (Dove Med Press).* 2017;9:313-23. doi: 10.2147/BCTT.S109763. PubMed PMID: 28503074; PubMed Central PMCID: PMC5426474.
 23. Osako T, Oguchi M, Kumada M, Nemoto K, Iwase T, Yamashita T. Acute radiation dermatitis and pneumonitis in Japanese breast cancer patients with whole breast hypofractionated radiotherapy compared to conventional radiotherapy. *Jpn J Clin Oncol.* 2008;38(5):334-8. doi: 10.1093/jjco/hyn030. PubMed PMID: 18417501.
 24. Habibollahi F, Mayles HM, Mayles WP, Winter PJ, Tong D, Fentiman IS, et al. Assessment of skin dose and its relation to cosmesis in the conservative treatment of early breast cancer. *Int J Radiat Oncol Biol Phys.* 1988;14(2):291-6. PubMed PMID: 3338951.

25. Kulik A, Lyczek J, Kawczyn Ska M, Gruszczyn Ska E. Cosmetic effect in patients with early breast cancer treated with breast conserving therapy (BCT) and with HDR brachytherapy (HDR-BT) "boost". *J Contemp Brachytherapy*. 2009;1(2):77-86. PubMed PMID: 27795716; PubMed Central PMCID: PMCPMC5075992.
26. Beadle GF, Silver B, Botnick L, Hellman S, Harris JR. Cosmetic results following primary radiation therapy for early breast cancer. *Cancer*. 1984;54(12):2911-8. PubMed PMID: 6498767.
27. Dewar JA, Benhamou S, Benhamou E, Arriagada R, Petit JY, Fontaine F, et al. Cosmetic results following lumpectomy, axillary dissection and radiotherapy for small breast cancers. *Radiother Oncol*. 1988;12(4):273-80. PubMed PMID: 3187067.
28. Liss AL, Ben-David MA, Jagsi R, Hayman JA, Griffith KA, Moran JM, et al. Decline of cosmetic outcomes following accelerated partial breast irradiation using intensity modulated radiation therapy: results of a single-institution prospective clinical trial. *Int J Radiat Oncol Biol Phys*. 2014;89(1):96-102. doi: 10.1016/j.ijrobp.2014.01.005. PubMed PMID: 24613813; PubMed Central PMCID: PMCPMC5446776.
29. Stegman LD, Beal KP, Hunt MA, Fomier MN, McCormick B. Long-term clinical outcomes of whole-breast irradiation delivered in the prone position. *Int J Radiat Oncol Biol Phys*. 2007;68(1):73-81. doi: 10.1016/j.ijrobp.2006.11.054. PubMed PMID: 17337131.
30. Katz LM, Perez CA, Gerber NK, Purswani J, McCarthy A, Das IJ. Skin recurrence in radiation treatment of breast cancer. *And Radiat Oncol*. 2018;3(July/Sep):458-62. doi: <https://doi.org/10.1016/j.adro.2018.04.014>.
31. Gerbi BJ, Meigooni AS, Khan FM. Dose buildup for obliquely incident photon beams. *Med Phys*. 1987;14(3):393-9. doi: 10.1118/1.596055. PubMed PMID: 3600530.
32. Akino Y, Das IJ, Bartlett GK, Zhang H, Thompson E, Zook JE. Evaluation of superficial dosimetry between treatment planning system and measurement for several breast cancer treatment techniques. *Med Phys*. 2013;40(1):011714. doi: 10.1118/1.4770285. PubMed PMID: 23298084.
33. Randomized phase III clinical trial evaluating post-mastectomy chestwall and regional nodal xrt and post-lumpectomy regional nodal xrt in patients with positive axillary nodes before neoadjuvant chemotherapy who convert to pathologically negative axillary nodes after neoadjuvant chemotherapy. NSABP PROTOCOL B-51/RTOG PROTOCOL 1304.
34. Gage I, Schnitt SJ, Recht A, Abner A, Come S, Shulman LN, et al. Skin recurrences after breast-conserving therapy for early-stage breast cancer. *J Clin Oncol*. 1998;16(2):480-6. doi: 10.1200/JCO.1998.16.2.480. PubMed PMID: 9469331.
35. Cowen D, Houvenaeghel G, Jacquemier J, Resbeut M, Largillier R, Bardou VJ, et al. [Local recurrences after conservative treatment of breast cancer: risk factors and influence on survival]. *Cancer Radiother*. 1998;2(5):460-8. PubMed PMID: 9868388.
36. Boulle G, Saint-Martin C, De La Lande B, Laki F, Bidoz NF, Berger F, et al. Photons without bolus versus electrons with bolus after upfront mastectomy without immediate reconstruction in breast cancer patients. *Int J Radiat Oncol Biol Phys*. 2019;104(4):877-84. doi: 10.1016/j.ijrobp.2019.03.029. PubMed PMID: 30926576.
37. Almberg SS, Lindmo T, Frengen J. Superficial doses in breast cancer radiotherapy using conventional and IMRT techniques: a film-based phantom study. *Radiother Oncol*. 2011;100(2):259-64. doi: 10.1016/j.radonc.2011.05.021. PubMed PMID: 21624698.
38. Soleymanifard S, Aledavood SA, Noghreiyani AV, Ghorbani M, Jamali F, Davenport D. In vivo skin dose measurement in breast conformal radiotherapy. *Contemp Oncol (Pozn)*. 2016;20(2):137-40. doi: 10.5114/wo.2015.54396. PubMed PMID: 27358592; PubMed Central PMCID: PMCPMC4925725.
39. Dogan N, Glasgow GP. Surface and build-up region dosimetry for obliquely incident intensity modulated radiotherapy 6 MV x rays. *Med Phys*. 2003;30(12):3091-6. doi: 10.1118/1.1625116. PubMed PMID: 14713075.
40. Chakarova R, Gustafsson M, Back A, Drugge N, Palm A, Lindberg A, et al. Superficial dose distribution in breast for tangential radiation treatment, Monte Carlo evaluation of Eclipse algorithms in case of phantom and patient geometries. *Radiother Oncol*. 2012;102(1):102-7. doi: 10.1016/j.radonc.2011.06.021. PubMed PMID: 21741719.
41. Chow JC, Jiang R, Leung MK. Dosimetry of oblique tangential photon beams calculated by

- superposition/convolution algorithms: a Monte Carlo evaluation. *J Appl Clin Med Phys*. 2010;12(1):3424. doi: 10.1120/jacmp.v12i1.3424. PubMed PMID: 21330989; PubMed Central PMCID: PMCPMC5718594.
42. Panettieri V, Barsoum P, Westermarck M, Brualla L, Lax I. AAA and PBC calculation accuracy in the surface build-up region in tangential beam treatments. Phantom and breast case study with the Monte Carlo code PENELOPE. *Radiother Oncol*. 2009;93(1):94-101. doi: 10.1016/j.radonc.2009.05.010. PubMed PMID: 19541380.
43. Ferrari A, Ivaldi G, Leonardi MC, Rondi E, Orecchia R. Prone breast radiotherapy in a patient with early stage breast cancer and a large pendulous breast. *Tumori*. 2009;95(3):394-7. PubMed PMID: 19688985.
44. Kirby AM, Evans PM, Donovan EM, Convery HM, Haviland JS, Yarnold JR. Prone versus supine positioning for whole and partial-breast radiotherapy: a comparison of non-target tissue dosimetry. *Radiother Oncol*. 2010;96(2):178-84. doi: 10.1016/j.radonc.2010.05.014. PubMed PMID: 20561695.

Appendix F: Permission to Publish Study 1

Journal of Applied Clinical Medical Physics <JACMPEditorial@wiley.com>

Nov 5, 2019, 1:47 AM ☆ ↩

to me ▾

Dear Dr. Pal,

Thank you for your email.

This is perfectly permissible without any written agreement from us. Please be advised that all articles published by JACMP are under a CC-BY license. <https://creativecommons.org/licenses/> This license allows the distribution, remix, tweak, and building upon the licensed work as long as you credit the original creation.

A correct citation, to the published article in JACMP, is the only real requirement. I hope this has been helpful.

Best,

Kate Marjorie Cabalar

Journal of Applied Clinical Medical Physics

JACMPEditorial@wiley.com

From: Amit Pal <amitpal97@gmail.com>

Sent: Tuesday, November 5, 2019 3:52 AM

To: Journal of Applied Clinical Medical Physics <JACMPEditorial@wiley.com>

Subject: Copyright to include in the dissertation

Dear Sir/Madam,

Our article below was published in 2018. I would want to use the article towards my dissertation, how can i get permission to use this article towards my dissertation?

Thank you,

Amit Saini

Appendix G: Permission to Publish Study 2



Powers, Kathryn (ELS-PHI)

to me ▾
Hi Amit,

Dec 2, 2019, 3:59 PM

I'm not sure if I responded to you previously, but if not, I apologize for the delay.

Authors can include their articles in full or in part in a thesis or dissertation for non-commercial purposes without requesting permissions.

Sincerely,

Katy Powers
Journal Manager
ELSEVIER | Research Content Operations
+1 (215) 239 3308 phone

To track the progress of your article in real time throughout the publication process, please use our [Article Tracking for Authors](#) service.
Feel free to also visit our [Customer Support](#) site where you can search for solutions on a range of topics and find answers to frequently asked questions.

From: Amit Pal <amitpal97@gmail.com>
Sent: Monday, November 4, 2019 10:55 PM
To: Powers, Kathryn (ELS-PHI) <k.powers@elsevier.com>
Subject: Permission to publish

*** External email: use caution ***

✉

Dear Kathryn,
Our article below is published now. I m wondering if you can please guide me towards the procedure to seek permission to use this article towards my dissertation?
Thank you,
Amit Saini

On Mon, Aug 5, 2019 at 11:51 AM <k.powers@elsevier.com> wrote:

PLEASE DO NOT ALTER THE SUBJECT LINE OF THIS E-MAIL ON REPLY

Dear Ms. Amitpal Singh Saini,

Thank you for publishing with *Practical Radiation Oncology*. We are pleased to inform you that the proof for your upcoming publication is ready for review via the link below. You will find instructions on the start page on how to make corrections directly on-screen or through PDF.

<https://live1.elsevierproofcentral.com/authorproofs/a4a5648b3af4a6bb4af723acd5181ef0>